THE INTEGRATION OF GPS HEIGHTS INTO THE AUSTRALIAN HEIGHT DATUM

R.D. HOLLOWAY

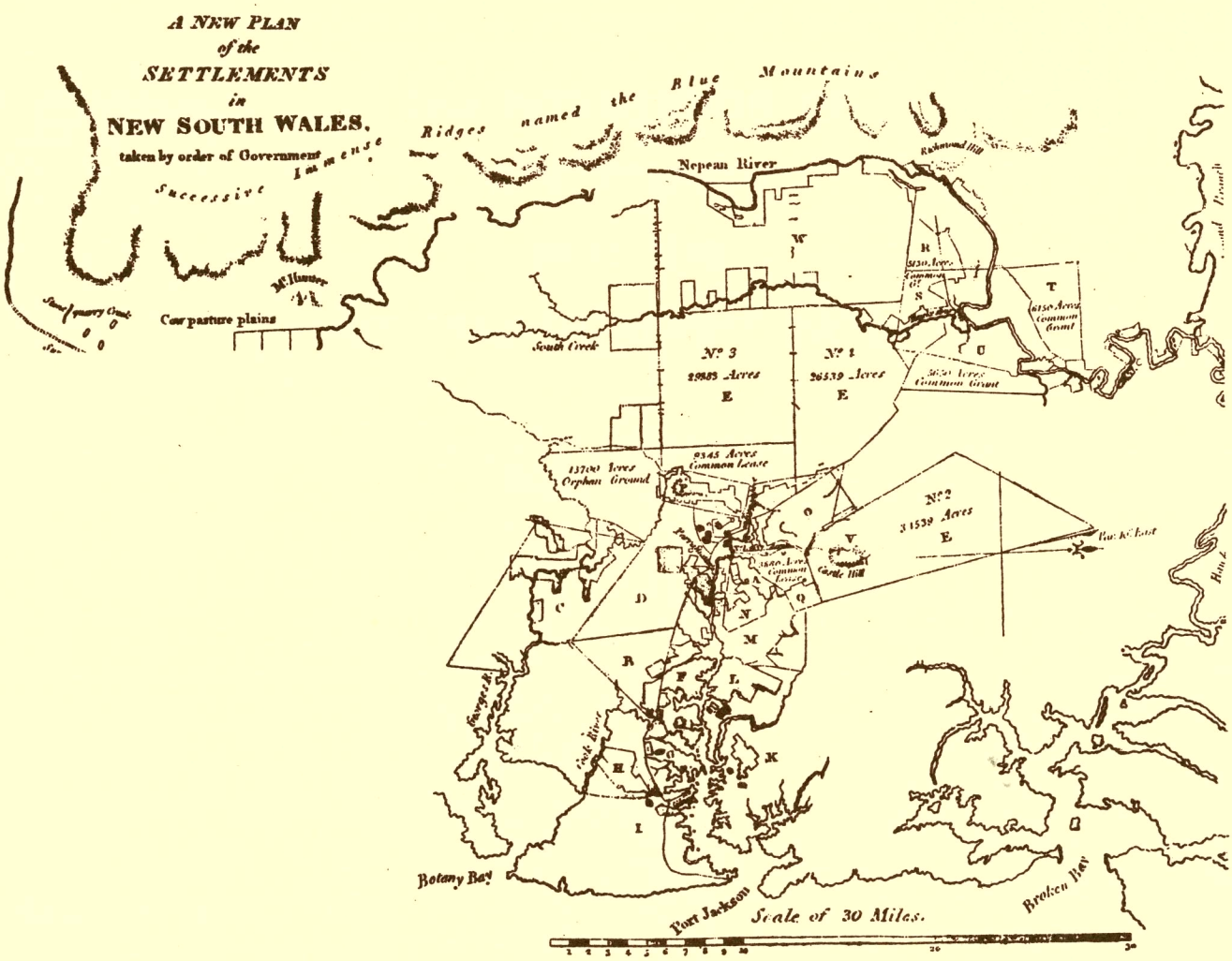

UNISURV S-33, 1988
Reports from
SCHOOL OF SURVEYING

THE UNIVERSITY OF NEW SOUTH WALES KENSINGTON, NSW AUSTRALIA 2033

UNISURV REPORT S - 33, 1988

THE INTEGRATION OF GPS HEIGHTS INTO THE AUSTRALIAN HEIGHT DATUM

R. D. Holloway

Received: October, 1988

SCHOOL OF SURVEYING
UNIVERSITY OF NEW SOUTH WALES
P.O. BOX 1,
KENSINGTON, N.S.W. 2033
AUSTRALIA

National Library of Australia

Card No. and ISBN 0 85839 051 5

Table of Contents

Figures

Tables

ACRONYMS

AGD	Australian Geodetic Datum
AHD	Australian Height Datum
ANGN	Australian National Gravity Network
ANS	Australian National Spheroid
ASO	Australian Survey Office
BMR	Bureau of Mineral Resources
DTM	Digital terrain model
DoD	United States Department of Defense
ESA	European Space Agency
GLONASS	Global Navigation Satellite System (Russian)
GPS	Global Positioning System
GRS67	Geodetic Reference System 1967
GRS80	Geodetic Reference System 1980
IAG	International Association of Geodesy
IGSN71	International Gravity Standardization Net 1971
IRI	International Reference Ionosphere
IUGG	International Union of Geodesy and Geophysics
NAVSTAR	Navigation Satellite Timing and Ranging
RINT	Ring Integration
RSS	root sum square
SECOR	Sequential Collation of Range
SLR	Satellite Laser Ranging
SST	sea surface topography
TEC	total electron content
UNSW	University of New South Wales
UTC	Universal Coordinated Time
WGS72	World Geodetic System 1972
WGS84	World Geodetic System 1984
WVR	Water Vapour Radiometer

UNITS OF GRAVITY

γ_e = 9.7803267715	ms^{-2}	normal gravity at equator (GRS80)
γ_e = 0.97803267715	kGal	1 kilogal = 10^3 Gal
γ_e = 978.03267715	Gal	
γ_e = 978032.67715	mGal	1 milligal = 10^{-3} Gal = 10^{-5} ms^{-2}
γ_e = 978032677.15	μGal	1 microgal = 10^{-6} Gal
γ_p = 9.8321863685	ms^{-2}	normal gravity at poles (GRS80)
$\bar{\gamma}$ = 9.797644656	ms^{-2}	average gravity over ellipsoid (GRS80)

ACKNOWLEDGEMENTS

This study has involved both the active and passive participation of a number of people who together have helped bring this project to fruition. I am not only indebted to those people and organisations who have directly contributed their resources but also to those people who created an environment in which discussion and inquiry were promoted.

Foremost, I am deeply grateful to my supervisor and employer, Dr. A.H.W. Kearsley who introduced me to the field of gravimetric geodesy, aroused my curiosity and guided me through its intricacies. His direction and encouragement has fuelled my sometimes lagging spirits.

I would like to thank Ken Alexander and the Western Australian Department of Land & Administration for making available the GPS data for the network in the South West Seismic Zone.

I would also like to thank Dean Warhurst and Doug Larden from the South Australian Department of Lands for making available the GPS data for the Phase I network in the Mallee region. I spent approximately six weeks in Adelaide analysing this data and received great cooperation and courtesy from all the staff of the department during my stay.

Adrian Roelse from the Australian Land Information Group (AUSLIG, formerly the Department of National Mapping) kindly provided me with research material and organised my visit to Canberra.

The Satellite, Navigation and Positioning Group (SNAP) within the School of Surveying at the University of New South Wales, under the chairmanship of Dr. Art Stolz and later Dr. Chris Rizos, has been an excellent forum to promote discussion on GPS topics amongst my fellow students and for the dissemination of research material. In particular, I would like to thank Don Grant, Brian Donnelly, Rod Eckels, Gary Chisholm and Robert Pascoe for their ideas and assistance in debugging my programs.

I have great admiration for my wife, Susan, who having a busy career in marketing is still able to share my enthusiasm for my studies and show great interest in matters of geoids and satellites. She has given me strength and I give her my love.

ABSTRACT

The Global Positioning System (GPS) is being used to determine ellipsoidal height differences (Δh) over baselines by organisations who are attracted to its efficiencies in use and accuracy of results compared to conventional surveying techniques. For these heights to be physically meaningful they must be integrated into the Australian Height Datum (AHD) to be compatible with other spirit levelled heights (ΔH). The GPS heights are referred to the reference ellipsoid of the satellite system whilst the reference surface of the AHD is observed mean sea level at 30 tide gauges around the Australian coastline being a close approximation of the geoid. The difference between the two surfaces at a point is the geoid-ellipsoid separation (N), or more commonly and more accurately, the difference in the geoid-ellipsoid separation (ΔN) when expressed over a baseline.

This study investigates the three components of the equation used to transform GPS heights into the AHD,

$$\Delta H = \Delta h - \Delta N$$

and finds that,

* heights in the AHD should be referred to as *normal orthometric heights* because normal gravity is used in the orthometric correction,
* heights in the AHD are referred to a warped surface not coincident with the geoid or any other equipotential surface because the levelling was adjusted between the mean sea level heights at 30 tide gauges around the Australian coastline,
* the difference between mean sea level and the geoid at each tide gauge station is equal to the sea surface topography at the tide gauge,
* there is a high probability that compensating gross errors in heights remain undetected in some levelling loops.

The principal systematic error sources in the GPS heights were found to be,

* the troposphere delay error,
* the *a priori* coordinates of the fixed station,
* the residual ionosphere delay error,
* errors in the satellite ephemerides.

Simulation studies show that with an appropriate observation and computation strategy the precision of GPS heights is 2-4 ppm. It was also found that there was no benefit in resolving the cycle ambiguities because the heights were not improved if the integer ambiguities were solved for correctly, which must be weighed against the risk of degrading the heights if the ambiguities are resolved incorrectly.

The precision requirements for the computation of the geoid-ellipsoid height differences vary with the application and the remoteness of the location. For the most precise heighting applications it is necessary to compute ΔN to the same precision as that of the GPS heights. The methods investigated in this study include,

* geometrical methods such as contouring N values and analytically fitting a plane surface to height control points,
* using high order geopotential models such as OSU81, GPM2 and OSU86E,
* using ring integration (RINT), which uses a high order geopotential model combined with integration of the local gravity field using Stokes' formula.

Each of these methods is evaluated by computing ΔN in two GPS observed networks, one in Western Australia and the other in South Australia. The relative precision of the results and complexity of computation are compared. It was found that GPS heights can be integrated into the AHD without loss of accuracy and that GPS heighting is a viable alternative to spirit levelling for all but the most accurate applications.

1 INTRODUCTION

Historically, surveyors have treated the observation of horizontal and vertical control networks quite separately. Horizontal coordinates, determined by classical surveying techniques such as triangulation, trilateration and traversing, are referred to either a local or global ellipsoid. The vertical coordinate, whether it be dynamic, orthometric or normal height is determined by spirit levelling and referred to mean sea level which is assumed to be coincident with the geoid. Both horizontal and vertical networks have also been adjusted separately.

The advent of the Global Positioning System (GPS) now means that the determination of position and height is possible both accurately and simultaneously. However the three dimensional GPS coordinates will be referred to the same global geocentric ellipsoid as that used for the satellite tracking. This will not usually be the same as the reference ellipsoid of the geodetic control network.

The transformation of GPS observed coordinates into the existing horizontal control network is achieved by the application of continental or regionally derived transformation parameters. These transformation parameters are determined empirically by comparison of coordinates in both systems at common points (Eckels, 1987).

The transformed coordinates will be consistent with the horizontal coordinates in the local geodetic network but the height component will not be with the vertical network as it is not referred to an equipotential surface, usually the geoid. If the separation at a point between the reference ellipsoid of the satellite datum and the geoid is known, then the GPS height can be transformed into a height in the Australian Height Datum (AHD).

This study investigates various methods of transforming GPS heights into the AHD, with emphasis on a gravimetric solution, and illustrates each procedure by analysis of two very different GPS observed networks. The first network, in the south west seismic zone in Western Australia consists of 10 stations, all of which have first or second order heights which were used as control against which the transformed heights were compared. The

second network, in the Mallee region in the south east of South Australia consists of 107 stations some of which have third order and fourth order heights which were again used as control.

Chapter 2 shows how levelled height differences, gravity and gravity potential are related and looks at the conceptual and practical differences between different height systems that are in use around the world. The chapter concludes by answering the question, "In which height system is the AHD?"

Chapter 3 reviews the history of the evolution of the AHD, the levelling accuracies, the adjustment and the departure of mean sea level from the geoid.

Chapter 4 describes the GPS system and looks at the origins and effects of the principal error sources in the transmission, propagation and reception of the satellite signal by reviewing the current literature. The behaviour of systematic errors in the GPS system, the instrumentation and the propagation medium and how they affect the final ellipsoidal heights is investigated by performing computer simulations.

Chapter 5 reviews the concepts and theoretical basis of various methods of transforming GPS heights into the AHD. The methods investigated are astro-geodetic, geometric, high order geopotential models and gravimetric solutions for the geoid-ellipsoid separation. The advantages or disadvantages and expected accuracies of each method are also discussed. An examination of the density and coverage of the gravity data over the Australian continent and near offshore areas is presented and also how well the gravity anomalies are able to be recovered using the high order geopotential model OSU81.

Chapter 6 looks more closely at a solution for the geoid-ellipsoid separation using ring integration (RINT, Kearsley, 1985) which involves the combination of an outer zone solution using a high order geopotential model with an inner zone solution integrating gravity data using Stoke's theorem. A system of computer programs to compute geoidal heights using the RINT technique has been developed at the University of New South Wales and is presented here.

Chapter 7 tests the various methods of determining the geoid-ellipsoid separation in the Western Australia and South Australia networks and presents the results. These techniques vary in complexity of computation, data requirements and accuracy of results. The user can decide which technique is the more appropriate for his application. He can, using only pen and ruler, graphically determine an interpolating surface to scale off geoid heights or determine the same surface analytically using program LESQPL (Annex D). High order geopotential models OSU81, GPM2 and OSU86E can be used to compute absolute geoid heights or, more accurately, differences in geoid heights. For the most precise applications, the RINT technique may be used.

The surveyor's office of the future, envisaged by Holloway and Williamson (1987), will soon be upon us and GPS will be an essential tool in that scenario. To obtain the full potential of this system, GPS heights will have to be transformed into heights in the AHD, as long as the reference surface for our height system is the geoid or our best estimation of the geoid. It is hoped that this study increases the understanding of the problems involved and provides a strategy to compute geoidal heights.

2 HEIGHT SYSTEMS

The *Oxford English Dictionary* defines height as "measure from base to top; elevation above ground or other (esp. sea) level." A more formal definition is given by Mueller and Rockie (1966) as "the distance between a surface (usually an equipotential surface) through the point in question and a reference surface, measured along a line of force or along its tangent."

When talking of the height of a point it is implicit with the figure quoted that the height is referred to a particular height system. A number of different height systems exist which differentiate measuring techniques and concepts. Some of these height systems can be considered "natural" and are based on physical mensuration. Therefore the natural height systems will incorporate measured gravity and be referred to the geoid. They have the inherent attribute of being able to show in which direction water will flow.

Other height systems can be considered "artificial" in that they have evolved as a mathematical approximation of the real earth to simplify calculations on an otherwise very complex shaped earth. Therefore the height in an artificial height system will refer to an ellipsoid closely approximating the geoid or incorporating normal gravity found by definition.

The difference in heights between height systems may not be numerically very large, as an ellipsoid of best fit to the geoid approximates the earth's surface within 0.03%. However, conceptually, they are different.

We must understand the different height systems to appreciate their strengths and weaknesses. This is particularly important at present when an increasing number of advocates are proposing we change from gravity inferred heights to earth-fixed geocentric heights because of the advent of satellite positioning systems (Schodlbauer, 1986).

It is also important we understand the concepts behind the Australian Height Datum (AHD) and the history of its evolution before we can

integrate heights from the Global Positioning System (GPS) into the AHD. Thus the first step in this treatise is to review the various concepts of height and definitions that are in use.

2.1 Geopotential Numbers.

An equipotential level surface (see Vanicek and Krakiwsky, 1986; Heiskanen and Moritz, 1967) can be considered to be a level surface at which the gravity potential anywhere on that surface will be constant and is normal to the direction of gravity everywhere. The gravity field of a point P on that surface will represent the gravity force ($\vec{g}$) of the equipotential surface whilst the gravity geopotential of the point P is the amount of work needed to overcome the force of gravity to remain stationary.

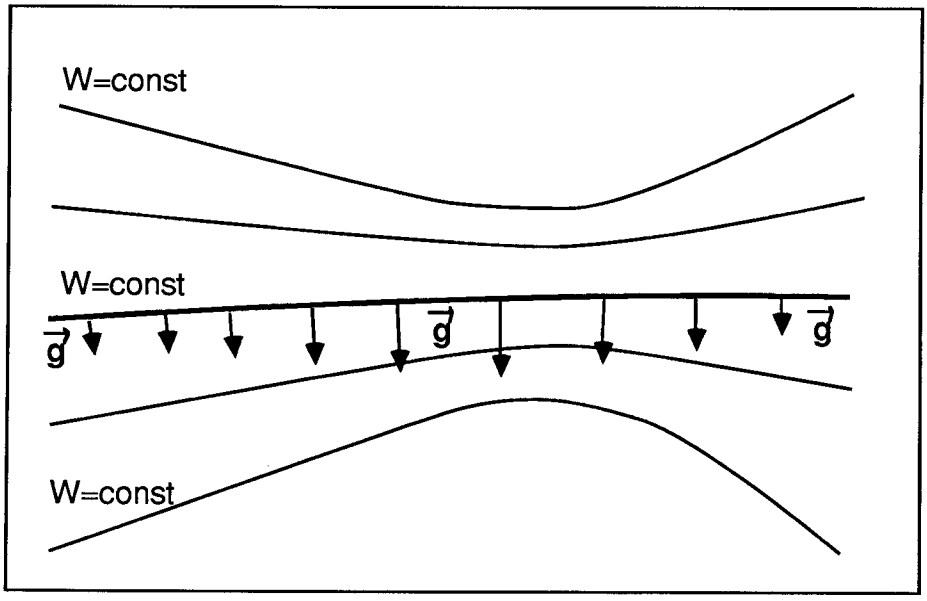

Figure 2.1 Gravity on an equipotential surface

There are an infinite number of equipotential or geopotential surfaces, each one unique and separate. The geopotential surfaces are not parallel to each other because they converge towards the poles due to the earth's oblateness in the global case and can converge or diverge due to mass irregularities inside the earth in the regional case.

However only one geopotential surface passes through any point and, there is only one value of potential (W_p) associated with each point. Therefore the geopotential represents one possible way of defining a unique height as a negative potential difference relative to a datum geopotential surface, usually the geoid, denoted W_0.

For a levelled point (P) on the earth's surface relative to the corresponding point on the geoid, the geopotential number (C) is given by (Heiskanen and Moritz, 1967, p. 162),

$$\begin{aligned} C &= W_0 - W_p \\ &= -\int_0^P dW \\ &= \int_0^P g\,.dh \end{aligned} \qquad (2.1)$$

As a potential difference, the geopotential number is said to be "route independent", that is the sum of the increments in height (dh) determined by perfect levelling will always be zero, no matter which route is used to find the total height difference. Mathematically, route independence can be shown as,

$$\oint dh = misclosure = 0$$

The geopotential number, C, is measured in geopotential units (gpu), where

1 gpu = 1 kGal metre, and since

$g \approx 0.98$ kGal

$$\begin{aligned} C &\approx g\,.H \\ &\approx 0.98\,H \end{aligned} \qquad (2.2)$$

The geopotential number is not expressed in length units, but kilogal metres (kGal m) the difference being approximately 2%.

The calculation of geopotential numbers, in practice, does not require a knowledge of the value of gravity at each bench mark, but may be interpolated with sufficient accuracy from surrounding values of gravity points providing the spacing is 2-3 km in flat country and every 1 km in high, mountainous country (Angus-Leppan, 1982).

2.2 Dynamic Heights.

To eliminate the "fault" of geopotential numbers not being expressed in length units (i.e. height in metres), dynamic heights (H^D) have been introduced. The dynamic height is found by scaling the geopotential number by a constant reference gravity g_R, i.e.,

$$H^D = \frac{1}{g_R} \int_0^P g.dh$$

$$= \frac{C}{\gamma_\phi} \qquad (2.3)$$

The reference gravity is usually the normal gravity associated with the mean reference ellipsoid at a reference geographic latitude (γ_ϕ). The normal gravity at sea level for latitude 45° is commonly used in Europe, whilst a convenient reference latitude can be chosen to suit the area of interest. This can be viewed as the scale factor needed to convert the geopotential number in units of potential to units of height in metres.

The normal gravity is calculated by an analytic function defined by the International Association of Geodesy (IAG). The first attempt to define the normal gravity field was proposed by Bowie and Avers (1914) as,

$$\gamma_0 = 980.624\,(1 - 0.002\,644\cos 2\phi + 0.000\,007\cos^2 2\phi) \quad Gal \qquad (2.4)$$

As can been seen it is a function of latitude (ϕ) only. A more accurate normal gravity formula was adopted by the IAG General Assembly in Stockholm in 1930 and became known as the *International Gravity Formula 1930.* It is,

$$\gamma_0 = 978.0490\,(1 + 0.005\,288\,4\sin^2\phi - 0.000\,005\,9\sin^2 2\phi) \quad Gal \qquad (2.5)$$

A third normal gravity formula was adopted by the IAG and became known as the *International Gravity Formula 1967*. It was considered to have a maximum error of 4 μGal.

$$\gamma_0 = 978.031\,85\,(1 + 0.005\,278\,895\,\sin^2\phi + 0.000\,023\,462\,\sin^4\phi) \quad Gal \tag{2.6}$$

This formula was replaced by the meeting of the IAG General Assembly meeting in Canberra by the *International Gravity Formula 1980* which is the latest. This formula has a maximum error of 0.7 μ*Gal.*

$$\gamma_0 = 978.032\,7\,(1 + 0.005\,279\,041\,4\,\sin^2\phi + 0.000\,002\,327\,18\,\sin^4\phi + 0.000\,000\,126\,2\,\sin^6\phi) \quad Gal \tag{2.7}$$

The dynamic height of a point will not be the correct geometrical height above the geoid, except at the reference latitude of the normal gravity. However all points on the same geopotential surface will have the same dynamic height.

2.3 Orthometric Heights.

Another system in common usage is the Orthometric Height (H^0). The orthometric height of a point P is the geometric distance between the geoid and a point on the earth's surface, measured along the curved plumbline of P. The units of orthometric height are metres.

The equation for orthometric height is

$$H^0 = \frac{1}{\bar{g}} \int_0^P g\,.dh$$

$$= \frac{C}{\bar{g}} \tag{2.8}$$

where $\bar{g}$ is the mean gravity on the plumbline between the geoid and P on the earth's surface. This cannot be measured practically as it lies inside the earth, and so some assumptions as to the density of matter within the earth have to be made.

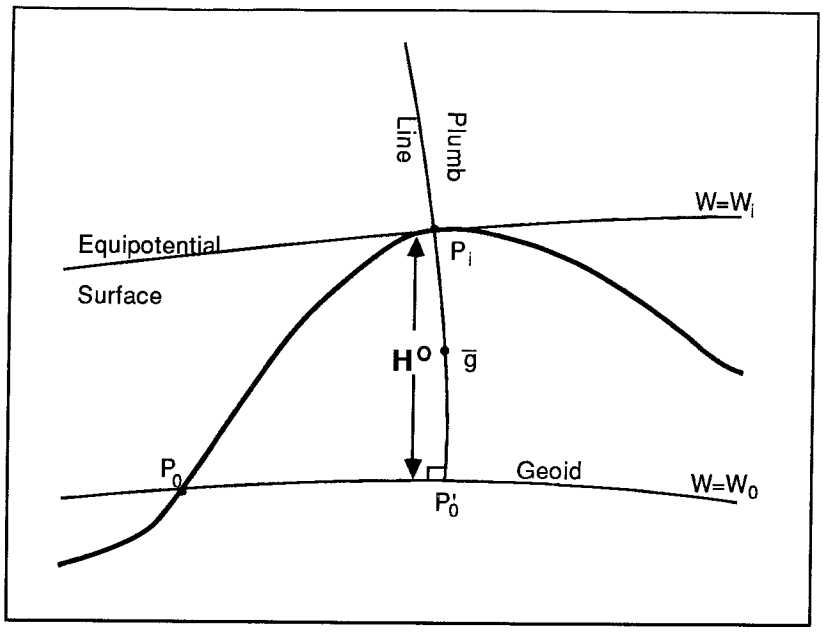

Figure 2.2 Orthometric height.

However, there are some methods to approximate $\bar{g}$, which will lead to a special kind of orthometric height.

If the normal gravity (γ) is used to calculate the mean normal gravity ($\bar{\gamma}$) from (2.8) instead of the mean gravity ($\bar{g}$), the height system is called *Normal Orthometric height* (Bomford, 1971, p. 230)

$$H^{NO} = \frac{C}{\bar{\gamma}} \tag{2.9}$$

Another method proposed by Helmert is called the *Helmert Orthometric height* (H^H) and takes the form

$$H^H = \frac{C}{g^H} \tag{2.10}$$

where $g^H = g + 0.0424\ H$.

and g is the gravity, in Gal, observed on the earth's surface. H is the height of the mid-point, in km, between the geoid and the earth's surface. The numerical coefficient follows directly from the use of the simple Prey

gravity gradient for terrain with an infinite Bouger plate of constant density (Vanicek and Krakiwsky, 1986, p. 371; Heiskanen and Moritz, 1967, p. 167).

It is evident that the orthometric height is closely associated with the geopotential number. However two points with the same orthometric height may not necessarily lie on the same geopotential surface, especially at high altitudes because of the uncertainty of the earth's density and hence the value of the mean gravity on the plumbline. The heights will be equal at sea level (i.e. on the geoid).

2.3.1 Orthometric Correction.

Heights are usually determined by observing successive height increments (dh) using a level and staff. However, as has already been mentioned, summing the observed height increments around a loop will not necessarily sum to zero. Therefore an orthometric correction can be applied to levelled height increments to convert them to orthometric height differences

$$\Delta H^0_{AB} = dh^{meas}_{AB} + OC_{AB} \tag{2.11}$$

where OC = orthometric correction between points A and B on the earth's surface and is given by Heiskanen and Moritz, (1967, p. 168),

$$OC_{AB} = \int_A^B \frac{g-\gamma_\phi}{\gamma_\phi}.dh \quad + \quad \int_0^A \frac{g-\gamma_\phi}{\gamma_\phi}.dH_A \quad - \quad \int_0^B \frac{g-\gamma_\phi}{\gamma_\phi}.dH_B \tag{2.12}$$

$$OC_{AB} = \sum_A^B \frac{g-\gamma_\phi}{\gamma_\phi}.dh \quad + \quad \frac{\overline{g}_A-\gamma_\phi}{\gamma_\phi}.H_A \quad - \quad \frac{\overline{g}_B-\gamma_\phi}{\gamma_\phi}.H_B \tag{2.13}$$

where $(\overline{g}_A)$ and $(\overline{g}_B)$ is the mean value of gravity along the plumbline at point A and B on the earth's surface and the geoid, and γ_ϕ is the normal gravity at a reference latitude.

Once again, a knowledge of the mean value of gravity on the plumbline is required. However an error analysis shows that for a point in the Swiss Alps with an altitude of 2504 metres, an error in the mean value of gravity

on the plumbline $\delta\bar{g}$ of 1 mGal will correspond to an error in the height of 3mm. An error in the value of the density of matter ($\delta\rho$) inside the earth for the point in the Alps between the surface and the geoid of 0.1 gcm^{-3} results in an error in the mean gravity of 10.5 mGal. This causes an error in the height of 10 mm (ibid, p 169).

The mean terrain height in Australia is approximately 500 metres, with few places attaining a height of that used in the example above. Therefore the errors caused by an inexact knowledge of the density inside the earth or of the mean gravity value on the plumbline will be small. The orthometric heights can be found with a high accuracy by applying an orthometric correction using these simple models.

2.4 Normal Heights.

In 1954 Molodenski proposed a new system of height which obviated the need for a knowledge of the value of gravity between the earth's surface and the geoid. Normal heights (H^N) would equal orthometric heights if the geoid coincided with the reference ellipsoid, and if the gravity was normal. While the orthometric height system uses the mean value of gravity along the plumbline between the geoid and the earth's surface, normal heights use mean normal gravity along the normal of the reference ellipsoid between the reference ellipsoid and the telluroid. (The telluroid being a point below the earth's surface along the normal plumbline from the reference ellipsoid at which the spheropotential is equal to the geopotential of a point on the surface.) See Heiskanen and Moritz, (1967, p. 292) and Vanicek and Krakiwsky, (1986, p. 372) for a detailed discussion.

The equation for normal height is written,

$$C = \int_0^P g\,.dh$$

$$H^N = \frac{C}{\bar{\bar{\gamma}}} \tag{2.14}$$

where $\bar{\gamma}$ is the mean normal gravity between the reference ellipsoid and the telluroid.

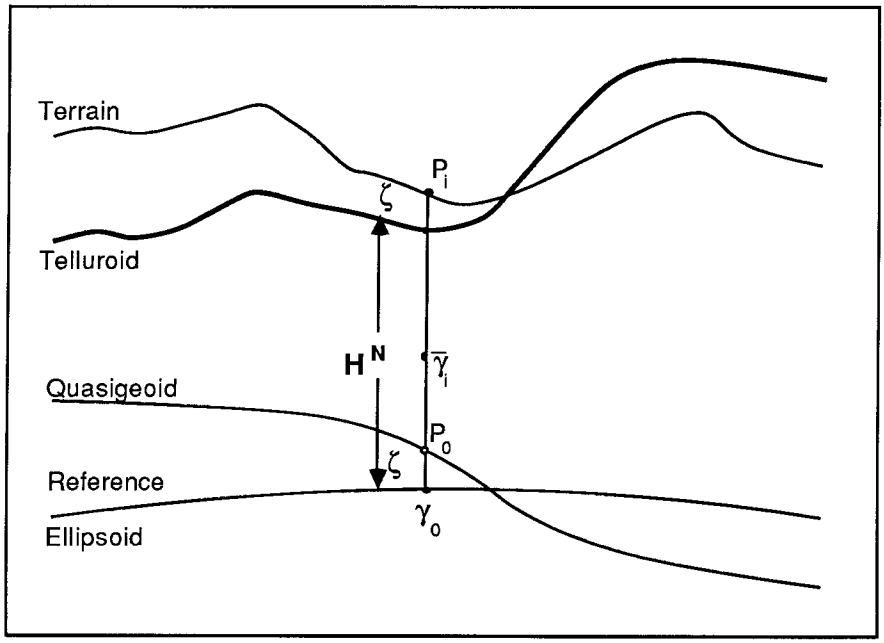

Figure 2.3 Normal height.

A simpler method of determining the mean normal gravity $\bar{\gamma}$ was proposed by Vignal in which the mean normal gravity was evaluated by applying a vertical gravity gradient to the normal gravity at the reference ellipsoid. The gravity gradient he chose was the free-air gravity gradient (Vanicek and Krakiwsky, 1986, p. 373).

$$H^V = \frac{C}{\gamma_0 - 0.1543H} \tag{2.15}$$

The normal and Vignal heights are numerically quite close. Vignal heights have been adopted for the unification of the European levelling networks, while normal heights are used extensively in the USSR and the east European countries (ibid). Both height systems are probably less appropriate today, however, because of the density of observed gravity stations in developed countries and the availability of low cost, accurate and portable gravimeters.

2.5 Ellipsoidal Heights.

The ellipsoidal height (h) of a point P on the earth's surface can be defined as the linear distance of that point above or below the reference ellipsoid measured along the normal of that ellipsoid. The heights are unique to the reference ellipsoid, being directly related to the defining parameters and orientation of the ellipsoid. The reference ellipsoid may be geocentric with it's centre coinciding with the centre of mass of the earth and the axes coincident with the poles and equator or the reference ellipsoid may be locally defined, such as the Australian National Spheroid[1] (ANS) to give a "best fit" to a region. Figure 2.4 shows ellipsoidal heights h_1 and h_2 for a point P on the earth's surface with respect to different geocentric ellipsoids E_1 and E_2.

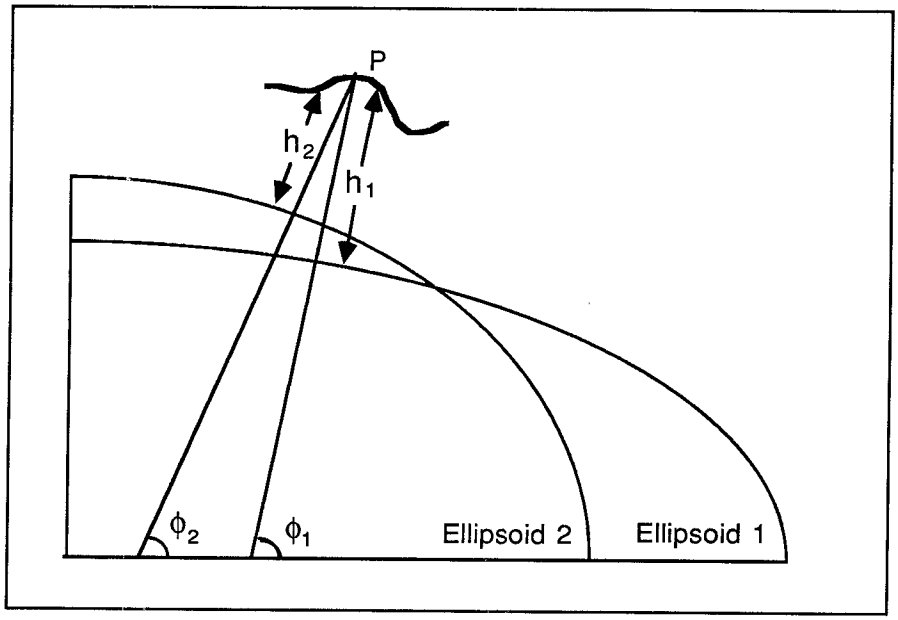

Figure 2.4 Different ellipsoid heights h_1 and h_2.

Ellipsoidal heights have no relation with the actual or model gravity field of the earth. Therefore they are purely geometrical in concept and are unable to tell in which direction water will flow.

1 The terms ellipsoid and spheroid are often used synonymously. However the literal meaning of spheroid is a sphere-like body rather than a biaxial ellipsoid.

The height differences obtained from GPS baseline observations will be ellipsoidal heights referenced in the same ellipsoidal coordinate system as the satellites are in, currently World Geodetic System 1984 (WGS84). However, the GPS heights cannot strictly be considered to be WGS84 ellipsoidal heights because of

* errors in coordinates of the satellite tracking stations defining the satellite datum,

* errors in the absolute heights, usually found by pseudo-range observations, of the GPS stations (see origin error, Section 4.3).

The ellipsoidal height, referred to the ellipsoid of the geodetic reference system (the ANS in Australia), between two points on the earth's surface can be found by vertical angle observations between the stations and a knowledge of the components of the deflection of the vertical in the direction of the line (Heiskanen and Moritz, 1967, p. 173). Alternatively, ellipsoidal heights in the satellite system can be transformed into heights in the geodetic reference system if the transformation parameters are known (Eckels, 1987, p. 140).

2.6 In Which Height System is the AHD?

We have now examined all the major height systems and it can be seen that they differ in only how they scale the geopotential number. The geopotential number is of more interest to the scientific community because it uniquely defines an equipotential surface. However, its units of kGal m means that it is not a height in a geometrical sense.

The dynamic height has at least the dimension of height, but no geometrical meaning. One advantage is that points on the same level surface have the same dynamic height. The dynamic correction for points with a large separation in latitude from the reference latitude, at which the normal gravity is calculated, will be very large.

"Orthometric heights are the natural heights above sea level, that is, heights above the geoid. They thus have an unequalled geometrical and physical significance" (Heiskanen and Moritz, 1967, p. 172). The computation is relatively laborious and requires a knowledge of the gravity gradient inside the earth between the geoid and the surface unless the simpler Helmert orthometric height is used.

"The physical and geometrical meaning of the normal heights is less obvious; they depend on the reference ellipsoid used. They have a somewhat artificial character as compared to orthometric heights, but are easy to compute rigorously" (ibid).

The Australian Height Datum corrects measured height differences by applying an orthometric correction (OC) as in (2.11). However the orthometric correction does not depend upon a knowledge of the mean value of gravity along the plumbline as in (2.12) and (2.13). The orthometric correction is found by the expression (Rapp, 1961)

$$OC = (A.H + B.H^2 + C.H^3)\,\delta\phi \tag{2.16}$$

where H = mean height of the two end points of the section
$\delta\phi$ = difference in latitude of the end points
A, B and C are coefficients varying with latitude.

However, the C term was considered to be negligible under Australian conditions and so (2.16) was reduced to (Roelse et al, 1975)

$$OC = (A.H + B.H^2)\,\delta\phi \tag{2.17}$$

and the values of A and B were defined as (Rapp, 1961)

$$A = 2\sin 2\phi\,\alpha'\left(1+\cos 2\phi\left(\alpha' - \frac{2\kappa}{\alpha'}\right) - 3\kappa\cos^2\phi\right).Q \tag{2.18}$$

$$B = 2\sin 2\phi\alpha' t_2\left(t_3 + \frac{t_4}{2\alpha'} + \cos 2\phi\left(\frac{3}{2}t_4 + 2\alpha' t_3 - \frac{2\kappa t_3}{\alpha'}\right)\right).Q \tag{2.19}$$

where; Q = value of 1' of arc in radians = 0.000290888209

$$\alpha' = \frac{\beta}{2+\beta+2\varepsilon}$$

$$\kappa = \frac{-2\varepsilon}{2+\beta+2\varepsilon}$$

$$t_2 = \frac{2(1+\alpha+c')}{a(1+\frac{\beta}{2}+\varepsilon)}$$

$$t_3 = 1 - \frac{(3\alpha - 2.5c')}{2}$$

$$t_4 = 1 - t_3$$

and parameters a, α, β, ε, c' are defined or derived constants on the Geodetic Reference System 1967 (GRS67) with,

a = semi-major axis = 6378160
α = flattening = $(298.247167427)^{-1}$
β = gravity constant = 0.005278895
ε = gravity constant = 0.000023462
c' = constant = 0.00344980143430

Heights in the Australian Height Datum are popularly thought of as being orthometric heights. However it is obvious from the foregoing definition that the orthometric correction does not include any measured gravity either on the earth's surface or reduced to a mean gravity on the plumbline between the surface and the geoid. This is contrary to the fundamental definition of orthometric heights and so it can be concluded that the AHD is not an orthometric height system.

That the orthometric correction is dependent upon normal gravity referred to the GRS 67 ellipsoid at a mean height H suggests that the criteria of (2.9) is satisfied and that heights in the AHD should be correctly referred to as normal orthometric heights. However, even though orthometric heights and normal orthometric heights are conceptually quite different they are numerically very similar (see Section 3.2).

3 THE AUSTRALIAN HEIGHT DATUM

Before 1972 Australia had a multitude of levelling datums, each of which was adopted by a government utility to suit its own particular need in a region. The levelling datums were usually based upon a local tide gauge and used for engineering projects or the determination of waterbound cadastral boundaries. Blume (1975) records the existence of five such datums in Sydney in the 1800's with different datums again, in Newcastle and Wollongong. The existence of many levelling datums caused much confusion and loss of accuracy for surveyors at the time. Figure 3.1 shows some of the levelling datums that have been used in Sydney based upon the tide gauge at Fort Denison.

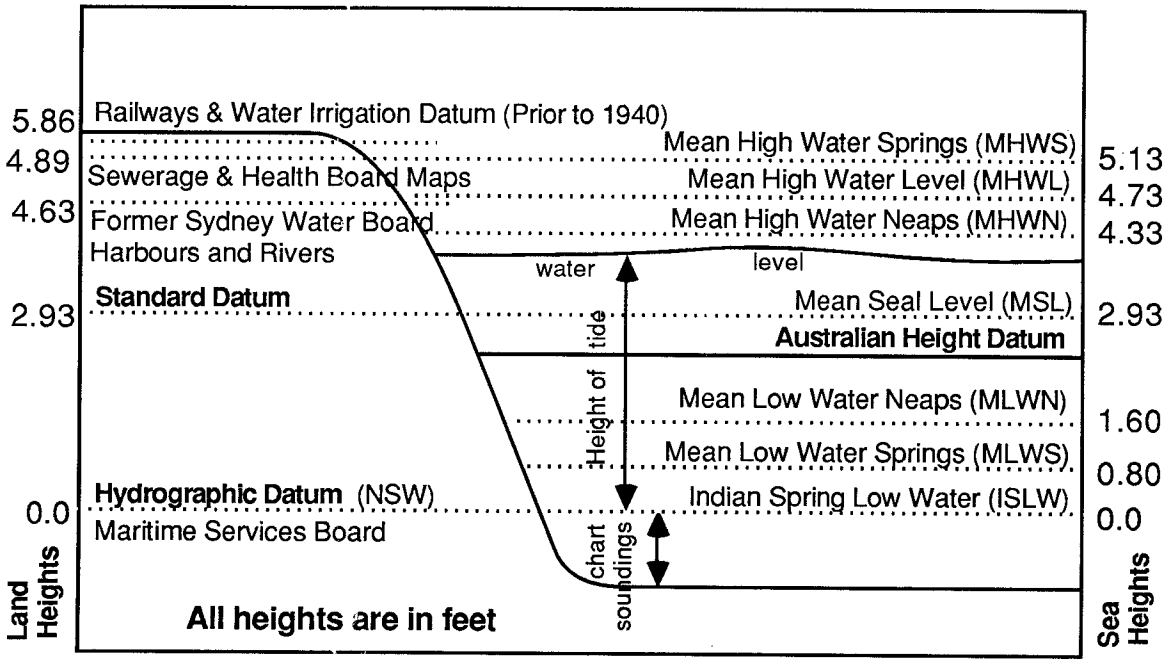

Figure 3.1 Levelling datums that have been used in Sydney.

In 1972 the National Mapping Council of Australia adopted the Australian Height Datum as the primary national levelling datum over mainland Australia. The simultaneous adjustment of 97,320 km of primary levelling observed between 1945 and 1970 was "fixed" at a mean sea level height of 0.000 metres to 30 tide gauge stations around the Australian coastline to form a single homogeneous levelling network (Roelse et al,

1975; Granger, 1972). It is the adjusted heights of 497 junction points forming 261 independent loops that define the Australian Height Datum to which all vertical control for mapping is to be referred.

Concurrent with the fixed adjustment, a "free" adjustment of the levelling network was performed holding the Johnston Geodetic Station in the centre of Australia to an arbitrary height. A comparison of the fixed and free adjustments by Roelse et al (1975, Annex D) shows the strain put on the mathematical model of the land-based levelling by the introduction of the height constraints of the 30 tide gauges. It is particularly evident that a north-south gradient in the difference contours exists with the worst case of 1.7 metres being up the north Queensland coast to Cape York.

The discrepancies between heights from geodetic levelling and the heights on tide gauges has become known as the "sea slope problem" and is of particular concern to potential users of GPS as a heighting tool because the reference surface of the AHD, mean sea level, is **not coincident** with the geoid.

An evaluation of the sea slope problem requires an investigation into the sources and magnitude of the errors in the three basic measurements;

1) the levelled height differences between tide gauges,

2) the determination of local mean sea level at the tide gauges, and

3) the sterically determined height differences between tide gauges.

The problem is further compounded in that geodetic levelling is "time consumptive" and that "various discrepancies are due chiefly to intrasurvey movement," particularly in tectonically active areas such as the Pacific coast of the United States, with "resultant distortion of geodetically defined height differences between tide stations" (Castle and Elliot, 1982).

3.1 Errors in the Australian Levelling Network.

Apart from some first order levelling in eastern New South Wales, parts of Victoria and south and east of Perth in Western Australia, most of

the levelling in the Australian levelling network was observed to third order standard, where the orders of tolerances refer to the agreement between a forward and backward level run. These tolerances are prescribed in the specifications for levelling by the National Mapping Council of Australia, (1970) as,

First Order $4\sqrt{k}$ mm.

Second Order $8.4\sqrt{k}$ mm.

Third Order $12\sqrt{k}$ mm.

where k is the distance levelled in kilometres.

These orders were used to weight the *a priori* variance factor s^2 in the adjustment according to the ratio (Roelse et al, 1975, p. 76),

$g_1 = 9\ s^2/D$ for first order levelling,

$g_2 = 2\ s^2/D$ for second order levelling,

$g_3 = 1\ s^2/D$ for third order levelling,

where g_1, g_2 and g_3 were the weights used and D is the distance levelled in miles.

A variance factor (s^2) of 0.001256 (imperial units) was adopted giving a precision of the adjusted levelling (1σ) of $8.1\sqrt{k}$ mm. The estimate of the precision of relative height differences in the adjustment between the centre of Australia and the coastline is given by Granger (1972) and Roelse et al (1975) as 0.34 metres. This figure agrees closely with the global empirical formula developed by NASA to find the standard deviation in the height H as it propagates over distance S kilometres (Vanicek and Krakiwsky, 1986, p. 99),

$$\sigma_H = 0.0018\, S^{\frac{2}{3}} \quad metres \tag{3.1}$$

Substituting in the above equation a distance S=3000 km approximately equal to the distance from the centre of Australia to the coastline, σ_H = 0.37 metres. However these figures are an estimate of the internal precision of the modelled parameters only and do not account for any unmodelled external errors.

The unmodelled errors in levelling, as with all survey measurements, can be classified as being gross, systematic or random errors. Gross errors should be easily detected and eliminated by the use of self checking procedures for all observations and reductions. However, compensating gross errors (that is, two errors of approximately the same magnitude and of opposite sign) within the same loop can remain undetected.

Rush (1986) reports the detection of a number of compensating errors, one of them being 0.4 metre in a project in central Queensland caused by three transcription errors from analysis sheet to printout. In 1975 the Department of National Mapping reobserved the same level lines along the north Queensland coast as in the 1971 adjustment. The new levelling found differences with the original levelling of 0.727 metre between Rockhampton and Mackay and 0.539 metre between Mackay and Townsville, but had little effect on the closes of the network loops when the new levelling was incorporated (Department of National Mapping internal report, undated). There must remain other undetected gross errors within the Australian levelling network, degrading the AHD, which may be caused in part to the haste in which the original levelling was done.

The origins of systematic errors in levelling are well known and detailed in Prijanto (1987), Jeremy (1973) and Cumerford (1987). They may be categorised as instrumental errors, environmental or personal error.

Instrumental errors such as compensator error in an automatic level, misalignment of the plate in a parallel plate micrometer, collimation error and staff calibration error can be minimised or even eliminated by adherence to correct levelling procedures. Similarly for environmental errors such as the earth's curvature or refraction effects can be minimised by observing equal backsights and foresights, although a residual refraction effect may occur depending upon the terrain slope, vegetation or meteorological conditions.

The effect of the use of normal gravity instead of observed gravity in the orthometric correction (see Section 2) to the measured height differences has been investigated by Mitchell (1973, p. 56) over the Australian continent and found to be negligible. He found the difference to be 1.1 cm north-south and 1.9 cm east-west across the continent.

The presence of an hitherto undetected systematic error or non-adherence to correct levelling procedures of the magnitude of 0.07 mm in observed height for each levelling set-up, assuming a staff separation of 100 metres, will result in differences in height of 2 metres over a distance equal to that as along the north Queensland coastline (Mitchell, 1973, p. 205). This systematic error, if present, would remain undetected until level connections are made to tide gauge stations or the lines observed with GPS.

3.2 Tide Gauges, MSL and the Geoid.

The adjustment of the Australian levelling network was constrained to fit mean sea level by level connections to 30 tide gauge stations around the Australian coastline from records over three years, 1966-68, of simultaneous data. This was based on the premiss that the surface of the oceans at rest, mean sea level, is coincident with the geoid.

However the oceans are not homogeneous and not in hydrostatic equilibrium and therefore the ocean surface will depart from the geoid by an amount equal to the sea surface topography (SST). Also, the tide gauges themselves are subject to errors in their readings due to their supports sinking or being sited in estuaries with the water level not being representative of mean sea level (see Wyndham tide gauge; Roelse et al, 1975, p. 26).

There are a number of physical phenomena that can influence the local height of mean sea level at a tide gauge station. These include

* changes in sea level due to variations in water density of the ocean. This can be caused by a change in gravity due to uplift or subsidence or changes in water temperature, salinity and air pressure.

* changes in sea level due to wind effects. Wind effect has three components; wind stress caused by the friction of moving air on the water surface, wind pile-up results in water moved by the wind being piled against a coastline, and storm surges.

* apparent changes in sea level due to local changes to the gauge station if sited in a harbour or estuary, such as a change in the topography of the sea floor caused by dredging operations or silting or changes to the amount of fresh water inflow during periods of drought or high rainfall.

* changes in sea level due to "tsunamis" or tidal waves.

* changes in sea level due to secular changes such as a rise or fall in the land level due to tectonic movements or post-glacial uplift, or changes in the volume of sea water as a result of evaporation, precipitation or melting of the polar ice caps.

* changes in sea level due to long term periodic astronomic effects such as the semi-annual tide (period of 182.6211 days), the solar annual tide (period of 365.2422 days), the pole tide (period of 428 days) and the nodal tide (period of 18.6 years).

"A one year measurement interval is the shortest period that could be conveniently chosen as a basis for the calculation of local sea level" as "shorter periods would introduce a seasonal bias for the calculation of local mean sea level" (Castle and Elliot, 1982, p. 6991). Mitchell (1973, p. 168) concludes that the nodal tide has a range in magnitude of between 1 mm and 32 mm and that differences in mean sea level calculated from 5 years of tide data than from 19 years of tide data is negligible.

Castle and Elliot (1982, p. 6995) suggest that the discrepancies between the height of the tide gauge stations and the geodetic levelling, particularly up the north Queensland coast, is due to the quality of the levelling and that the length of some of the network loops, up to 3000 km, may contain large errors whilst still satisfying the rejection criteria.

4 THE GLOBAL POSITIONING SYSTEM

That the Global Positioning System has already had an enormous impact on the surveying, navigation and geodetic communities is evident from the amount of interest expressed by current users. Research into processing software, equipment design and evaluation and field testing to find optimal methods and new applications is happening at a frenetic pace. However, I believe this is only the tip of the iceberg and that in the future the impact of GPS will be even greater. Receiver costs are dropping as the receivers are getting physically smaller and more sophisticated so that even more position related problems can be solved with GPS.

Looking at the evolution of satellite positioning systems, we can trace the first attempt at positioning on the earth's surface by measurements to an artificial orbiting satellite to SPUTNIK I which was launched on 4th October, 1957.

Some of the other systems developed since then have included photographing satellites against the star background, satellite laser ranging (SLR) to the satellite LAGEOS and the US Army's SECOR (sequential collation of range) system. These systems have generally been replaced by the next generation of satellite positioning system because of the cost of receivers, their portability, complexity of the computations involved or the accuracies obtained.

The TRANSIT system, in 1967, became the first commercially available satellite positioning system that could be used by non-government agencies. A detailed description of TRANSIT positioning can be found in Hoar (1982) and Eckels (1987), but a brief comparison with GPS is relevant.

The TRANSIT system consists of six satellites in polar orbits at an approximate altitude of 1100 kilometres with one complete orbit taking 107 minutes. An observer has to wait 1 to $1^1/_2$ hours between each satellite pass, with many passes required to obtain an accurate geodetic position. Typically this can take approximately two days, compared to a GPS observation period of about 1 hour.

The relatively low altitude of the orbiting satellites in the TRANSIT system, compared to the the 20,200 km orbits of the GPS satellites, makes it difficult to model and then predict future orbits because the perturbing effect of the gravity field is greater close to Earth and not as well known. The atmospheric drag is also much greater at the lower altitude. Therefore the broadcast ephemerides, which is the "extrapolated" position of the satellite using prior tracking data and an orbit model, will reflect these errors. The user can use the precise ephemerides, which is the "interpolated" position of the satellite from tracking data concurrent with the observing session. However, there will inevitably be a delay in the dissemination of the precise ephemerides or it may even be restricted to military users only.

The advantages of GPS over other systems make it the preferred satellite positioning system of the surveying, navigation and geodetic communities for the remainder of this century and into the next. That the full constellation of GPS satellites will not be launched and in place until 1991-92 (see Table 4.1) has prompted the US Department of Defence (DoD) to announce that the TRANSIT system will be supported until 1995, after which it will be phased out.

There are a number of other satellite positioning systems proposed or already in operation which may or may not affect the future use of GPS. The Russian Global Navigation Satellite System (GLONASS) first launched on 12th October 1982, is very similar to the GPS system. It is intended to be available to the military of the USSR only. Despite this, it has been reported by Klass (1987) that it is possible to design a single receiver capable of using both GLONASS and NAVSTAR GPS signals for civil users who are reluctant to depend solely on a single system operated by the military establishments of the two superpowers.

The European Space Agency (ESA) is exploring the possibilities of NAVSAT, a civilian targeted system involving continuous two way communications between ground control stations, the satellites and ground receivers. There would be 6 geostationary satellites in an equatorial orbit and up to another 12 in highly elliptical orbits to provide world wide coverage. There are, however, no firm deployment plans yet.

SAT #	GPS #	CARRIER	DATE
1	13	MLV[1]	OCT 1988
2	14	MLV	JAN 1989
3	16	MLV	APR
4	17	MLV	JUN
5	18	MLV	JUL
6	19	MLV	SEP
7	20	MLV	OCT
8	21	MLV	JAN 1990
9	15	MLV	MAR
10	22	MLV	JUN
11	23	MLV	AUG
12	24	MLV	SEP
13	25	MLV	NOV
14	26	MLV	JAN 1991
15	27	MLV	MAR
16	28	MLV	APR
17	29	MLV	JUN
18	30	PAM-DII[2]	AUG
19	31	MLV	OCT
20	32	MLV	JAN 1992
21	33	MLV	APR
22	34	PAM-DII	JUL
23	35	MLV	OCT
24	36	MLV	JAN 1993
25	37	MLV	APR
26	38	MLV	JUL
27	39	MLV	JAN 1994
28	40	MLV	JUL

Table 4.1 Proposed GPS launch schedule of Block II satellites. (GPS Bulletin, 1988)

Another system proposed by commercial interests in the United States is the STARFIX described by Dennis (1986). It will be a user pays system utilizing differential pseudo-range measurements to three geosynchronous satellites giving initial coverage of the US continent which could be extended later on.

4.1 GPS System Description.

The Navigation Satellite Timing and Ranging Global Positioning System (NAVSTAR/GPS) was introduced with the launching of the first satellite on the 2nd February 1978. It has been described by Wooden (1985) as a "space based radio positioning, navigation and time transfer system"

1 MLV = Multiple Launch Vehicle (Delta II rocket).
2 PAM = Payload Assist Module (Shuttle)

which provides "highly accurate three dimensional position and velocity information along with Coordinated Universal Time (UTC) to an unlimited number of suitably equipped users under all weather conditions, continuously, anywhere on or near the surface of the Earth."

The system was designed and financed by the US Department of Defence to satisfy their requirements for a positioning system that it

* is capable of 50 metre point positioning accuracy in real time anywhere in the world,
* can determine the velocity vector of a vehicle and work in a high kinematic situation,
* is independent of weather conditions,
* uses compact, inexpensive receivers,
* is not jammable by the enemy,
* can combine military and civilian use in one system.

It has never been the intention of the U.S. DoD to develop GPS to satisfy the needs of the surveying and geodetic communities. Nevertheless, they have been able to develop techniques for high precision applications that are essentially outside the initial intention of the system.

The GPS system will, in its final configuration consist of a satellite constellation with 18 satellites in 6 orbital planes with an inclination of 55° plus 3 spares. This means there will be 3 satellites in each orbital plane and will be spaced 120° apart. The satellites will orbit the earth at an approximate altitude of 20,200 km taking 12 hours to complete one orbit. There will be between 4 and 7 satellites "visible" above the horizon at any instant with a pass lasting up to 5 hours. Table 4.2 shows the planned positions of the 18 satellites in their GPS orbits expressed in Keplerian elements.

Each satellite transmits a unique signal on two L-band frequencies which are exact multiples of the satellite's fundamental frequency of 10.23 MHz, kept by the onboard oscillator. The L1 frequency of 1575.42 MHz is a carrier onto which a C/A (Coarse Acquisition) Code of 1.023 MHz and a P (Precise) Code of 10.23 MHz are modulated. The L2 frequency of 1227.60

MHz is a carrier for the P-Code only, and depending on future US government policy may be restricted to military use only by encrypting the signal (see Scherrer, 1985).

Sat. No.	a (m)	e	ω (deg)	i (deg)	Ω (deg)	M (deg)
1	26 560 001.0	0.003	0.0	55.0	0	0
2	26 560 002.0	0.003	0.0	55.0	0	120
3	26 560 003.0	0.003	0.0	55.0	0	240
4	26 560 004.0	0.003	0.0	55.0	60	40
5	26 560 005.0	0.003	0.0	55.0	60	160
6	26 560 006.0	0.003	0.0	55.0	60	280
7	26 560 007.0	0.003	0.0	55.0	120	80
8	26 560 008.0	0.003	0.0	55.0	120	200
9	26 560 009.0	0.003	0.0	55.0	120	320
10	26 560 010.0	0.003	0.0	55.0	180	120
11	26 560 011.0	0.003	0.0	55.0	180	240
12	26 560 012.0	0.003	0.0	55.0	180	0
13	26 560 013.0	0.003	0.0	55.0	240	160
14	26 560 014.0	0.003	0.0	55.0	240	280
15	26 560 015.0	0.003	0.0	55.0	240	40
16	26 560 016.0	0.003	0.0	55.0	300	200
17	26 560 017.0	0.003	0.0	55.0	300	320
18	26 560 018.0	0.003	0.0	55.0	300	80

Table 4.2 Future GPS 18 satellite constellation.
(Nakiboglu et al, 1985)

where; a is the semi-major axis of orbit.
e is the eccentricity of orbit.
ω is the argument of perigee.
i is the angle of inclination between the orbital and equatorial planes.
Ω is the right ascension of the ascending node.
M is the Mean Anomaly, the position of the satellite in the orbital plane.

The wavelengths of the C/A and P code on the L-band frequencies are found by the relation,

$$\lambda = \frac{c}{f} \tag{4.1}$$

where; λ = carrier wavelength in metres
c = speed of light in a vacuum (299,792,458.0 $msec^{-1}$)
f = code or carrier frequency in hertz.

These frequencies are equivalent to nominal wavelengths of 19 cm and 24 cm for the L1 and L2 carrier signal compared to 29.3 metres and 293 metres for the P code and C/A code. They are nominal because the signal is retarded or "delayed" as it travels through the atmosphere and also the doppler effect on the carrier frequency due to the relative motion of the satellite with respect to the receiver. The wavelengths are therefore inexact.

GPS receivers use a number of different techniques to record the transmitted satellite signals. The collected data are known as observables, and can be processed according to the observation type to determine a receiver's position or baseline vector between two receivers. A detailed analysis of GPS signal structure can be found in Eckels (1987), King et al, (1985) and Wells et al, (1986).

The intended method of measurement, for which GPS was designed, is to use the P and C/A code signals to measure ranges to the satellites. This is known as the "pseudo-range" observable because the ranges contain an error due to oscillators in the satellites and the receivers not being synchronised. The pseudo-range is found by scaling the time delay of the signal from the satellite to the receiver by the speed of light. By measuring the pseudo-range to four satellites simultaneously the observer can solve for the three positional elements of the receiver's location plus the clock offset to GPS time.

This is analogous, in the surveying sense, to a resection for the receiver's location, by distance measurements to four surrounding control points whose positions are known. The satellites can be considered to be those control points whose instantaneous positions are determined by interpolating the satellite orbits, found from the Broadcast Ephemeris or the Precise Ephemeris.

The resolution of the pseudo-range measurement depends on the accuracy of the time measurement made by aligning the satellite's transmitted P or C/A code with the receiver's generated code. The relatively longer wavelengths of the code signals to the L band signals make accurate signal alignment not possible. The P code was designed for point positioning to the 10 metre level while the C/A was designed to achieve point positioning at the 100 metre level (King et al, 1985, p4).

The accuracy from pseudo-range observations is generally unacceptable for surveying and geodetic applications and so this technique will not be mentioned further in this study (see section 4.2.7). The preferred observation is the measurement of the L band carrier waves with two or more suitably equipped receivers in a relative mode.

The principle of carrier wave phase measurement is that the range between the satellite and the receiver consists of an integer number of carrier waves (the ambiguous term) and a residual fractional part of a cycle of the carrier wave. The ambiguous term can be resolved using post-processing techniques providing sufficient observations are available to resolve the integer cycle biases. The "sufficient" number of observations relates to the length of the arc the satellite travels during the observation period as well as the actual number of measurements made.

The remaining fractional part of the carrier wave cycle is found by comparing or "beating" the reconstructed carrier wave with another carrier wave of the same frequency generated by the receiver. The resultant carrier beat phase when multiplied by the wavelength of the L1 or L2 carrier wave gives the fractional part to an accuracy of millimetres.

The fundamental carrier phase observation equation can be expressed as,

$$\lambda\Phi_i^k = -\rho_i^k - dI_i^k - dT_i^k + c\Delta t_i^k + \lambda C_i^k + \varepsilon \qquad (4.2)$$

where λ = carrier wavelength in metres

Φ_i^k = observed carrier beat phase in cycles

ρ_i^k = geometric range between satellite and receiver

dI_i^k = ionosphere phase delay

dT_i^k = troposphere phase delay
Δt_i^k = time difference between satellite and receiver clock
C_i^k = integer carrier phase ambiguity term
ε = error associated with the observation
i and k refer to receiver i and satellite k.

It is apparent from the above equation that the error sources, such as satellite orbits, satellite and receiver clocks and atmospheric propagation errors, will be strongly correlated between receiver sites. If the carrier phase measurements are differenced between receivers, between satellites or between epochs, the errors common to the measurements being differenced will be removed. However if the correlation is not perfect, there will be an unmodelled residual error which will propagate into the solution adversely affecting the result. The next section attempts to identify and quantify these error sources and particularly how they affect GPS heights.

4.2 Error Sources in GPS Heights.

Historically, estimates of the magnitude of height errors in networks observed with GPS have been made after examination of height loop closures. This has led to claims of differing precisions for GPS heights by various authors, for example,

"relative geocentric spheroidal heights to within a few millimetres"	Rush (1986)
"3 ppm"	Schwarz et al, (1985)
"2-3 ppm for lines 10-70km length"	Delikaraoglou et al, (1985)
"cm, or even sub-centimetre accuracy over distances of the order of 100km"	Hein, (1985)
"2 ppm horizontal, 4 ppm vertical"	Stolz, (1987)
"1cm + d(1 ppm) d = length in km"	Hothem et al, (1985)
"about 1.6 ppm"	Engelis and Rapp, (1984)
"half the precision of horizontal coordinates"	GPS Users Group

"ellipsoidal height differences with cm order accuracy for distances up to 100 km"	Denker et al, (1986)
"1 ppm over baselines 50-100 km and in the near future perhaps 0.1 ppm"	Hein, (1986)
"± (0.5mm + 1-2 ppm)"	Zilkoski and Hothem, (1988)

Here the error being quoted is the error in height over the baseline length expressed in parts per million (ppm). This method is the most common in usage and will be adhered to in this study.

The errors in GPS observed heights can be subdivided into random errors and systematic errors (or biases). Random errors are a result of the observation process itself and neither the magnitude nor the sign of the error is known. However, repeated observations will allow an estimate to be made of the error source which can statistically be propagated into the final solution.

Biases have the same, but often unknown, magnitude and sign under the same observation conditions because the mathematical model accounting for them is in error or incomplete. They can be greatly minimised or even eliminated as an error source by modelling the error in the solution or differencing the observations.

The accuracy of heights obtained by GPS is dependent on both the random errors and biases inherent in the observation and the geometric strength of the satellite configuration being observed. This determines how the errors propagate into the final solution.

The errors that influence GPS measurements fall into the following categories (Wells et al, 1986)

BIASES

Satellite Dependent

* Orbit errors due to an incorrect satellite ephemeris.
* Satellite clock model biases.

Station Dependent

* Receiver clock biases.
* Station coordinates.

Observation Dependent

* Ionospheric delay.
* Tropospheric refraction.
* Carrier phase ambiguity.

RANDOM ERRORS

* Residual biases.
* Cycle slips.
* Multipath.
* Antenna phase centre movement.
* Random observation error.

The user, by his choice of observation procedure and processing strategy, has control over the propagation of some errors into the final solution. These include orbit errors, ionospheric delay, tropospheric delay and to some extent, multipath. Other errors are dependent on instrument type or are inherent in the GPS system. To this extent the user is somewhat at the mercy of the equipment manufacturers and the operators of the GPS space and control segments. These error sources are investigated in greater detail below.

4.2.1 Ionosphere.

The signal from a GPS satellite passes through 5 distinct layers in the Earth's atmosphere. These layers and the corresponding heights in which they occur are shown in Table 4.3.

ATMOSPHERIC LAYER	APPROXIMATE HEIGHT (km)	REFRACTIVE INDEX (n)
Troposphere	0 to 11	$n > 1$
Stratosphere	11 to 30	$n > 1$
Mesosphere	30 to 70	$n = 1$
Ionosphere	70 to 1000	$n < 1$
Exosphere	> 1000	$n = 1$

Table 4.3 Layers of the atmosphere.

The signals transmitted by the satellite are "delayed" as they pass

through these layers in the atmosphere. This increases the transit time of the signal from the satellite to the receiver and hence the range. Therefore, GPS measurements must be corrected for the ionospheric phase delay (dI_i^k) and tropospheric delay (dT_i^k) from (4.2).

In the ionospheric region, the ultra-violet radiation from the sun ionizes the gas molecules releasing free electrons into the ionosphere causing the region to become negatively charged. The correction for the ionospheric phase delay is dependent on this number of free electrons in the ionosphere, called the Total Electron Content (TEC), measured at the zenith. The units of TEC are expressed as N_e, the number of free electrons per square metre (el m^{-2}). Typical values for TEC range from a maximum of 2000 x 10^{15} el m^{-2} to a minimum of 10 x 10^{15} el m^{-2}.

The TEC is a function of,

* latitude - maximum TEC occurs at low to mid latitudes, the minimum at the poles.

* diurnal cycle - maximum occurs early afternoon, minimum in the early morning.

* sunspot cycle - 11 year cycle of solar activity.

* sudden ionospheric disturbances.

Figure 4.1 shows the typical range in the diurnal ionospheric delay for 2 two day periods, one in September 1980 and the other in May 1983. The first occurs during a peak in solar activity, whilst the second occurs towards a minimum. The 11 year cycle of solar activity is clearly seen in Figure 4.2. It can also be seen that isolated peaks of activity also occur which are overlaid on the longer period cycle.

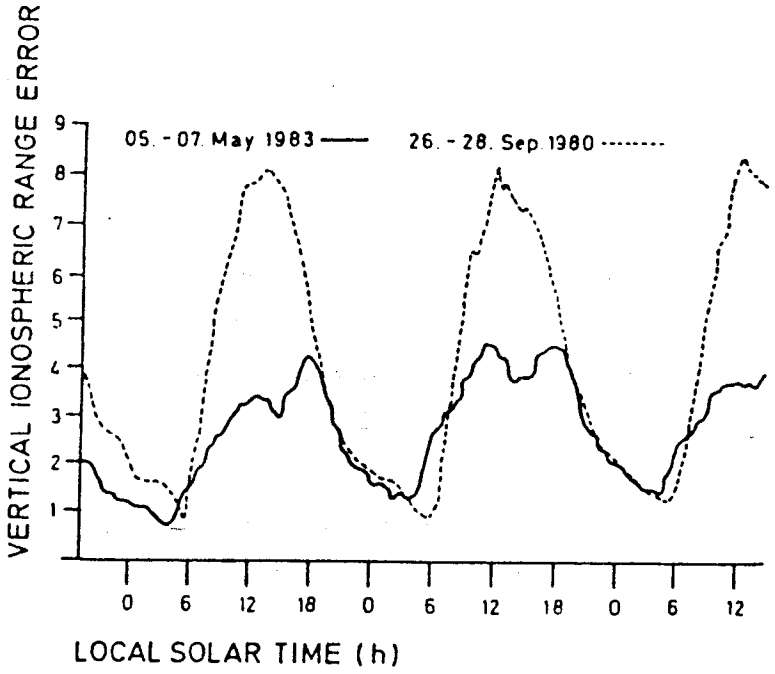

Figure 4.1 Typical diurnal variations in TEC.
(Campbell and Lohmar, 1985)

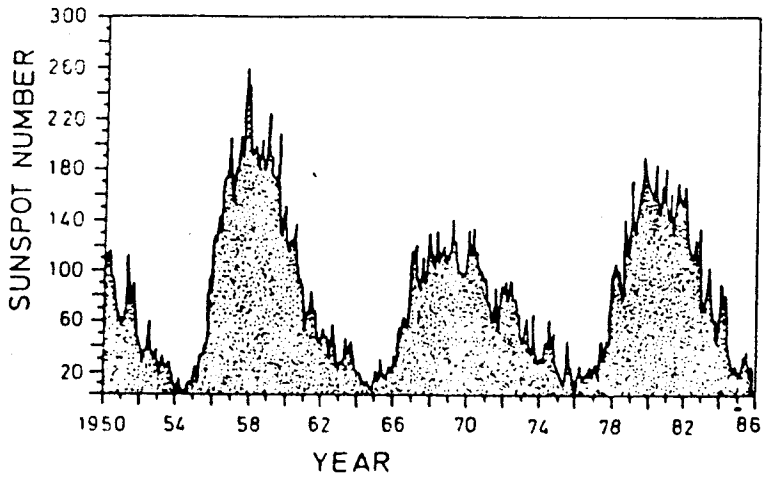

Figure 4.2 Monthly sunspot numbers 1950-1985.
(Campbell and Lohmar, 1985)

Observations made to the GPS satellites will, typically, be away from the zenith which will increase the value of the TEC and hence amplify the ionospheric phase delay. The amount of amplification is approximately

proportional to the secant of the zenith angle of the geometric path from the receiver to the satellite. At a zenith angle of 75° this is about 3.9 times the TEC at the zenith.

Various strategies have been devised to correct phase observations for the ionospheric phase delay. They differ greatly in complexity and attainable accuracy. Table 4.4 shows the expected accuracy of the vertical ionospheric range error of several models and in comparison the accuracy expected from dual frequency observations.

	Ionospheric Range Error
Without correction	2 - 15 m
Klobuchar model	1 - 8 m
Bent model	0.5 - 4 m
Bent model + updating	0.25 - 2 m
Two-frequency observations	< 0.01 m

Table 4.4 Expected residual error for different ionospheric correction methods in the zenith direction.

Depending upon the separation of the two receivers and the stability of the ionosphere, double differencing phase measurements between station sites will tend to cancel most of the ionospheric delay. For example, two GPS receivers 10 km apart access the signal simultaneously from a satellite. The signal paths will be virtually the same and so double differencing will tend to cancel the ionospheric effects. However, if the two receivers have a large separation the signal paths will be very much different causing a relative residual ionospheric error after double differencing.

A residual error in the absolute ionospheric delay tends to propagate into the final solution of a baseline or network more as a scale error and does not significantly affect height determination. Georgiadou et al, (1988) report a reduction in baseline length of 0.25 ppm for a 1 m residual ionospheric delay whilst Beutler et al, (1987) state that a "network contracts by 0.7 ppm if a TEC of 10^{17} in the zenith direction is neglected." However, a residual error in the relative ionospheric delay between two

stations will be reflected as an error in the GPS height differences. This would tend to occur over long baselines, particularly those oriented north-south.

4.2.1.1 Dual Frequency Observations.

The ionospheric delay is frequency dependent owing to the dispersion effect of radio waves in the ionosphere and so measurements made simultaneously on both L1 and L2 frequencies will eliminate most or almost all of the ionospheric correction. This is the most accurate method of correcting carrier phase observations. From King et al, (1985, equation 5.83),

$$\phi_c = \phi_{L1} - 1.984(\phi_{L2} - 0.779\phi_{L1}) \tag{4.3}$$

The "combined, ionosphere free, phase observable ϕ_c can be used for geodetic positioning in exactly the same manner as single frequency observables." For short baselines affected by multipath, however, the ambiguity biases may be harder to resolve for the combined ionosphere free phase observations than single frequency observations because the signal noise is amplified.

4.2.1.2 Broadcast Ionospheric Correction Model.

Most GPS receivers used today are single frequency only. This is because of the uncertainty of future US DoD plans for access denial of the P-code on the L2 frequency and also the extra cost involved in building a dual frequency receiver. Therefore, the L1 carrier phase observable has to be corrected by application of a model that represents the ionospheric phase delay, to obtain geodetic accuracies. One ionospheric correction model is broadcast in the GPS navigation message on subframe 4.

This model was developed by Klobuchar in 1982. It is a compromise between accuracy and an acceptable level of complexity. It uses an algorithm containing eight coefficients to model the ionospheric delay. The model is quoted as having an accuracy of 50% root sum square (RSS) of the

correction on a global basis (Klobuchar, 1986). However, at this accuracy, the model is unable to accurately fit significant day-to-day fluctuations and, indeed, there could be periods when the model actually degrades the observations (Campbell and Lohmar, 1985).

4.2.1.3 Other Ionosphere Correction Methods.

There are other methods to correct for the ionospheric delay which have shown encouraging results but have not gained universal acceptance because of their complexity or cost. One method described by Campbell and Lohmar, (1985) and Partis, (1988) is to use dual frequency Doppler data from the NAVSAT satellites transmitted at 150 and 400 MHz and then used to calculate the ionospheric delay at the GPS frequencies.

Henson and Collier, (1986) report on combining the group delay obtained from pseudo-range measurements with the phase delay from carrier phase measurements. These delays are nearly the same but of opposite sign, in common distance units, the difference being the ionospheric correction.

A number of empirical regional and global models have been developed to model the TEC from data from ionosonde observations by means of vertical looking HF-radar to measure peak electron density. Two global models that have found wide interest are the Bent Ionospheric Model (Llewellyn and Bent, 1973) and the International Reference Ionosphere (IRI) (Rawer et al, 1978).

4.2.2 Troposphere.

The troposphere, sometimes referred to as the neutral atmosphere, is a non-dispersive medium, unlike the ionosphere. Therefore the tropospheric propagation delay is dependent not the transmitting signal frequency but on the refractive index (n) of the medium along the signal path. The refractive index can, alternately, be expressed as refractivity (N) by the expression

$$N = 10^6(n-1)$$

The refractivity is the sum of a dry component (N_D) and a wet component (N_w) and depends on the temperature (T) in degrees Kelvin, air pressure (P) in mbar and the pressure of the water vapour (e) mbar of the troposphere. The formula of Smith and Weintraub (1953) give this as

$$N = N_D + N_W \qquad \text{where;}$$

$$N_D = 77.6\,P/T \quad \text{and} \quad N_W = 3.73\text{x}10^5\,(e/T^2)$$

The tropospheric delay (dr) is then expressed as the integral of the refractivity along the line of sight (LOS) from the satellite to the receiver.

$$dr = \int_{LOS} (N_D + N_W)\, dh \tag{4.4}$$

Typically, the dry component makes up between 80-90% of the zenith range delay of approximately 2.3 metres in the first 7 km above the earth's surface. Close to the horizon, the range delay can be up to 20 metres. This can be modelled within 2-5% using surface meteorological data (Landau and Eissfeller, 1986).

However, the wet component, which typically contributes a zenith range delay of 10-20 cm, depends on the atmospheric conditions along the signal path from the receiver to the upper level of the troposphere. Under some conditions, it is questionable whether the surface temperature or the water vapour pressure truly reflects the meteorological conditions at higher altitudes or that horizontal variations in the water vapour content do not exist.

For example, the surface water vapour pressure measured in fog or in an inversion layer would be very different to measurements taken only a few hundred metres above the ground. Also Rothacher et al (1986) report on a GPS observed network in the Swiss Alps with station height differences of up to 900 metres exhibiting very different meteorological conditions at each station. It is for this reason that researchers have taken a great interest in the determination of the water vapour pressure along the line of sight from satellite to receiver.

The various options that are available to correct GPS range or phase measurements for the troposphere delay are,

* No correction - that is, ignore the tropospheric delay, hoping that the double difference observations will tend to cancel. This will be essentially true for short baselines in flat topography under stable weather conditions.

* Model the tropospheric delay using a standard model based upon a standard atmosphere or upon surface weather data. Table 4.5 shows various tropospheric correction models available for the zenith correction (Coco and Clynch, 1982). These models generally give accuracies of a few centimetres.

* Radiosonde data - measuring temperature and water vapour pressure profiles from balloon launches at a nearby weather station.

* Water Vapour Radiometer (WVR) observations - these measure very accurately the microwave radiation emitted by the water vapour in the atmosphere along the line of sight. The WVR's are very expensive, however, and generally beyond most operator's budgets.

The most common method for commercial GPS processing software to correct for the tropospheric delay is to use one of the models in Table 4.5. The Wild-Magnavox GPS processing software, PoPS^{tm}, (WM Satellite Survey Co., 1987) allows the user to select from a choice of three models, Saastamoinen, Hopfield I and Hopfield II or use no model at all, whilst the Trimble software, TRIMVEC^{tm}, (Trimble, 1986) uses the Marini or modified Hopfield model. Both programs allow the user to input measured surface temperature, pressure and relative humidity readings or use a default standard atmosphere.

MODEL	NOTES
Hopfield	Based on a quartic model of the refractivity.
Black	empirical model, no surface measurement inputs, depends only on latitude.
Berman	empirical model with different parameters for day and night cases.
Chao 73	assumes adiabatic law rather than perfect gas law, semi-empirical model
Saastamoinen	assumes a linear decreasing temperature as a function of altitude.
Saastamoinen/ Marini	a variation of the Saastamoinen model

Table 4.5 Tropospheric correction models.

A differential residual error in the tropospheric correction between two stations is the major source of GPS height errors, (assuming the orbit errors or the error in the ionospheric delay are not abnormally large). This is in agreement with Beutler et al, (1987) who state "a bias of 1mm in the zenith direction of" (the relative) "tropospheric correction causes a height bias of approximately 2.9mm." However, an absolute error in the tropospheric correction causes a scale error in the baseline, the effect being to stretch the baseline if the troposphere is neglected altogether.

Two methods have been suggested by Grant (1987) to minimise the error in the heights due to a differential residual error in the tropospheric correction between two stations. The first is to model this error at each station as a time invariant bias in the solution. The success of this method will depend on how stable the troposphere was during the observing session. The second method is to model the residual error at each station and at each epoch using a Kalman filter. The success of this method will depend on how well the dynamic model reflects the changing troposphere.

4.2.3 Orbit Errors.

The satellite emphemeris is a set of coordinates describing the position of an orbitting satellite with respect to the earth's centre of mass as a function of time. The satellite orbit obeys Kepler's three laws of planetary motion but is "perturbed" from an idealized orbit by gravitational and non-gravitational disturbing effects upon the satellite. These are,

* gravitational perturbations caused by the earth's non-sphericity, the mass of the sun and the moon, earth and ocean tidal effects.

* non-gravitational perturbations caused by atmospheric drag on the satellite, solar radiation pressure and Albedo.

An orbit generation program involves tracking a satellite's orbit from tracking stations around the world, using an appropriate force model reflecting the disturbing effects on the satellite and then predicting future orbits which are then uploaded from the ground Master Control Station to become the broadcast ephemeris. Errors in the broadcast ephemeris are caused by,

* errors in the defining elements of the reference ellipsoid (WGS84).
* errors in the positions of the tracking stations.
* errors in the position and velocity of the satellite (the initial state) caused by tracking errors.
* errors in the force model of the disturbing effects.

An error in a satellite's orbit may be described in the HCL system. The L or along-track error is in the direction of the satellite's motion, the across-track error, C, is perpendicular to the along-track error and the radial error, H, is mutually perpendicular to the other two and in the direction from the satellite to earth. Typically, the along-track error is the largest of the three (Grant, 1988).

No matter how accurately the ranges between the receivers and the satellites are determined, an error in the satellite orbit will result in an incorrect receiver position, scaled by a factor dependent upon the strength

or weakness of the satellite geometry. As a general rule, the relationship between an error in the satellite's orbit and the error in a measured baseline will obey the approximate law (King et al, 1985; Colombo, 1986)

baseline error (ppm) = ephemeris error/altitude of satellite

That is, an error of 20 metres in the satellite orbits will result in a baseline error of approximately 1 ppm. The effect of an along-track error has been investigated geometrically by Beutler et al, (1987) who looked at the particular case of a single satellite passing through the zenith of a ground station. They found that an along-track error of 1" in the plane of the observer as viewed from the ground station will affect the height component by an amount caused by a rotation of the network by 1" about an axis perpendicular to the orbit plane. The error achieves a maximum when the direction of the baseline is the same as the motion of the satellite.

4.2.4 Receiver and Satellite Clock Errors.

The satellite and receiver clock biases for differential positioning have three components,

* an epoch offset from Universal Coordinated Time (UTC),
* an epoch difference between the two receivers,
* and a time rate difference between the two receivers and the satellites.

An epoch offset from UTC, common to both receivers, will result in the satellite emphemerides being interpolated for the incorrect time. The error is a function of the time bias from UTC and the satellite along-track velocity. The receiver clocks need to be synchronised to UTC within 7 milliseconds for a baseline error below 1 ppm (King et al, 1985) and if the two receiver quartz clocks are synchronised to each other within 3 microseconds that error reduces below 1 cm (ibid).

The frequency stability of the satellite and receiver clocks depends on the type of clocks used. The measure of this stability is the Allan Variance ($\sigma\gamma(\tau)$) (Stolz, 1987). The stability of the various clocks used in the GPS satellites is given in Table 4.6.

STABILITY AT 1 DAY	QUARTZ	RUBIDIUM	CESIUM
$(\sigma\gamma(\tau))$	$1x10^{-9}$ secs	$1x10^{-12}/10^{-13}$ secs	$2x10^{-13}$ secs

Table 4.6 Allan variance of satellite clocks.

The types of clocks in the present (Block 1) satellites are given in Table 4.7 (King et al, 1985).

NAV ID #	SV ID #	LAUNCH DATE	CLOCK TYPE
1	4	22/02/78	Quartz
3	6	7/10/78	Rubidium
4	8	11/12/78	Rubidium
5	5	9/02/80	Cesium
6	9	26/04/80	Cesium/Rubidium
8	11	14/07/83	Rubidium
9	13	13/06/84	Cesium
10	12	10/09/84	Cesium

Table 4.7 Satellite clocks.

The satellite and receiver clock biases are eliminated by the differencing in the solution for the baseline components. A single difference is the difference in phase of a "simultaneous" measurement between one satellite and two receivers. A double difference is the difference of two single differences (between station differences) related to two different satellites at the same epoch. These methods cancel any clock biases and any instabilities in the receiver and/or the satellite clocks.

4.2.5 Carrier Phase Ambiguity.

The ambiguity term C_i^k in the carrier phase observation equation 4.2 is the unknown integer number of cycles between the satellite and the receiver. The ambiguity is unique to each satellite-receiver combination and will not change during an observing session unless a cycle slip occurs or the receiver loses lock.

The process of ambiguity resolution involves the selection of the nearest integer value of the ambiguity parameters based on the estimate from a first ambiguity free solution. This estimate of the bias free ambiguities may not be well determined if the observations contain

* unmodelled ionospheric effects,

* unmodelled tropospheric effects,

* instrumental errors such as multipath,

and will also depend on the

* length of the observation session,

* length of the baseline,

* and, the number of satellites observed.

After the integer values of the cycle ambiguities have been resolved, a second ambiguity fixed solution for the geodetic parameters only, can be performed holding the ambiguities fixed to their estimated integer values. If the ambiguities have been fixed to their correct integer values then a increase in precision of the solution for the geodetic parameters of interest will occur. However, the solution will be degraded if incorrect values are chosen in the ambiguity fixed solution. In these cases an ambiguity free solution will give a more accurate estimate of the geodetic parameters (King, 1987; Henson and Collier, 1986).

An alternative method to estimating the ambiguity bias is to eliminate it using triple differences, i.e. double differencing between measuring epochs. However, the favoured method which gives the most accurate results (Eckels, 1987, p. 115) is the first method. This reduces the number of parameters in the solution which increases the redundancy and hence increases the precision of the results.

4.2.6 Multipath.

Signal multipath errors occur if the received signal at the antenna is composed of two or more constituents which have propagated along paths of different length causing the signals to interfere at the receiver. The different propagation paths is usually caused by part of the signal being

reflected off some nearby structure, the ground or body of water. Multipath effects are site and antenna independent and therefore the effects will not cancel when double differenced between receivers.

Reducing the effects of multipath can be achieved by the use of a well designed antenna that minimises interference and possibly incorporating an absorbent ground plane to cut out signal reflection. If suspected multipath errors are still thought to exist the receiver can be resited away from the suspected reflective surface. Unfortunately, too often during GPS campaigns, unexplained errors are attributed, perhaps unjustly, to multipath. Proof that a suspect error source is caused by multipath contaminating the GPS signal will be made if the error repeats one sidereal day later when the satellite-reflector-antenna geometry is the same.

4.2.6.1 Antenna Phase Centre Movement.

Antenna phase centre movement is the difference between the electrical phase centre and the geometrical phase centre of an antenna. The range of the incoming signal from the satellite will vary around the phase centre according to the azimuth and elevation of the satellite. The range error caused by the phase centre movement will be the projection of the deviation of the actual phase centre from the nominal centre onto the line of sight from the antenna to the satellite.

Experiments by Kleusberg (1986b) on the variability of phase centre with rotation and inclination of a TI-4100 antenna show a difference of 1.9 cm for the L1 frequency and 3.3 cm for the L2 frequency.

This error source can only be overcome by good antenna design. Collins (1986) suggests that the crossed dipole antenna used by Macrometer™ "has consistently provided the greatest accuracy under extreme conditions."

4.2.7 Random Observation Errors & Residual Biases.

GPS measurements contain additional observational random errors other than those described above. They are due to the limitations of the

electronics in the receivers, in the system and round off errors in the processing software. As a general rule, they are proportional to about 1% of the signal wavelength (Wells et al, 1986). Therefore they will be much greater for code measurements than carrier phase.

GPS SIGNAL	WAVELENGTH λ	1% OF λ
C/A Code	300 m	3 m
P-Code	30 m	30 cm
Carrier	20 cm	2 mm

Table 4.8 Magnitude of random observation errors.

The observations will also contain unmodelled residual biases which have not been accounted for. They are systematic and present because the model used to account for the error is either incomplete or incorrect. The purpose of much of the current GPS research is to investigate more complete error models that will account for all the errors, if this is possible. It may be found that the increased complexity of a better error model may not be warranted by all but the most demanding of users.

They can also be caused by differencing observations that do not contain common errors as in the case of differing ionospheric refraction at the ends of a long baseline due to the signal passing through a different part of the ionosphere. Another case could occur in the tropospheric delay, even on a short line, if observations are made under severe and changing weather conditions.

4.3 Simulations.

One method of looking at the effect of systematic errors on a GPS adjustment is to observe GPS under the conditions which are being investigated and comparing these results with known ground truth. The main disadvantages of this method are the time and cost involved in collecting the data, the uncertainty that the ground truth, "the yardstick", is error free and the difficulty in separating different error sources from

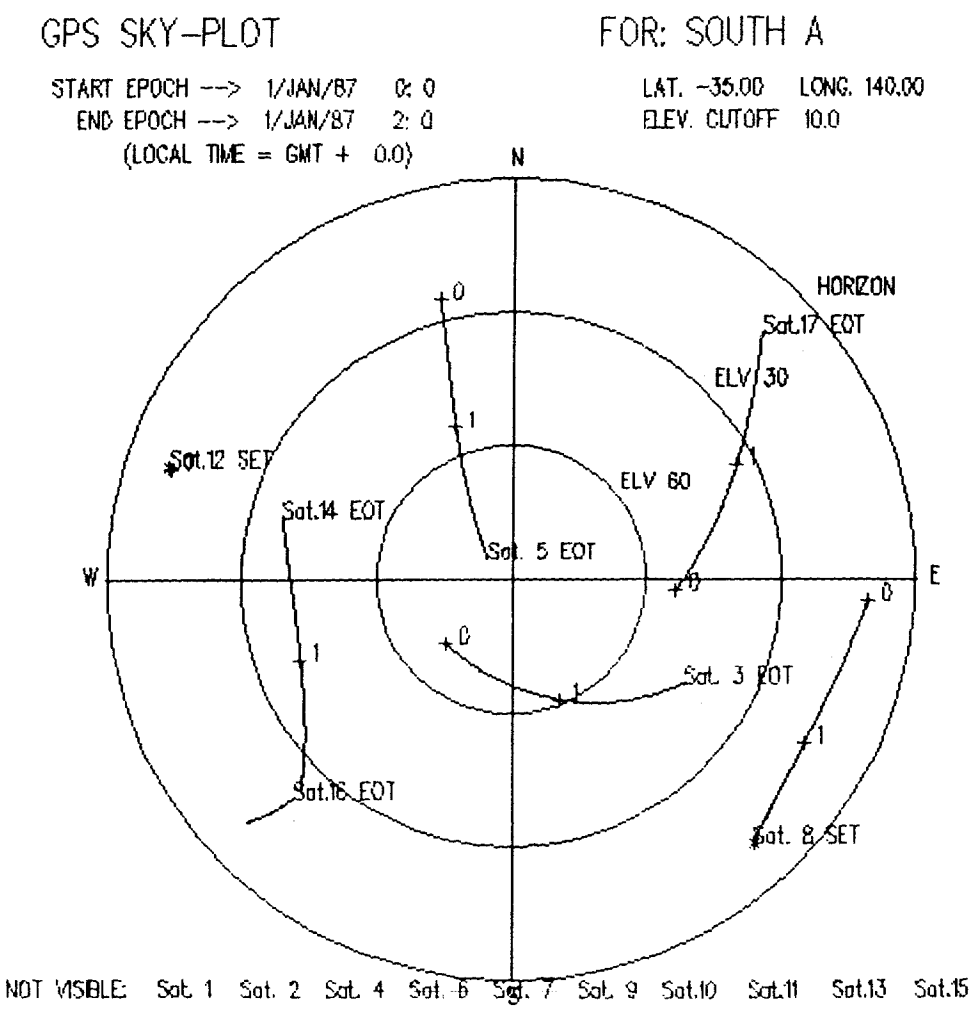

Figure 4.3 Skyplot of satellite constellation for simulation.

The errors considered in this study are,

1) errors in the station coordinates with respect to the earth fixed reference frame. The GPS baseline solution is with respect to a fixed station, the *a priori* coordinates of which are usually obtained from a pseudo-range solution or converting AGD84 coordinates to WGS84. The given error figures are $\sigma_e, \sigma_n, \sigma_h = 10$ metres and are assumed to be uncorrelated.

2) errors in the satellite orbits. The errors are given in the HCL system with the along track component L being the worst determined than the other two (Grant, 1988). Typical values are 6 m, 6 m and 18 m (HCL) giving a total error of 19.9 m. It is also assumed that these errors are uncorrelated and that there is no correlations between satellites.

3) the residual tropospheric delay error after the observations have been corrected *a priori* using surface meteorological data and a tropospheric model such as Hopfield or Saastamoinen. The zenith tropospheric delay

is estimated as a constant parameter which assumes the troposphere is stable during the observing session. The residual error of the zenith delay at a point is σ_{trop} with a correlation distance D_{trop} for a spatial correlation function given below (4.5). The values of σ_{trop} = 0.048 m, approximately equal to a residual error of 2% and D_{trop} = 75 km have been adopted for this simulation (Grant, 1988).

4) the error caused by the ionospheric delay of the signal from the satellite to receiver. For dual frequency receivers the error is negligible. However, most observations will be made with single frequency receivers as they are less expensive than the others. The values of σ_{ion} = 1 m and D_{ion} = 1000 km given below (4.6) have been adopted for this simulation. This appears to be a reasonable value for observations made near a solar minimum, at night-time or corrected with the ionospheric model by Klobuchar (1986).

5) random observational errors and residual biases in the observation process. These errors include multipath, antenna phase centre uncertainties, inter-channel biases and random noise in the electronics of the receivers. The effects of these errors will be independent of the length of the baseline and will thus be most noticeable on short baselines where the errors due to orbits and atmospheric propagation delay are smallest. An error of 5 mm in the undifferenced phase observations with one observation every 2 minutes has been adopted for this simulation. This is equivalent to a 10 mm uncertainty for observations taken every 30 seconds and is a conservative estimate (Grant, 1988).

The spatial correlation function used for the tropospheric and ionospheric delay D_{trop} and D_{ion} is given by the Gaussian function (ibid)

$$\rho(b) = \exp\left(-\frac{b^2}{D_{trop}^2}\right) \tag{4.5}$$

$$\rho(b) = \exp\left(-\frac{b^2}{D_{ion}^2}\right) \tag{4.6}$$

where $\rho(b)$ is the correlation between the two stations, b is the length of the baseline and D_{trop} and D_{ion} have already been defined. This corresponds to correlations for the simulated 5 km and 50 km baselines of,

Troposphere	5 km line	$\rho = 0.996$
	50 km line	$\rho = 0.641$
Ionosphere	5 km line	$\rho = 1.000$
	50 km line	$\rho = 0.998$

Two cases were investigated in the simulation. First, the case where the ambiguities were not able to be resolved at all for both lines. The second case where the ambiguities were able to be resolved correctly for the 5 km line. It was thought that this was the more realistic situation as the observational errors in the longer line would make it unlikely for the estimate of the ambiguities to be correctly fixed to integers.

It is understood that the ionospheric and tropospheric delay errors and the orbit errors will be anisotropic, that is azimuth dependent, to a certain extent. The ionospheric delay is dependent upon the TEC which exhibits a steep gradient from the equator to the poles. The propagation of orbit errors depends upon the relationship between the direction of the baseline to the direction of the groundtracks of the satellites (Beutler et al, 1987), whilst the residual tropospheric error is influenced by local topographic and climatic conditions. This study did not investigate the spatial behaviour of errors any further other than acknowledging some azimuth dependency. All errors in the simulation are considered isotropic.

Figure 4.4 shows that when the ambiguities are not resolved the dominant height error is the tropospheric error and is proportionally much the same for both baselines. The receiver noise error is constant and therefore has a much greater influence on the shorter line. The other errors are proportionally very similar to each other.

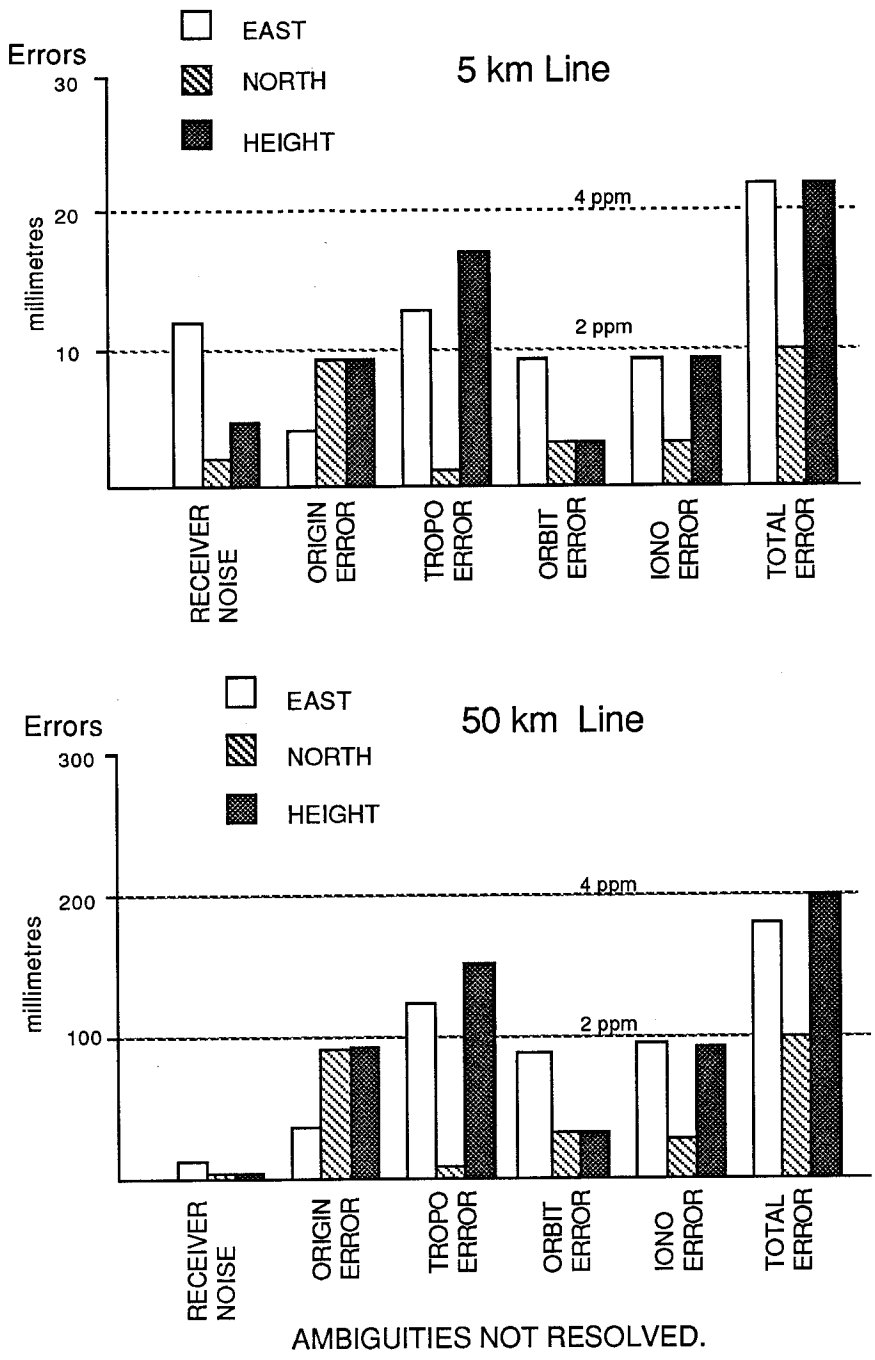

Figure 4.4 Simulated errors in 5 km and 50 km baseline.

Figure 4.5 shows that by resolving the ambiguities correctly the error in the easting coordinate is improved dramatically. The total receiver noise error has also been improved. The dominant error for the height component is still the residual tropospheric error with the errors in the ionosphere and the fixed station coordinates also being significant. It is also apparent that

the total height error is not improved whether the amiguities are able to be resolved or not, although the errors in the easting and northing components are improved.

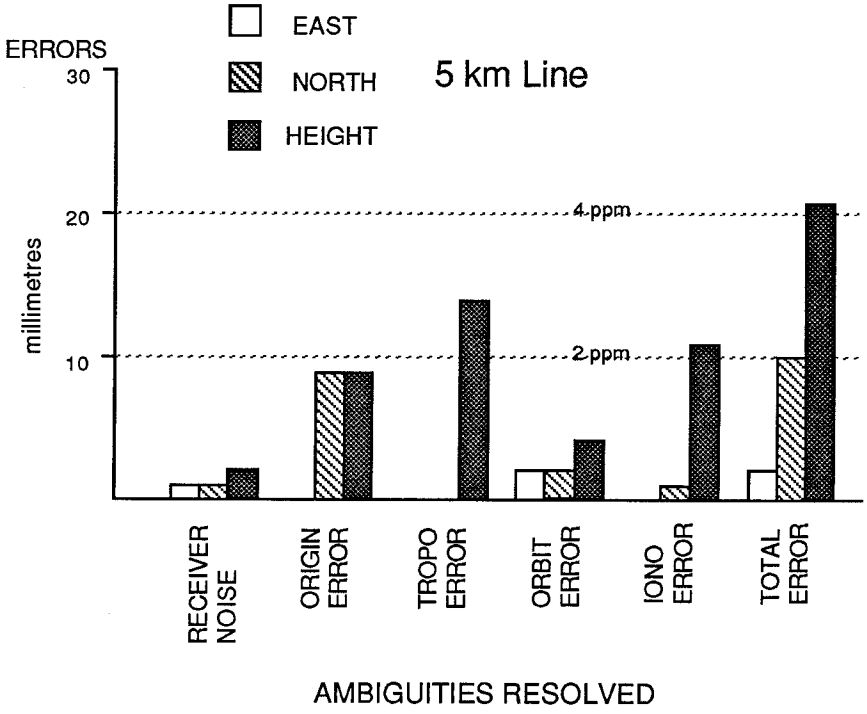

Figure 4.5 Simulated errors in 5 km baseline.

It can be concluded from the foregoing error simulations that GPS surveys observed primarily to obtain heights, such as connections between tide gauges or densification of levelling networks, that there is very little benefit in resolving the cycle ambiguities. The risk that the cycle ambiguities may be resolved incorrectly and degrade the observations must be weighed up against the very little improvement that correct ambiguity resolution brings.

When observing high precision GPS surveys for height, care should be taken to control the tropospheric error primarily and the ionospheric delay error and errors in the fixed station coordinates secondary. This can be achieved by a better determination of the wet component of the troposphere with the use of WVR's, the use of dual frequency receivers and perhaps a connection to a VLBI or TRANSIT doppler site.

5 METHODS OF TRANSFORMING GPS HEIGHTS TO AHD HEIGHTS

The determination of height by levelling is intrinsically more accurate than geodetic positioning by terrestrial measurements, but how accurate is levelling when compared to heights from GPS?

The simulation of systematic errors in the GPS system in Section 4.3 gives a standard error for heights of 4 ppm of the baseline length. This figure may be a little conservative as analysis of loop misclosures in a number of networks and the experience of researchers (Section 4.2) shows that the error in GPS heights is closer to 2-3 ppm.

To compare the accuracy of GPS heights with spirit levelling, we have to use the standard error (*s.e.*) of the levelling and not the prescribed tolerances. This can be found using Lallemand's formulae (Bomford, 1977, p. 244),

$$s.e. = \sqrt{(\eta^2 k + \sigma^2 k^2)} \qquad (5.1)$$

where k is the distance levelled in kilometres,
η is the random error in mm/km$^{1/2}$,
σ is the systematic error in mm/km.

Bomford gives figures for η and σ of 0.35 mm/km$^{1/2}$ and 0.04 mm/km based on analysis of the second geodetic levelling of Finland 1935-1955. These figures appear to be too optimistic to be used in the Australian situation. Roelse et al (1975, p. 76) estimated the precision of the Australian levelling after adjustment as $8.1\sqrt{k}$mm. This figure does not account for any systematic errors in the levelling but is the best estimate available for the Australian levelling. This error figure is also quite close to the tolerance for second order levelling. Therefore, as an illustration only, table 5.1 is given which compares the accuracy of GPS heights, adopting an accuracy figure of 2 ppm, to the prescribed tolerances of first, second and third order levelling.

The figures above the dark solid line show at which distances GPS heights are more accurate than spirit levelling whereas for the figures below, the reverse is true. By inspection, first order levelling is more accurate than GPS heights over all distances, while third order levelling is not as accurate as GPS heights up to a distance of 35 kilometres. As most of the levelling in the Australian levelling network is of third order standard (Roelse et al, 1975, p. 75), GPS can be considered a valid alternative to spirit levelling for all heighting other than the most precise applications.

Baseline Length	GPS Heights	LEVELLING		
	Accuracy 2 ppm	First Order $4\sqrt{k}$	Second Order $8.4\sqrt{k}$	Third Order $12\sqrt{k}$
km	mm	mm	mm	mm
5	10	8.9	18.8	26.8
10	20	12.6	26.6	37.9
15	30	15.4	32.5	46.5
20	40	17.9	37.6	53.7
25	50	20.0	42.0	60.0
30	60	21.9	46.0	65.7
35	70	23.7	49.7	71.0
40	80	25.3	53.1	75.9
45	90	26.8	56.3	80.5
50	100	28.3	59.4	84.9

Table 5.1 Comparison of GPS heights with levelling.

However the normal orthometric heights of the AHD are measured with respect to the geoid (Section 3) whilst GPS heights are referred to an

ellipsoid (WGS84). The difference between the orthometric height *(H)* and the ellipsoidal height *(h)* is the geoid-ellipsoid separation[3] *(N)*. The relation between the two is shown in Figure 5.1.

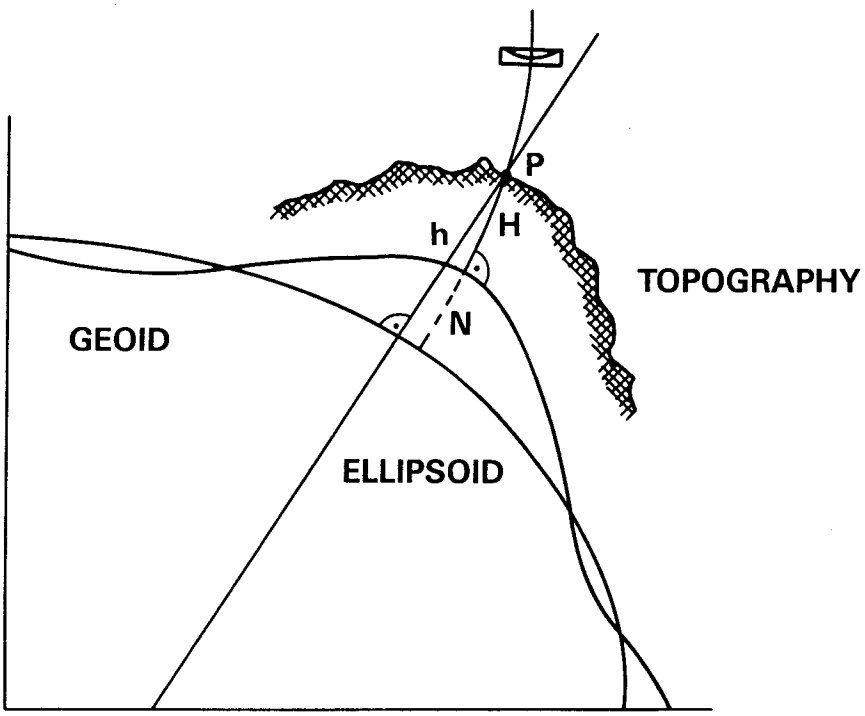

Figure 5.1 The geoid-ellipsoid separation.
(Scherrer, 1985)

From Figure 5.1,

$$H = h - N \tag{5.2}$$

H is measured from the geoid along the curved plumbline and h is measured normal to the ellipsoid. The difference in direction is the deflection of the vertical. For small deflections of the vertical, equation 5.2 holds true and the two can be considered coincident.

However, GPS heights are most accurately determined in the differential mode as many of the systematic errors inherent in the system are minimised when observations from two stations are differenced. Spirit levelling is also most accurate in the determination of relative height

3 The geoid-ellipsoid separation can also be called the geoidal height or geoidal undulation.

differences because mean sea level is not coincident with the geoid. The absolute orthometric height of a point on the coast will be in error by an amount equal to the sea surface topography at that point. Likewise, the determination of relative geoidal heights ΔN will be much more precise than the determination of absolute N because many of the systematic errors will cancel.

Equation 5.2 now becomes,

$$\Delta H = \Delta h - \Delta N \tag{5.3}$$

The precision required for H will depend upon the purpose for which the heights are being used. Some tasks will only require H to a few metres, in which case the constraints on the determination of h and N can be relaxed. For the highest order requirements, the precision to which Δh can be found limits the precision of ΔH, and dictates the precision requirements for ΔN. ΔN will need to match Δh in precision, 2 to 4 ppm, so that the precision of ΔH will not be seriously eroded (Kearsley, 1984 and Kearsley, 1988a).

The sections below outline different methods for determining N and ΔN and will refer to a worked example of each method for two GPS observed networks, one in South Australia and the other in Western Australia.

5.1 Astro-geodetic Methods.

The major control network that extends over the Australian continent has been computed on the Australian Geodetic Datum (AGD) which is referenced to a local best-fitting ellipsoid, the Australian National Spheroid (ANS). A station referenced to this ellipsoid by measurement of directions and distances will have geodetic coordinates ϕ and λ.

To control the orientation error throughout the network, astronomical observations were made at junction points and astronomical coordinates Φ and Λ calculated. The relationship between the geodetic coordinates referenced to the local ellipsoid and the astronomic coordinates observed in

the local gravity field and therefore referenced to the geoid, gives the deflection of the vertical. The two components of the deflection of the vertical in the meridian (ξ) and prime vertical (η) are found by direct comparison (Heiskanen and Moritz, 1967),

$$\xi = \Phi - \phi \tag{5.4}$$

and,

$$\eta = (\Lambda - \lambda)\cos\phi \tag{5.5}$$

The total deflection of the vertical, (θ), between the plumbline and the ellipsoidal normal is given by (ibid),

$$\theta = \sqrt{\xi^2 + \eta^2} \tag{5.6}$$

and the deflection component, (ε), between surface points A and B, whose azimuth is α,

$$\varepsilon = \xi\cos\alpha_{AB} + \eta\sin\alpha_{AB} \tag{5.7}$$

The geoid-ellipsoid separation of point B with respect to A is (ibid),

$$\Delta N_{AB} = -\int_A^B \varepsilon \, . \, ds \tag{5.8}$$

A profile of geoidal heights is found when this calculation is repeated between a series of stations. If the density of the stations is sufficient, geoidal heights can be interpolated between the stations to form a geoid map.

It is interesting to note a further application of this method is in the determination of a best-fitting ellipsoid for a region. If the geodetic positions are observed and adjusted with respect to an arbitrary initial point (i.e., Johnston Geodetic Station) with an assumed deflection of the vertical and geoidal height equal to zero, the position and inclination of the local ellipsoid with respect to the earth can be found by a least squares adjustment such that,

$$\Sigma(\xi^2 + \eta^2) = minimum \tag{5.9}$$

and,

$$\Sigma N^2 = minimum \tag{5.10}$$

The least squares adjustment would be extended over many astronomical points covering the continent.

The astro-geodetic determination of geoidal heights would refer to the ANS reference ellipsoid. This is not particularly helpful if we wish to transform GPS observed heights referred to WGS84. Therefore the geoidal heights would have to be transformed using appropriate transformation parameters such as those by Higgins (1987). The geoidal heights would then relate to the WGS84 ellipsoid and could be transformed to AHD heights using equation 5.3.

In practice, this method is unsuitable for the transformation of GPS heights to heights on the AHD because astronomic determinations of latitude and longitude are labour intensive and time consuming and hence very expensive. Also, it is questionable whether astro-geodetic N values are actually representative of the local geoid-ellipsoid separation as the astronomic observations are usually made on the top of the highest mountains in a region and thus ε may not represent the general slope of the geoid in the locality.

5.2 Geometric Methods.

If a number of control stations exist in a height network which have both GPS and AHD heights, then geoidal heights can be found directly at the control stations using equation 5.2. Three or more noncolinear control stations will define a surface of geoidal heights from which N values can be determined for other stations. If the control stations surround the other stations then the process is one of interpolation or if the stations are outside the control stations then the process is one of extrapolation.

The surface of N values can be defined graphically which is described in Section 5.2.1, or it can be defined analytically which is described in Section 5.2.2. The surface will contain datum errors due to the adoption of incorrect ellipsoidal coordinates for the origin station used in the GPS

relative mode. The "absolute" ellipsoidal coordinates of the origin station are usually found by a pseudo-range solution which will be contaminated by errors in the satellite ephemerides and errors in the coordinates of the tracking stations. The rest of the network is built up by processing and adjusting baselines or multi-station networks relative to the origin station. Therefore the surface of N values **can only be used** to interpolate AHD heights from GPS heights **for stations observed and adjusted in the same campaign.**

The main advantages of the geometric methods of determining N values is that they are conceptually simple and also quick and easy to implement. However it is very much a case of **user beware** as there are few checks with geometric methods to detect errors. An error in either the GPS or AHD height will result in an erroneous value for N which propagates directly into the definition of the interpolation surface.

Geometric methods make the assumption that the geoid is regular between the data points defining the interpolation surface. This is why researchers usually impose areal limits, determined empirically, on the suitability of these methods such as, "adequate for areas up to 50 x 50 km where the geoid is smooth" (King et al, 1985, p. 94). This should be tempered with the warning from Gilliland (1986, p 279) that "linear interpolation over distances as small as 25 km could result in errors much greater than 10 cm" (> 4 ppm). It is therefore advantageous for the user to have some knowledge of the nature of the geoid in the area in which he is performing the calculation as well as the precision of the result he desires. The behaviour of the geoid is not always dependent on the roughness of the terrain as for example, the Officer Basin in central Australia exhibits large geoid undulations while the terrain is quite flat.

5.2.1 Contouring.

One geometrical method of defining an interpolation surface is to contour N values established from control points which have both GPS and

AHD heights. The method is very simple and convenient, requiring no computer resources, just a pencil and ruler. The accuracy of the method is limited to,

* the scale of the drawing and the plotting accuracy,
* the contour interval,
* the behaviour of the geoid between the data points,
* the presence of errors in either the GPS or AHD heights.

This method was adopted by Collins for a GPS survey of 42 stations in Montgomery County (PA), although no accuracies were given (Collins and Leick, 1985, p 688). Ladd (1986, p. 1114) also used contoured geoid heights for a survey of 21 stations in California and said, "interpolation can be performed successfully at the few centimetre level if the vertical control used to originally generate the contours comes from the same levelling campaign and levelling adjustment."

5.2.2 Least Squares Plane Fits.

The interpolating surface can be defined analytically if three or more noncolinear points exist with both AHD and GPS heights. The simplest surface to generate is a first-order plane surface. This often gives the wrong impression that the plane surface is flat. Actually, it represents the linear relationship between the plane and the curved geoid. The analytical function of a plane surface will be of the form (Eckels, 1987, p. 160),

$$N = Ae + Bn + C \tag{5.11}$$

where; A, B and C are coefficients defining the plane.
e and n are the easting and northing in an UTM system.
N is the geoid-ellipsoid separation at point (e,n).

If more than three points exist then the plane is overdetermined and the coefficients A, B and C can be solved for by Least Squares and takes the form,

$$\hat{x} = (A^T A)^{-1} \quad (A^T l) \tag{5.12}$$

where $\hat{x}$ is the least squares estimate of the coefficients, A, B and C, and matrix A is the design matrix of parameter coefficients and l is the geoid-ellipsoid separation at each control station. It is assumed, in this case, that the weight matrix of the observations is an identity.

$$\hat{x} = \begin{pmatrix} A \\ B \\ C \end{pmatrix} \tag{5.13}$$

$$A = \begin{pmatrix} e_1 & n_1 & 1.0 \\ e_2 & n_2 & 1.0 \\ e_3 & n_3 & 1.0 \\ . & . & . \\ . & . & . \\ e_n & n_n & 1.0 \end{pmatrix} \tag{5.14}$$

$$l = \begin{pmatrix} N_1 \\ N_2 \\ N_3 \\ . \\ . \\ N_n \end{pmatrix} \tag{5.15}$$

This strategy has been adopted for program LESQPL listed in Appendix D. The program reads data from an input file in two sections. The first section contains the control points that have both GPS and AHD heights which are used to determine the coefficients A, B and C defining the plane. The size of the residuals at each point and the standard deviation of the residuals gives an indication of how well each point fits the plane. Other elements computed are the deflections of the vertical in the meridian and prime vertical and the maximum slope and direction of the geoid. The second section of the data file contains the points with GPS heights only, which are transformed to AHD heights by back substitution.

It is possible to generate higher order surfaces such as second order surfaces, trigonometric functions or bicubic splines fitted to the control points to interpolate N values. However, these methods tend to become

unstable when the point data is irregularly spaced. Cases have occurred in which "height values have been interpolated which are hundreds of metres above the highest point on the mountain" (Kearsley, 1985, p. 88).

5.3 High Order Geopotential Models.

In the past few years the description of the earth's gravity potential in terms of spherical harmonic coefficients has been extended to degree and order n_{max}=360. These high degree expansions can be used to evaluate quantities such as geoidal heights, gravity anomalies, gravity disturbances and deflections of the vertical with respect to a geocentric ellipsoid. The theory of spherical harmonics used to determine the potential of the earth is given in Heiskanen and Moritz (1967, p. 57) and Torge (1980, p. 26).

The coefficients, C_{nm} and S_{nm}, up to degree (n) and order (m) for a high order geopotential model are determined by a combination of data from analysis of orbit perturbations of satellites, mean terrestrial gravity values for different sized blocks and N values at crossover points in ocean areas measured by satellite altimetry. The long wavelength geoidal features determined from satellite analysis are found in the low order terms of the model whilst the short wavelength, higher frequency information found from the satellite altimetry and terrestrial gravity is reflected in the higher order terms. Geopotential models to degree 180 are capable of detecting geoidal features with a half wavelength of 1°, or 110 km, to an accuracy of ±0.2 m (Kearsley, 1984, p. 94) and ±0.5 m in Canada (Schwarz and Sideris, 1985, p. 16).

The most commonly used high order geopotential models and the input data used to determine them is given in Table 5.1.

Geopotential model OSU86E excludes geophysically predicted gravity anomalies and OSU86F includes such gravity anomalies over areas where there is no terrestrial gravity data such as Africa, South America and USSR. The use of either model should make little difference over Australia because of the good coverage of gravity data over the continent.

MODEL	DEGREE	ORIGIN	DATE	INPUT DATA
OSU81	180	Rapp	1981	GEOS 3 data + 1° surface gravity + SEASAT altimetry
GRIM 3	36	Reigber	1983	
GEM-L2	20	Lerch	1984	SLR + GEM 9 data
GPM2	200	Wenzel	1985	GEM-L2 + 1° surface gravity + altimetry
OSU 86C, D	250	Rapp, Cruz	1986	as above
OSU 86E, F	360	Rapp, Cruz	1986	as above + 30' surface gravity

Table 5.1 Earth gravity models.

The geoidal height (N_L) and gravity anomaly (Δg_L) of a point, in spherical harmonics, is (Rapp, 1982)

$$N_L = \frac{kM}{\gamma R} \sum_{n=2}^{n_{max}} \left(\frac{a}{R}\right)^2 \sum_{m=0}^{n} P_{nm}(\cos\theta)\,(C_{nm}\cos m\lambda + S_{nm}\sin m\lambda) \tag{5.16}$$

$$\Delta g_L = \frac{kM}{R^2} \sum_{n=2}^{n_{max}} (n-1) \sum_{m=0}^{n} P_{nm}(\cos\theta)\,(C_{nm}\cos m\lambda + S_{nm}\sin m\lambda) \tag{5.17}$$

where; kM is the gravitational constant,

R is the geocentric radius,

γ is the normal gravity from (2.7),

θ is the geocentric latitude,

λ is the geocentric longitude,

a is the equatorial radius of the reference ellipsoid,

C_{nm} and S_{nm} are the fully normalised potential coefficients,

n and m are the degree and order of the geopotential model,

$P_{nm}(\cos\theta)$ are the associated Legendre functions of the first kind.

The computation must be performed on a computer as there are 16,471 coefficients each for C_{nm} and S_{nm} for a geopotential model with n_{max}=180, such as OSU81 and 65,341 coefficients for a geopotential model with n_{max}=360, such as OSU86E,F.

Intuitively we would expect that with higher order models the geoidal heights would be more accurate. This is generally, but not always, so. The accuracy of geoidal heights varies from region to region throughout the world. The principal error sources in the high order terms of the geopotential coefficients comes from the gravity data itself, the sampling and smoothing techniques. Rapp and Cruz (1986, p. 10) estimate that the magnitude of the noise is equal to the signal near degree 175 and that there is a 100% uncertainty in the coefficients above that degree for models OSU86E,F.

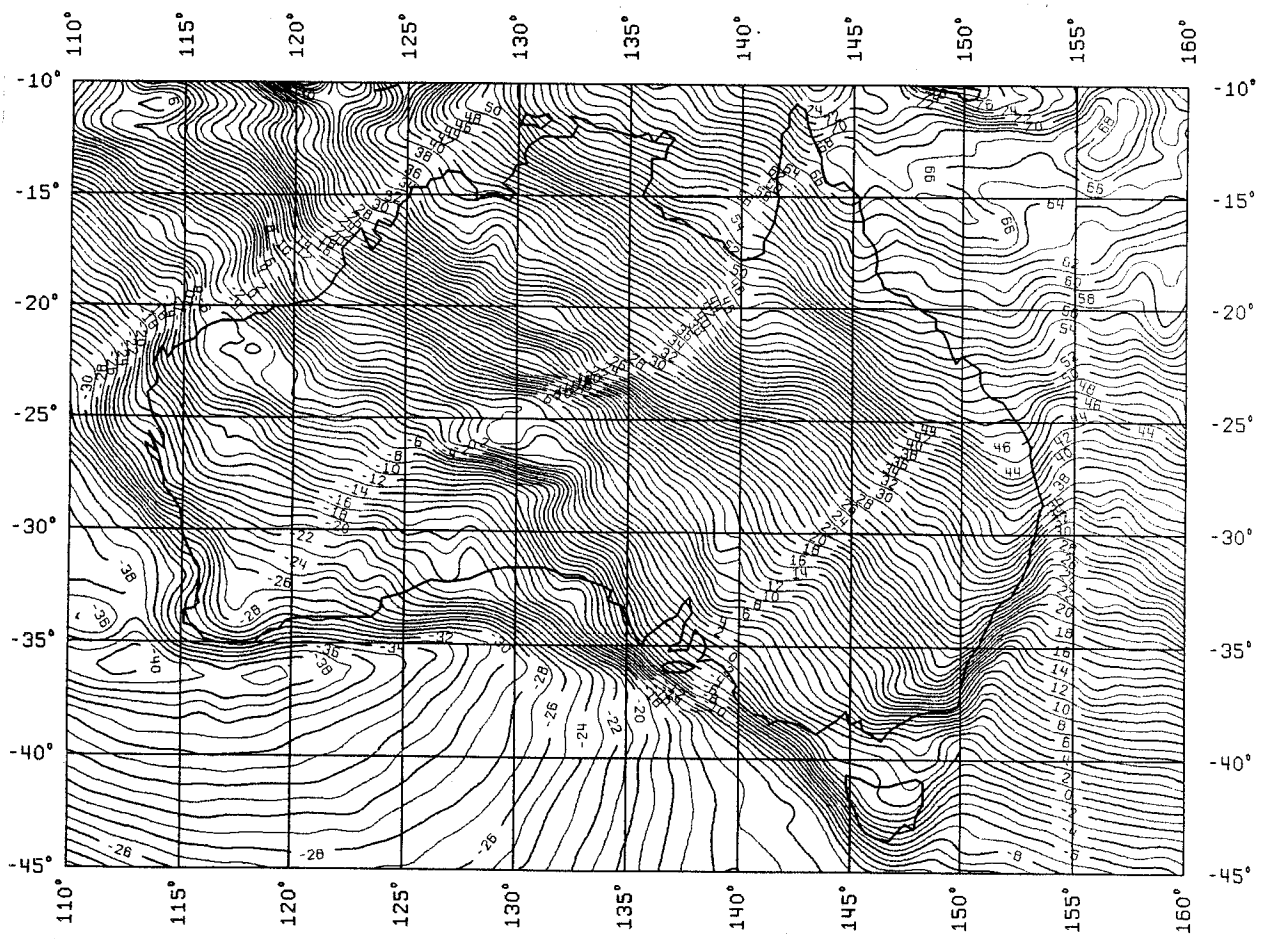

Figure 5.2 Australian geoid based on OSU86F to degree 360.
(Rapp and Cruz, 1986)

They also warn that "just because we have a high degree field, it does not mean we have a highly accurate high degree field" (ibid, p 21). However, it is still the best estimate of the higher order coefficients we have and can be used to recover a lot of useful information. Figure 5.2 shows a geoid map of Australia generated on a 1°x1° grid using geopotential model OSU86F to degree 360 showing very fine detail.

The agreement between gravity anomalies generated from geopotential model OSU81 at degree 180 and observed gravity anomalies for a 2°x2° grid over the Australian continent is investigated in Section 5.4.1.

5.4 Gravimetric Methods.

The first gravity measurement made in Australia was in 1819 by a Frenchman named Freycinet in Sydney using a one second pendulum (Dooley and Barlow, 1976). Very few gravity observations were made thereafter until the 1950's when the government introduced the Petroleum Search Subsidy Act which offered financial assistance to private oil exploration companies and the Bureau of Mineral Resources (BMR) to search for oil. Helicopters were also able to be used to gather data which greatly increased the number of observations that could be made.

Gravity observations were connected to first order gravity base stations across Australia which were then tied into the international gravity network called the Potsdam system. All the gravity traverses were adjusted by least squares to form the Australian National Gravity Network (ANGN) Isogal 65. In 1971 the International Union of Geodesy and Geophysics (IUGG) adopted a new international gravity reference system, the International Gravity Standardization Net 1971 (IGSN 71), which differed from the old system at Potsdam by -14.0 mGal. A provisional formula allows gravity data in the Isogal 65 system to be converted to the IGSN 71 system in Australia (ibid, p 268).

All onshore and offshore gravity data observed by the BMR and private companies has been collected together to form the Australian gravity

database and is in the custody of the BMR. The gravity data is kept in two formats, the first is a file of all gravity stations with each record containing the following information,

1) the BMR gravity station number,

2) the latitude and longitude of the station,

3) the observed gravity value, adjusted and referenced to the Isogal 65 system,

4) the terrain and station height adjusted to AHD (they are usually the same).

The second format gives mean Bouger gravity anomalies on a 6'x6' grid covering the continent and near offshore areas.

The School of Surveying at the University of New South Wales (UNSW) has an edited version of the BMR point gravity database which is used for all gravimetric geoid solutions. The editing has purged all detected gross errors from the BMR gravity data and grouped the data into geographically defined files. Data purged from the BMR database falls into one of the following categories,

* all header information,

* all duplicate points,

* all records with missing information,

* all points with a ground height greater than Mt. Kosciusko,

* all points north of latitude 8°,

* all points where the free air gravity anomaly is greater than 250 mGal.

The UNSW version of the gravity database contains 443,754 gravity data points in 7 files ordered in approximately 5° latitude bands across Australia.

FILE	LATITUDE LIMITS (degrees)	GRAVITY POINTS
1	-46.23 to -40	15,616
2	-40 to -35	35,682
3	-35 to -30	68,265
4	-30 to -25	130,459
5	-25 to -20	92,766
6	-20 to -15	72,181
7	-15 to - 8	28,785
	TOTAL	443,754

Table 5.2 Gravity data in the UNSW gravity database.

The density of gravity stations over the Australian continent varies greatly from no gravity data at all in the Gulf of Carpentaria, sparse coverage off the south east coast of Australia to very dense coverage off the north west Australian coast, Kimberely region and centre of the continent.

The average spacing between gravity stations is 11 km except in South Australia and Tasmania where the average spacing is 7 km (Gilliland, 1987, p. 578). Figure 5.3 shows the number of gravity data points in 2°x2° blocks over the continent and near offshore areas.

The accuracy of the gravity data in the national network is estimated to have a standard error of ± 0.2 mGal (Anfiloff et al, 1976, p. 275) to ± 0.5 mGal (Gilliland, 1987, p. 579) relative to the network as a whole. The precision of the marine surveys is estimated from the differences of gravity misties at line intersections to be ± 2-6 mGal (Anfiloff et al, 1976). With these accuracies the gravity data fulfils the requirements for the computation of a gravimetric geoid to an accuracy of 5 cm outlined by Kearsley (1986, p. 9200) providing there is no significant deterioration in accuracy when estimating mean values for 10km x 10km blocks.

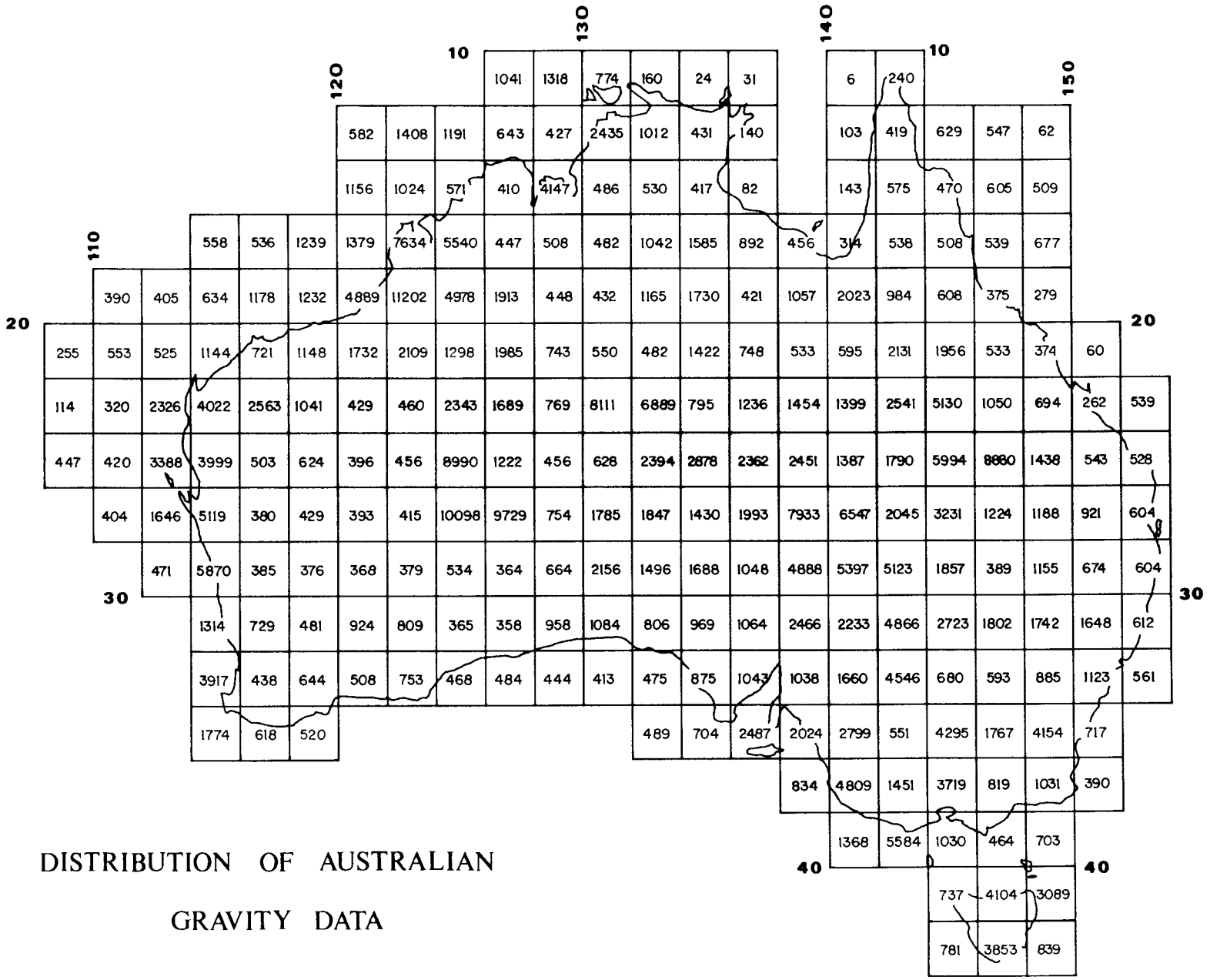
110
120
130
140
150
10
20
30
40
DISTRIBUTION OF AUSTRALIAN
GRAVITY DATA

Figure 5.3

5.4.1 The Agreement Between OSU81 and the ANGN.

It was said in Section 5.3 that the ability of high order geopotential models to model the geoid and terrestrial gravity varies according to the model used, the degree and order of the model and the behaviour of the geoid in the region in which the computation is made. We have investigated this further by computing gravity anomalies using model OSU81 to degree 180 and comparing them to terrestrial gravity anomalies over the Australian continent. The comparisons were made at all gravity points and grouped into the same 2°x2° blocks in Figure 5.3. An average value was then computed for each block.

The procedure used was to compute gravity anomalies (Δg_L) using equation (5.17) and the coefficients from geopotential model OSU81 to n_{max}=180 on a 0.1°x0.1° grid. A computer program by Rizos (1979) was used to compute the mesh of Δg_L.

Each terrestrial gravity point at a height H in a block was reduced to the geoid by applying the free air correction,

$$g' = g + 0.3086H \tag{5.18}$$

and the free air anomaly computed by subtracting the normal gravity (γ) found from equation (2.7),

$$\Delta g = g' - \gamma_\phi \tag{5.19}$$

A model gravity anomaly was then interpolated from the gravity anomalies at the grid intersections for the same position as the gravity point. A surface was used whose equation is

$$\Delta g_L = ax + bxy + cy + d \tag{5.20}$$

where x and y are the local coordinates of the gravity point in a block, and
a, b, c and d are the coefficients defining the surface.

The grid intersections of a block were assigned local coordinates,

$$\begin{array}{ll} (0,1,\Delta g_2) & (1,1,\Delta g_4) \\ (0,0,\Delta g_1) & (1,0,\Delta g_3) \end{array}$$

so that the coefficients a, b, c and d could be easily solved,

$$a = \Delta g_3 - \Delta g_1$$
$$b = \Delta g_4 - \Delta g_3 - \Delta g_2 + \Delta g_1$$
$$c = \Delta g_2 - \Delta g_1$$
$$d = \Delta g_1$$

The residual gravity anomaly ($\Delta g'$) was then found by simply subtracting the two,

$$\Delta g' = \Delta g - \Delta g_L \tag{5.21}$$

This procedure was repeated for each gravity point in a block and a mean residual gravity anomaly calculated by,

$$\overline{\Delta g'} = \sum_{i=1}^{n} \frac{\Delta g'}{n} \tag{5.22}$$

where n is the number of gravity points in each 2°x2° block. The means of all the blocks were then placed into four categories in increasing magnitude. We have found from experience that these categories approximately relate to differences in geoidal heights differences (δN), found using Equation (6.4), expressed as a fraction of the baseline length in parts per million (Kearsley and Holloway, 1987),

Category 1	0-5m Gal	$\rightarrow \delta N$ = 0-5 ppm,
Category 2	5-13 mGal	$\rightarrow \delta N$ = 5-10 ppm,
Category 3	13-21 mGal	$\rightarrow \delta N$ = 10-15 ppm,
Category 4	>21 mGal	$\rightarrow \delta N > 15$ ppm.

The results are presented in Figure 5.4. One can see that OSU81 is able to model gravity anomalies over 60% of the Australian continent to within 5 mGal and over 90% of the continent to within 13 mGal. However, the west coast of Australia, near Perth and the centre of the continent are very poorly represented by OSU81. This is probably due to short wavelength geoidal features in these areas not being detected by the geopotential model. There is also a noticeable decay on the east coast of Australia at the coastline which is probably due to the land-water boundary and the mountain ranges that run parallel to the east coast.

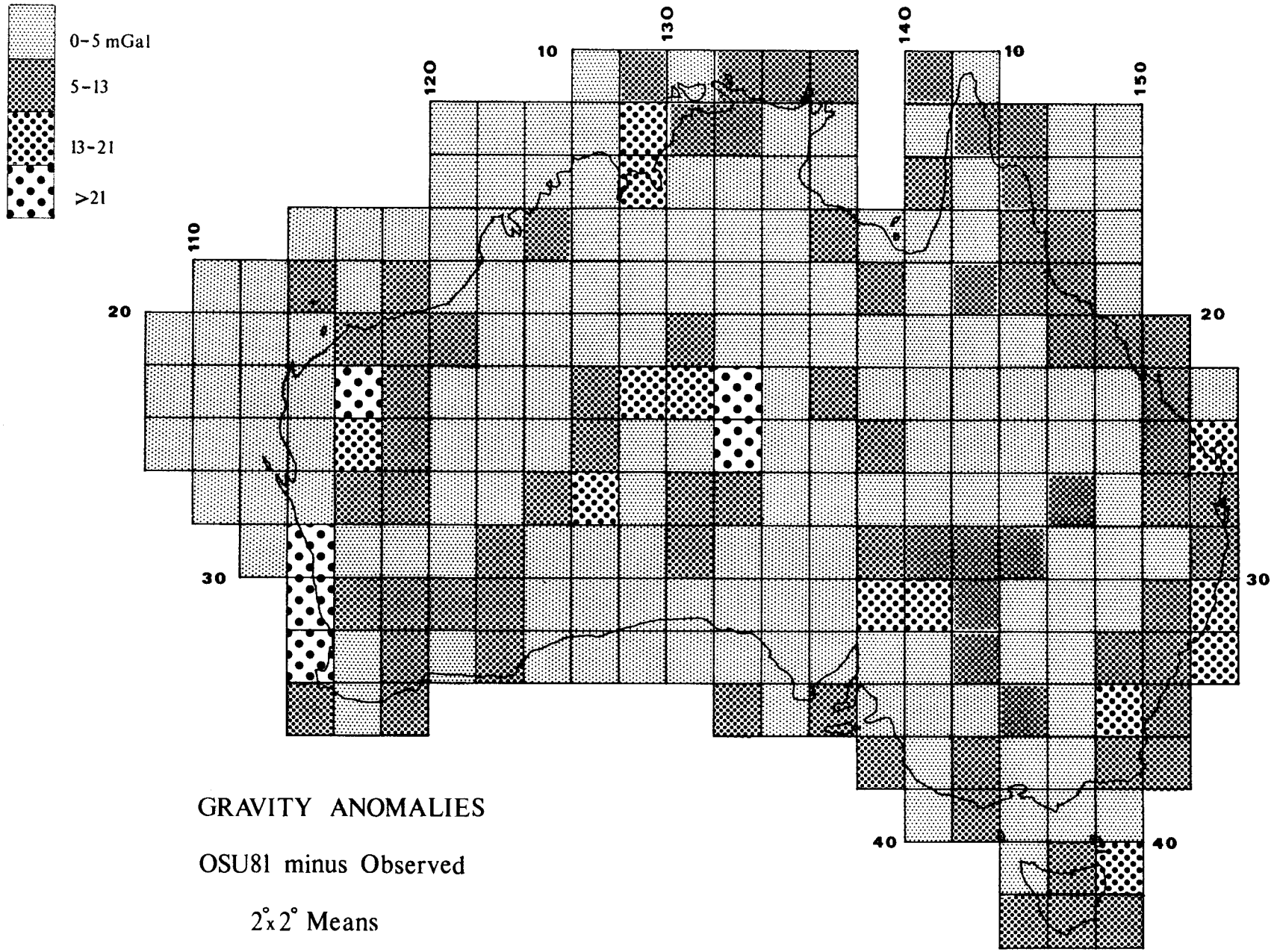
0-5 mGal
5-13
13-21
>21
110
120
130
140
150
10
20
30
40
GRAVITY ANOMALIES
OSU81 minus Observed
2°x2° Means

Figure 5.4

5.5 Stokes' Theorem.

The classical form of the geodetic value problem can be expressed by the disturbing potential (T) defined by,

$$T = W - U \tag{5.23}$$

where W is the actual gravity potential and U is the potential referenced to an ellipsoid. If the centrifugal forces of the geoid and ellipsoid are equal, then the Laplace equation

$$\nabla^2 T = 0 \tag{5.24}$$

is satisfied external to all the masses of the earth. This presupposes that all gravity measurements have been reduced to the geoid. The height N of the geoid above the reference ellipsoid is given by Bruns' formula[4],

$$N_p = \frac{T_p - (W_p - U_q)}{\gamma_q} \tag{5.25}$$

the subscripts p and q denoting the points on the geoid and ellipsoid respectively and γ_q is the normal gravity on the ellipsoid. However, if a value of U_q is chosen to be equal to W_p (as the position of the reference ellipsoid can be selected arbitrarily without changing the gravity field), equation (5.25) reduces to,

$$N_p = \frac{T_p}{\gamma_q} \tag{5.26}$$

and N will refer to a "best fitting" geocentric reference ellipsoid.

The solution for the disturbing potential (T) can be accomplished by the Stokes' integral[5] (Torge, 1980, p. 157). However, by incorporating equation (5.26), it is more common for it to be used to solve for the geoidal height,

$$N_p = \frac{R}{4\pi\gamma_m} \int\int_{\sigma} \Delta g \, S(\psi) \, d\sigma \tag{5.27}$$

---

4 Bruns' Theorem in 1878.

5 George Gabriel Stokes (1819-1903) was an English physicist.

where R is the radius of the spherical model of the earth,

γ_m is the mean gravity of the earth,

Δg is the free air gravity anomaly associated with $d\sigma$,

ψ is the spherical distance between p and $d\sigma$,

$S(\psi)$ is the Stoke's function, equation (5.28)

$d\sigma$ is the element of surface area σ over which the integration is performed.

The function $S(\psi)$ is

$$S(\psi) = \operatorname{cosec}\frac{\psi}{2} - 6\sin\frac{\psi}{2} + 1 - 5\cos\psi - 3\cos\psi \ln\left(\sin\frac{\psi}{2} + \sin^2\frac{\psi}{2}\right) \tag{5.28}$$

The integration is, in theory, performed over the whole earth. This assumes we have a perfect knowledge of the continuous gravity field over all the oceans and land masses. However this is not so, as our knowledge of the gravity field is in the form of discrete points limited to only some of the oceans and land masses. Therefore, in practice, the surface integrals are replaced by a finite summation restricted to a limited area defined by geographical blocks or to a cap defined by rings and radial lines.

The former method of subdivision by grid lines fixed by geographical coordinates ϕ and λ is described in Heiskanen and Moritz (1967, p. 117-119) and is favoured by Gilliland (1982;1983) and others. The gravity anomalies (Δg_i) are replaced by the mean gravity anomaly ($\Delta \bar{g}_i$) for the midpoint of compartment i. Equation (5.27) becomes,

$$N_p = \frac{R}{4\pi\gamma_m} \sum_i S(\psi)_i \, \Delta \bar{g}_i \, d\sigma_i \tag{5.29}$$

The behaviour of the Stokes' function $S(\psi)$ is non-linear and tends to infinity close to the computation point (see Figure 5.5). To reduce the error in the $S(\psi)$ term the earth's surface is divided into several zones. The compartment size within each zone is reduced so that a finer and finer mesh of mean gravity anomalies is used as the summation approaches the computation point, that is, as $\psi \to 0$. Table 5.3 gives a typical computation strategy.

Zone	Range of ψ	Compartment size within zone
Outer	$\psi > 20°$	5° equal area blocks.
Middle	$5° < \psi < 20°$	1°x1° geographical blocks.
Near	$1.5° < \psi < 5°$	0.5°x0.5° geographical blocks.
Inner	$0.2° < \psi < 1.5°$	0.1°x0.1° geographical blocks.
Innermost	$\psi < 0.2°$	0.1°x0.1° geographical blocks and point values.

Table 5.3 Compartment sizes of geographic blocks.
(Gilliland, 1982, p. 50)

This method has the advantage that once the mean gravity anomalies have been computed for each compartment they can be stored efficiently in a computer and used again and again in subsequent computations.

An alternative method of computing N using the Stokes' formula is to perform the integration over a spherical cap centred on the computation point P with a maximum radius ψ_0. The compartments are formed by radial lines with azimuth α and concentric rings in increasing radius from 0 to ψ_0. Equation (5.26) now becomes,

$$N_p = \frac{R}{4\pi\gamma_m} \int_{\psi=0}^{\pi} \int_{\alpha=0}^{2\pi} \Delta g \, F(\psi) \, d\psi d\alpha \tag{5.30}$$

where the kernel function $F(\psi)$ is (Kearsley, 1985, p. 80)

$$F(\psi) = S(\psi) \sin\psi \tag{5.31}$$

and alternately,

$$F(\psi) = 2\cos\frac{\psi}{2} - \sin\psi\left(6\sin\frac{\psi}{2} - 1 + \cos\psi\left(5 + 3\ln\left(\sin\frac{\psi}{2} + \sin^2\frac{\psi}{2}\right)\right)\right) \tag{5.32}$$

Both the Stokes' function $S(\psi)$ and the modified Stokes' function $F(\psi)$ may be viewed as a weighting function that scales the gravity anomalies. They both go to zero near $\psi = 39°$ and $\psi = 118°$, but as $\psi \to 0$ $S(\psi) \to \infty$ whilst

$F(\psi) \to 2.0$. Therefore $F(\psi)$ has the great advantage over $S(\psi)$ in that it is much more stable as $\psi \to 0$. This means that any errors in the point gravity data or in the mean gravity anomalies of the compartments or blocks, and especially near the computation point, are contained.

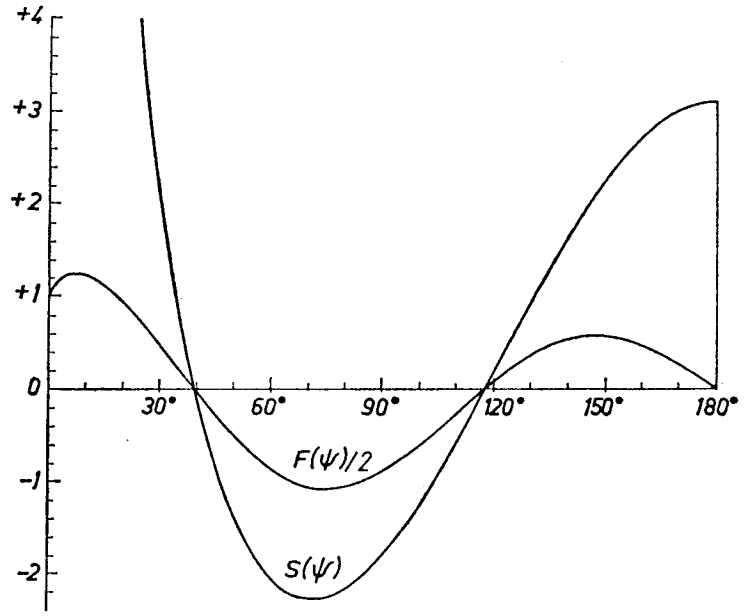

Figure 5.5 Behaviour of $S(\psi)$ and $F(\psi)/2$.
(Heiskanen and Moritz, 1967, p. 96)

This method of ring integration also has the great advantage of being both flexible and simple. Before the advent of the electronic computer the computation was performed partly graphically using a a template made by drawing rings on transparent material and placing it over a gravity map. The contribution of each compartment to the geoid height at P could then be calculated for all gravity points inside the rings on the template (Heiskanen and Moritz, 1967, p. 117). Today a computer can generate the rings at each point quickly and calculate the mean gravity anomalies for each compartment without the need to "precompute" mean gravity values for different sized zones as in the first method.

5.6 Collocation.

Least squares collocation (Lat.: collocare - to place together, combine), is a method of determining any quantity in the earth's anomalous gravity field by combining geodetic measurements of different kinds. The main purpose of collocation is to predict signal quantities from measurements that contain observational errors (noise) and filter the observations to estimate and then remove the noise.

The basic equation of the least squares adjustment can be written as,

$$measurement = mathematical\ model + noise + signal$$

which can be written in general vector notation (Torge, 1980, p. 193),

$$\underline{\hat{x}} = \underline{AX} + \underline{n} + \underline{s} \tag{5.33}$$

where $\underline{\hat{x}}$ is the vector of observations, such as gravity anomalies,
$\underline{A}$ is the design matrix from the mathematical model,
$\underline{X}$ is the vector of unknowns, such as geoidal heights and deflections,
$\underline{n}$ is the vector of random measuring errors (noise),
$\underline{s}$ is the vector of signal components in the observations,
$\underline{AX}$ is the systematic part, such as the ellipsoid reference system and modelled systematic errors.

The least squares estimates of $\underline{X}$ and $\underline{s}$ can be obtained by demanding that,

$$\underline{V}^T P \underline{V} = minimum$$

where $\underline{V}$ is the vector of residuals,$(\underline{n} + \underline{s})$,
P is the weight matrix,
$\underline{V}^T$ is the transpose of $\underline{V}$.

The parameter vector $\underline{X}$ can be an estimate of the geoidal height $\underline{N}$ by,

$$\underline{N} = (\underline{A}^T \overline{C}^{-1} \underline{A})^{-1} \quad \underline{A} \overline{C}^{-1} \Delta g \tag{5.34}$$

where $\underline{\underline{C}}$ is the covariance matrix, derived from the covariance function of the gravity anomalies (Δg) in the region of the computation.

Collocation is a very flexible method that has been used successfully by a number of researchers (Tscherning and Forsberg, 1986; Schwarz et al, 1987; Hein, 1985; Engelis et al, 1984) to compute geoidal heights. Its strength lies in the fact that it can use heterogeneous data such as gravity anomalies, deflections of the vertical and satellite altimetry together in the same prediction. However, instabilities may result when there is a large number of data points very close together creating a large covariance matrix which has to be inverted. In rugged terrain, collocation gives poor results unless the topography is accounted for by using a Digital Terrain Model (DTM) (Tscherning and Forsberg, 1986).

6 A COMBINED SOLUTION - RINT.

The technique in equation (5.30), preferred by Mather (1973) for high precision evaluations and shown by Kearsley (1984) to be capable of evaluating ΔN to a similar precision as that of Δh from GPS, is a combined solution called "ring integration" or RINT.

This method involves the evaluation of the Stokes' integral over an inner spherical cap to solve for the short wavelength contribution N_S which is combined with a remote zone contribution from a high order geopotential model to provide the medium to long wavelength contribution N_L. The total geoidal height will be the sum of the two components (Kearsley, 1988b)

$$N = N_L + N_S \tag{6.1}$$

The remote zone contribution to the geoid height N_L is found using geopotential model OSU81 and evaluated using equation (5.17) to degree n_{max}=180,

$$N_L = \frac{kM}{\gamma R} \sum_{n=2}^{n_{max}} \left(\frac{a}{R}\right)^2 \sum_{m=0}^{n} P_{nm}(\cos\theta)\,(C_{nm}\cos m\lambda + S_{nm}\sin m\lambda)$$

It is possible, in the future, that much higher order geopotential models may be able to compute N to sufficient accuracy by themselves. It is only the inconsistent coverage of gravity data in some parts of the world and the unavailability of a supercomputer, needed to compute the coefficients, that is retarding progress in this field.

The half wavelength signal in N is theoretically π/n_{max}, so that OSU81 at n_{max}=180 can recover geoidal features with half wavelengths of 1°. Therefore it is theoretically correct to compute N_S over a spherical cap with maximum radius $\psi_0 \approx 1°$ using Stokes' formula and the modified Stokes' function $F(\psi)$ from equation (5.32),

$$N_S = \frac{R}{4\pi\gamma_m} \int_{\psi=0}^{\psi_0} \int_{\alpha=0}^{2\pi} \Delta g' F(\psi)\, d\psi d\alpha \tag{6.2}$$

where the **residual** gravity anomaly ($\Delta g'$) is found by subtracting the modelled gravity anomaly (Δg_L) generated by OSU81 using equation (5.17) from the terrestrial gravity anomaly (Δg) using equation (5.19),

$$\Delta g' = \Delta g - \Delta g_L \tag{6.3}$$

The use of residual gravity anomalies avoids duplication of the signal when the inner zone is combined with a remote zone which would cause a "double counting" effect. An alternative method would be to omit the contribution of N_L inside the spherical cap.

The Stokes' integral is evaluated in compartments generated by concentric rings with radius $0 < \psi \leq \psi_0$ incrementing in $\approx 0.1°$ steps and radial lines radiating from the computation point with a constant change in azimuth ($d\alpha$) of 10° (Kearsley, 1985, p. 83). The contribution per mGal to N_S for each compartment inside the cap is $C_{N,}$ determined by Kearsley (1988b) to be 0.3 mm/mGal which reflects the density of gravity data available.

If N is evaluated at each end of a GPS baseline and then differenced, we call the change in geoid height ΔN_{grav}. By differencing over typical baseline lengths systematic errors will tend to cancel. Such errors may include,

* the assumption of a spherical earth adopted for the Stokes' formula,

* the reference surface of the levelling network not being coincident with the geoid introducing an error in the reduction of gravity data to the geoid,

* any errors in the high order terms of the geopotential model.

ΔN_{grav} is then compared with $\Delta N_{GPS-levelling}$ acting as control, using equation (5.3), at GPS stations that also have levelled heights,

$$\delta N = \Delta N_{GPS-levelling} - \Delta N_{grav} \tag{6.4}$$

The difference (δN) can be expressed as a fraction of the baseline length (s), in parts per million (ppm),

$$p = \left| \frac{\delta N_{AB}}{s_{AB}} \right| 10^6 \tag{6.5}$$

and the mean of the differences for n baselines in the network can be calculated by

$$m = \sum_{i=1}^{n} \frac{p_i}{n} \tag{6.6}$$

The flexibility of RINT is evident as accumulated ring contributions for successive rings, coupled with the remote zone contribution, can be analysed for all ring combinations from 0 (at which only the geopotential model is being tested) to ψ_0, to determine the smallest mean differences in m and hence the optimum cap size.

6.1 UNSW Gravimetric Geoid Programs.

The foregoing strategy to compute gravimetric geoids using RINT has been implemented in a suite of programs written in FORTRAN 77 and running on a VAX computer. A flowchart of the logic behind the programs is shown in Figure 6.1.

GRAV00 - is based on a program by Rizos (1979), calculates gravity anomalies (Δg_L) using a geopotential model on a 0.1°x0.1° grid covering the GPS network. The input parameters, such as the south west corner of the network, the extent of the network, grid interval and geopotential model used are read in from a separate file. The coefficients n, m, C_{nm} and S_{nm} for the geopotential model, usually OSU81, are also read in from a separate file.

GRAV06 - by Donnelley (1988), extracts the gravity data from the Australian gravity database for an area covering the GPS network. The gravity data is converted into the IGSN 71 system, reduced to the geoid and the normal gravity subtracted to give point gravity anomalies. A point gravity anomaly from the geopotential model is interpolated from the 0.1°x0.1° grid,

using equation (5.20). The residual gravity anomaly for all points in the network is then found using equation (6.3) and written to a file.

GRAV01 - by Kearsley (1985), generates the rings and performs the ring integration in the residual gravity anomaly field, output from GRAV06, using the Stokes' formula and the modified Stokes' function from equation (6.2). The residual gravity anomalies can be optionally supplemented with terrain height information from a DTM. An input parameters file tells the program the number of rings to generate, the contribution to N for each compartment per mGal (C_N) and the geographic coordinates of each station in the network. Output from the program is the accumulated contribution for each ring, at each point, to N_S.

GRAV02 - based on a program by Rapp (1982), calculates the remote zone contribution N_L at each point using the same geopotential model used in GRAV00. The input parameters file specifies the flattening factor of the reference geocentric ellipsoid, the degree and order of the model and the geographic coordinates of each station in the network.

GRAV08 - compares ΔN_{grav} for all points in the network with $\Delta N_{GPS-levelling}$ at those stations that have both GPS heights and AHD heights. An input points file gives the point number, geographic coordinates and GPS height for all points in the network. The lines file specifies each line to be analysed as the difference between two points. The statistics generated include the individual baseline lengths, the differences in δN, the differences in δN as a fraction of the baseline length in ppm and the means and standard deviations of all of the above.

The UNSW gravimetric geoid programs have been used successfully to calculate ΔN for GPS networks in New Mexico and Ohio, USA (Kearsley, 1985), Ontario and Manitoba, Canada (Kearsley, 1988b) and Western Australia and South Australia detailed in Section 7.

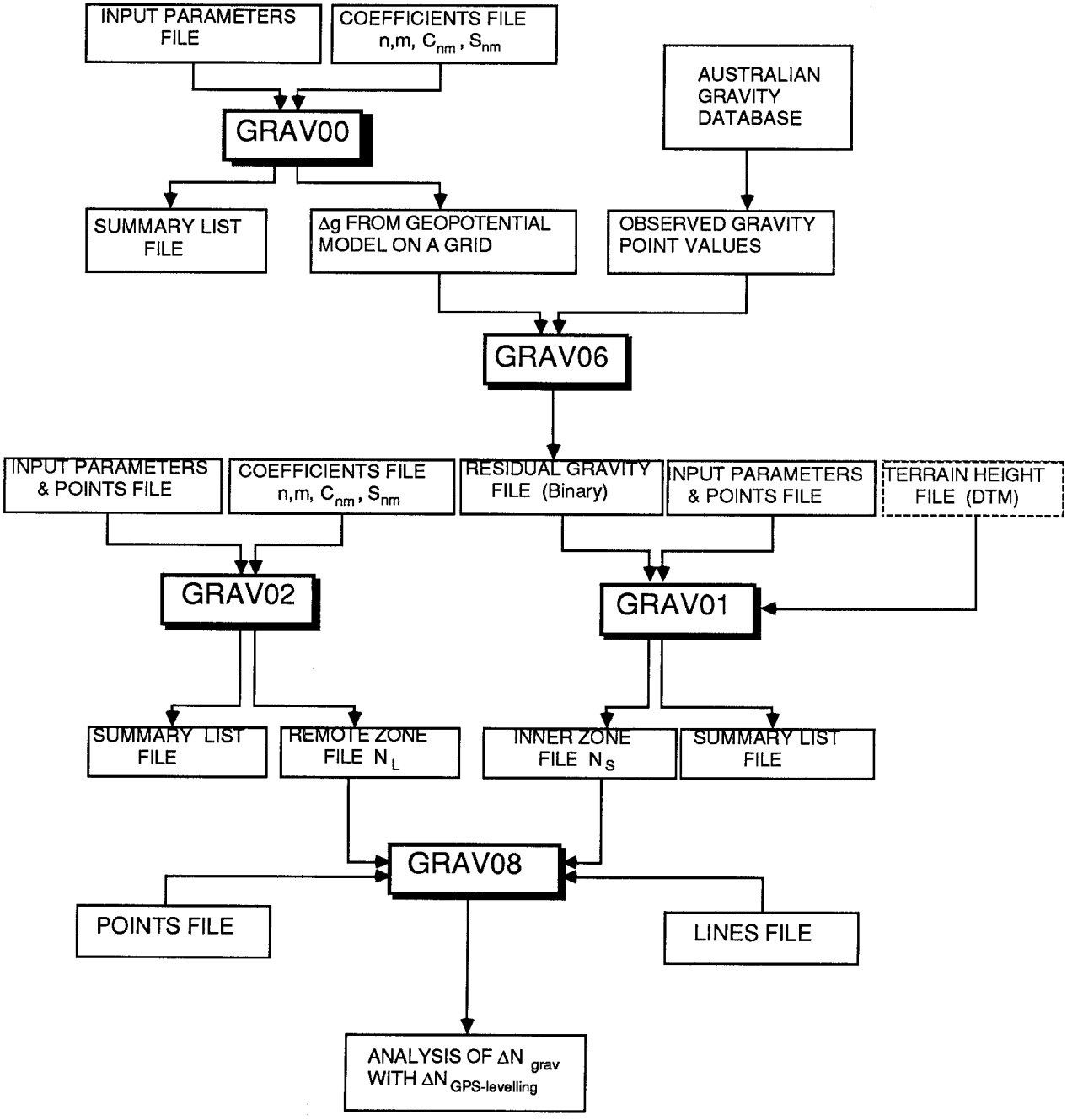
INPUT PARAMETERS FILE
COEFFICIENTS FILE n,m, C_{nm}, S_{nm}
AUSTRALIAN GRAVITY DATABASE
GRAV00
SUMMARY LIST FILE
Δg FROM GEOPOTENTIAL MODEL ON A GRID
OBSERVED GRAVITY POINT VALUES
GRAV06
INPUT PARAMETERS & POINTS FILE
COEFFICIENTS FILE n,m, C_{nm}, S_{nm}
RESIDUAL GRAVITY FILE (Binary)
INPUT PARAMETERS & POINTS FILE
TERRAIN HEIGHT FILE (DTM)
GRAV02
GRAV01
SUMMARY LIST FILE
REMOTE ZONE FILE N_L
INNER ZONE FILE N_S
SUMMARY LIST FILE
GRAV08
POINTS FILE
LINES FILE
ANALYSIS OF ΔN_{grav} WITH $\Delta N_{GPS\text{-}levelling}$

Figure 6.1

7 NETWORKS ANALYSED

The accuracy requirements for users of height information, the precision of σ_N or $\sigma_{\Delta N}$, vary with the type of application, the region in which the heights are required and the user's access to geopotential models and terrestrial gravity data. The models are readily available from their authors and the gravity data from the BMR, at a cost, and so should not inhibit the evaluation of ΔN to the highest possible precision.

Usually heights are not needed to the same precision in remote areas of Australia as in urban areas and therefore a strategy to compute ΔN should reflect this. Either a lower order method could be selected, or gravity databases computed on a grid interval matching the requirements and needs of the region, similar to the "red line" concept advocated by Kearsley (1988a, p. 16) which has been used for standard mapping in Australia.

For users of height information, the orders of accuracy required and possible methods of evaluating N or ΔN have been summarised by Kearsley (1988a,p 17), and reproduced in Table 7.1.

N used for	Accuracy specification for N	Possible means of evaluating N
1. geophysical exploration and reconnaissance surveys	Low: $\sigma_N \approx \pm$5-10 m	Low order (n_{max}=36) geopotential models
2. Transforming between geodetic datums	3rd order: $\sigma_N \approx \pm$1-2 m	High order (n_{max}=180) geopotential models
3. Control surveys for large scale mapping, engineering projects	2nd order: $\sigma_{\Delta N} \approx \pm$10-20 cm over 20 km (5-10 ppm)	a) Surface fitting of N - program LESQPL b) Detailed gravimetric solution - RINT
4. Height control	1st order: $\sigma_{\Delta N} \approx \pm$20-30 cm over 110 km (2-3 ppm)	Detailed gravimetric solution - RINT

Table 7.1 Geoid requirements and methods of evaluation.

A comparison of these methods to first, second and third order accuracies was undertaken for this study for two very different GPS observed networks. The GPS networks are situated in Western Australia and South Australia.

The Western Australian network is situated in the south west seismic zone, approximately 110 km from Perth and consists of 10 stations (see Appendix A). The extent of the network is approximately 76 km north-south and 40 km east-west, the bounds being,

$$-31.5° < \phi < -30.8°$$
$$116.5° < \lambda < 117.0°$$

All the stations have been observed previously by conventional surveying techniques at different epochs in order to determine tectonic movements in the area. The stations have first or second order heights which were used as control to determine $\Delta N_{GPS-levelling}$.

The South Australian Phase 1 GPS network is situated east of Adelaide in the Murray Mallee region which abuts the state border with Victoria. The network was observed to extend the major first order geodetic network over this region. There are 107 stations in the network, of which only the northerly 73 stations were used in this study (see Appendix B). The extent of the network is approximately 170 km north-south and 125 km east-west, the bounds being,

$$-35.8° < \phi < -34.3°$$
$$139.5° < \lambda < 141.0°$$

Height control within the network was sparse, with those stations on the northern, western and southern perimeter of the network having AHD heights. The heights were generally of third or fourth order accuracy spirit levelling and also with some trigonometric heights. These heights were supplemented, after the completion of the GPS survey, by additional spirit levelled heights by the Australian Survey Office (ASO) throughout the network. These additional heights were generally of second order accuracy.

Both the Western Australian and South Australian networks were observed in October-December, 1985 by Geo/Hydro, Inc. for the Western Australian Department of Land Administration and the South Australian Department of Lands using three to four Macrometer V-1000 GPS receivers and a Trimble 4000A time receiver which was used to obtain UTC for the synchronisation of the other receivers (Geo/Hydro, 1986; Larden et al, 1986).

7.1 Western Australian Network.

The Western Australian GPS network consists of 10 stations, making 19 lines observed (see Figure 7.1). The GPS observations were processed using Macrometer programs INTRFT and LSQT on a baseline by baseline basis using the broadcast ephemerides. The computed baseline vectors were given in spherical coordinates as latitude (ψ), longitude (λ) and radius *(R)* from the centre of the earth to the station in the WGS72 system (Geo/Hydro, 1986). The geodetic coordinates (ϕ,λ,h), were found by converting the spherical coordinates first to cartesian coordinates (x,y,z) using (Heiskanen and Moritz, 1967, p. 40),

$$\begin{aligned} x &= R\cos\psi\cos\lambda \\ y &= R\cos\psi\sin\lambda \\ z &= R\sin\psi \end{aligned} \tag{7.1}$$

and then iteratively finding the inverse solution for ϕ,λ,h (Heiskanen and Moritz, 1967, p. 182),

$$\begin{aligned} x &= (\nu + h)\cos\phi\cos\lambda \\ y &= (\nu + h)\cos\phi\sin\lambda \\ z &= (\nu(1-e^2) + h)\sin\phi \end{aligned} \tag{7.2}$$

where ν is the radius of curvature in the prime vertical,

$$\nu = \frac{a}{\sqrt{(1 - e^2\sin^2\phi)}} \tag{7.3}$$

and a and e^2 are the radius of the semi-major axis and the first eccentricity of the reference ellipsoid (WGS72). The difference in GPS heights (Δh) between stations is found simply by subtracting the two.

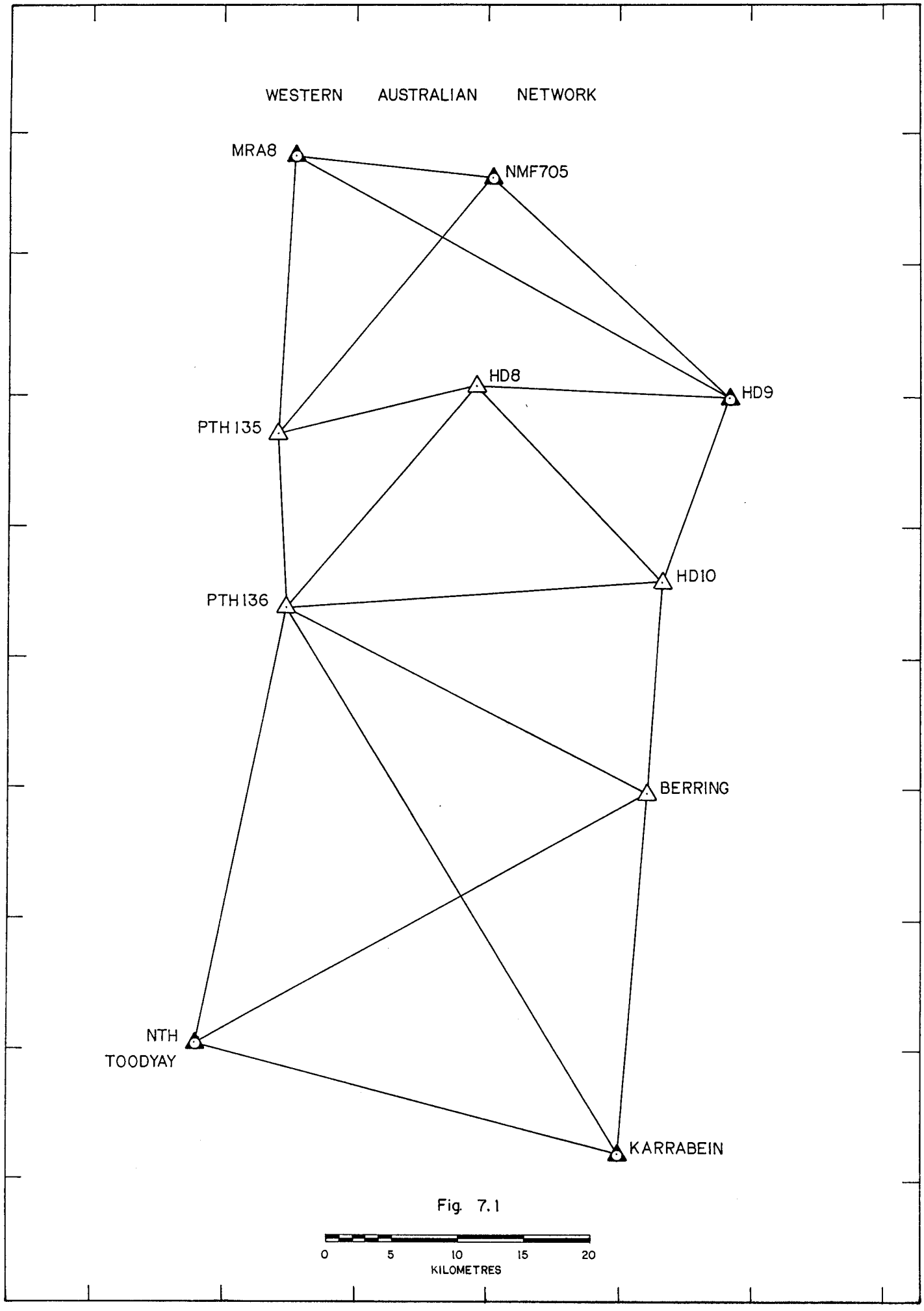
WESTERN AUSTRALIAN NETWORK
MRA8
NMF705
HD8
HD9
PTH135
HD10
PTH136
BERRING
NTH
TOODYAY
KARRABEIN
0
5
10
15
20
KILOMETRES

Fig. 7.1

WESTERN AUSTRALIAN NETWORK

ELLIPSOIDAL HEIGHT MISCLOSES OF LOOPS

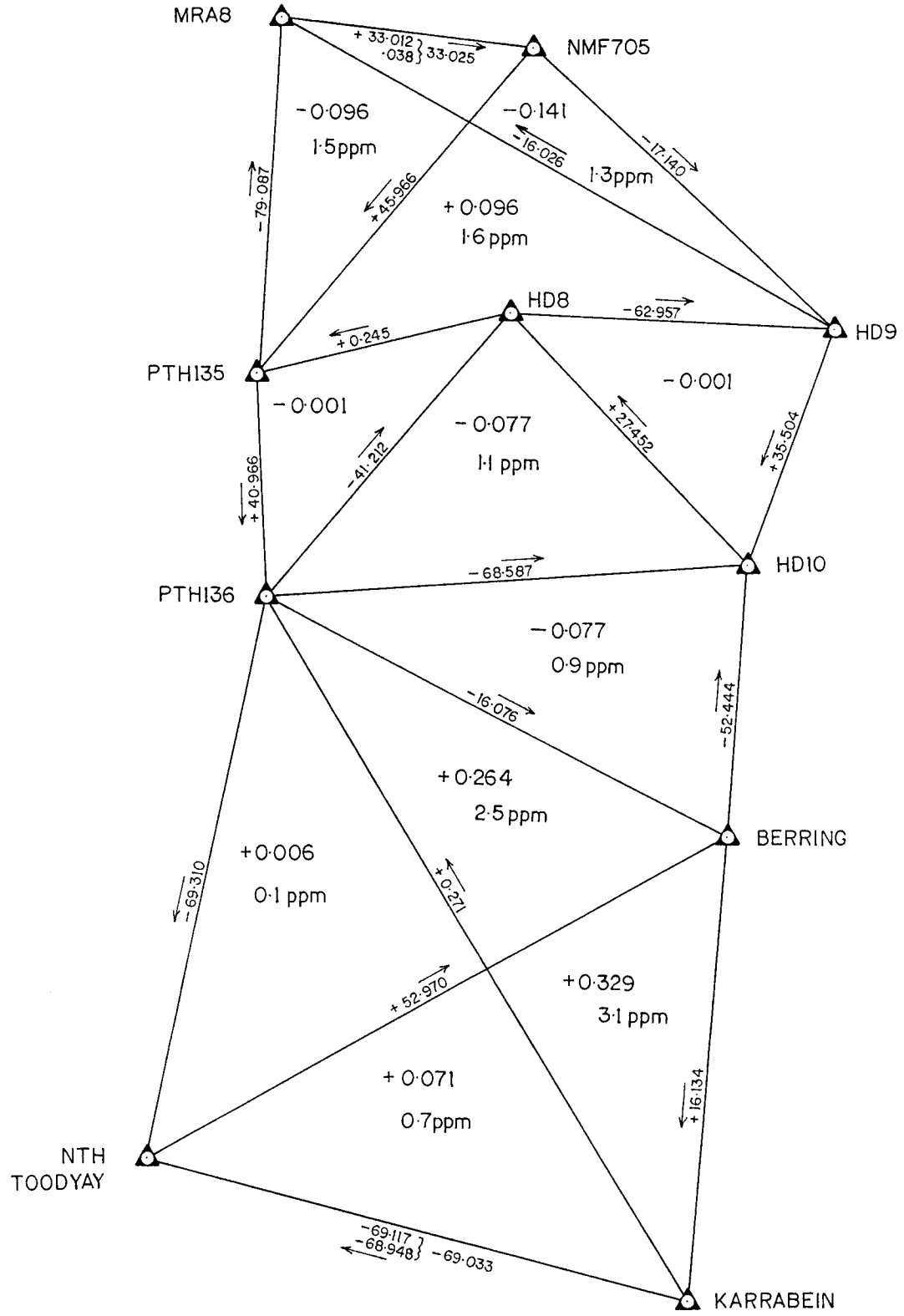

Figure 7.2

0 5 10 15 20

KILOMETRES

By repeating this procedure, the observed height differences and the height misclosures were found for all identifiable loops. Lines MRA8 to NMF705 and NTH TOODYAY to KARRABEIN were observed twice on different days. The difference between the two observations was 0.026 m and 0.169 m respectively. A mean value for both these lines was used for all calculations. Figure 7.2 shows the observed height differences and the loop misclosures. The mean height misclosure for the 11 most obvious loops was 1.2 ppm with a range from 0 to 3.1 ppm.

7.1.1 Interpolation of *N* from Contours.

By determining N, using equation 5.2, at the three northerly stations, MRA8, NMF705 and HD9 and also at the two southerly stations NTH TOODYAY and KARRABEIN a contoured surface was able to be drawn. In Figure 7.3 the contours, drawn with a contour interval of 5 cm, show that the geoid is rising uniformly to the north east from -24.9 m to -23.5 m.

Geoidal heights were interpolated from the contour plot for the remaining 5 intermediate stations, PTH135, HD8, HD9, HD10 and BERRING and compared to $N_{GPS-levelling}$. The mean differences between the interpolated geoidal heights and the control was 11 cm.

7.1.2 Interpolation of *N* from a Least Squares Fitted Plane.

Another method of determining N values, is to interpolate them from a plane surface fitting the same five control points used for the contour plot in the previous section. This method was described in Section 5.2.2.

Program LESQPL was used to determine the coefficients A, B and C of the plane as (see Appendix E),

A = +2.0386494E-05
B = +1.2325885E-05
C = -114.6127

with a standard deviation of the residuals being 0.016 m.

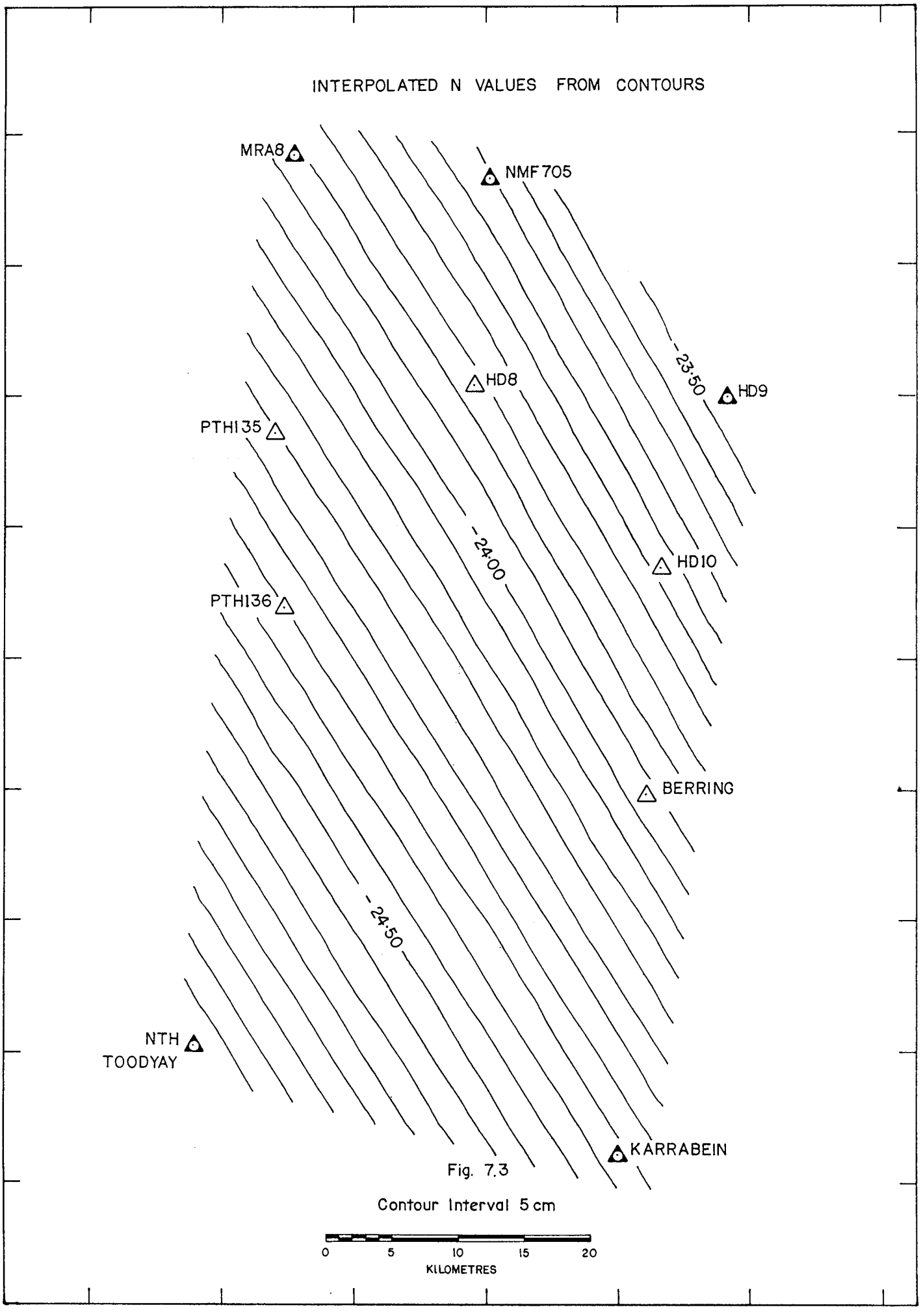
INTERPOLATED N VALUES FROM CONTOURS
MRA8
NMF 705
HD8
HD9
PTH135
PTH136
HD10
BERRING
NTH
TOODYAY
KARRABEIN
-23·50
-24·00
-24·50
Contour Interval 5 cm
0
5
10
15
20
KILOMETRES

Fig. 7.3

The *a posteriori* variance is unrealistically low because the weight matrix is assumed to be an identity which also assumes the *a priori* variance for each height is 1 metre. Realistic relative weights would be difficult to assign to the heights because there is no information of their precisions. The slope of the geoid, with respect to the plane, was calculated and found to rise 23.8 mm/km in the direction 59° (i.e., nearly north east).

The coordinates of the five intermediate stations were next substituted back into the equation of the plane to give N values at those stations. The N values were subtracted from the GPS heights to give interpolated AHD heights and compared with the actual AHD heights of the stations in Table 7.2.

Station	N (levelling)	N (interpolated)	Difference
PTH135	338.041	338.182	-0.141
PTH136	297.256	297.371	-0.115
HD8	338.010	338.057	-0.047
HD10	365.463	365.369	+0.094
BERRING	313.307	313.161	+0.146
		mean (without sign)	0.109

Table 7.2 Interpolated heights from Least Squares Plane.

The methods of contouring and LESQPL used to determine N in the Western Australian network gave very similar results. The contouring method was simple and required very little equipment but was time consuming in its application. The LESQPL method, on the other hand, required a computer and was very quick. An indication of how well the plane "fits" the control points is also given by the size of the residuals, which is not given by a contour plot.

With the height information available, the behaviour of the geoid within the region of the Western Australian GPS network appears to be benign, making it an ideal surface to interpolate geoidal heights. The geoid rises uniformly, the AHD heights are of first or second order specifications, the GPS heights have an average loop misclosure of 1.2 ppm and the extent

of the network is small enough that the approximation of a plane surface is adequate. However, I would suggest that all these conditions occurring together is not common and users of these techniques must bear in mind that an error in the height of a control station will propagate directly into the interpolating surface.

7.1.3 Evaluating N Using a Geopotential Model.

A method of computing geoidal heights for low and third order requirements is to use a geopotential model (see Section 5.3). Equation (5.17) is evaluated to the maximum degree and order of the model using the coefficients C_{nm} and S_{nm} for that model.

N values were calculated for the Western Australian network using geopotential models, OSU86E, OSU81 and GPM2, all to n_{max}=180 and compared to $N_{GPS-levelling}$ in Table 7.3.

It is evident that a bias of 1-2.5 m exist in the models when compared to $N_{GPS-levelling}$, which probably reflects the differences in the values for a and f adopted for the WGS72 (a=6378135.0, f=1/298.26) and GRS80 (a=6378137.0, f=1/298.257223563) reference ellipsoids. These "errors in the geopotential solution can be considered as a type of datum error" (Schwarz and Sideris, 1985, p. 5).

Station	N OSU86E	N OSU81	N GPM2	N GPS-levelling
MRA8	-26.69	-26.37	-24.90	-23.92
NMF705	-26.11	-25.75	-24.26	-23.65
HD9	-25.82	-25.43	-23.90	-23.45
PTH135	-27.17	-26.79	-25.29	-24.07
HD10	-26.20	-25.76	-24.25	-23.83
PTH136	-27.36	-26.95	-25.45	-24.24
BERRING	-26.48	-26.03	-24.54	-24.12
KARRABEIN	-26.83	-26.38	-24.96	-24.37
NTH TOOD	-28.11	-27.70	-26.26	-24.90
HD8	-26.46	-26.05	-24.55	-23.81

Table 7.3 Comparison of N from Geopotential Models at degree 180.

The accuracy of the geoidal heights from geopotential models will be greatly improved if we look at the differences in geoidal heights (ΔN) as the biases will tend to cancel.

Figure 7.4 shows the mean differences (errors) in ΔN, evaluated using OSU86E, OSU81 and GPM2 from degree 30 to their n_{max}, over all GPS observed baselines in the Western Australian network. These differences were found by comparing ΔN_{model} to $\Delta N_{GPS-levelling}$ for all the baselines. The error was expressed as a fraction of the baseline length in ppm for each line and then averaged for all lines in the network (Equations 6.5 and 6.6). This error reaches a maximum of approximately 15 ppm at degree 180 for all models.

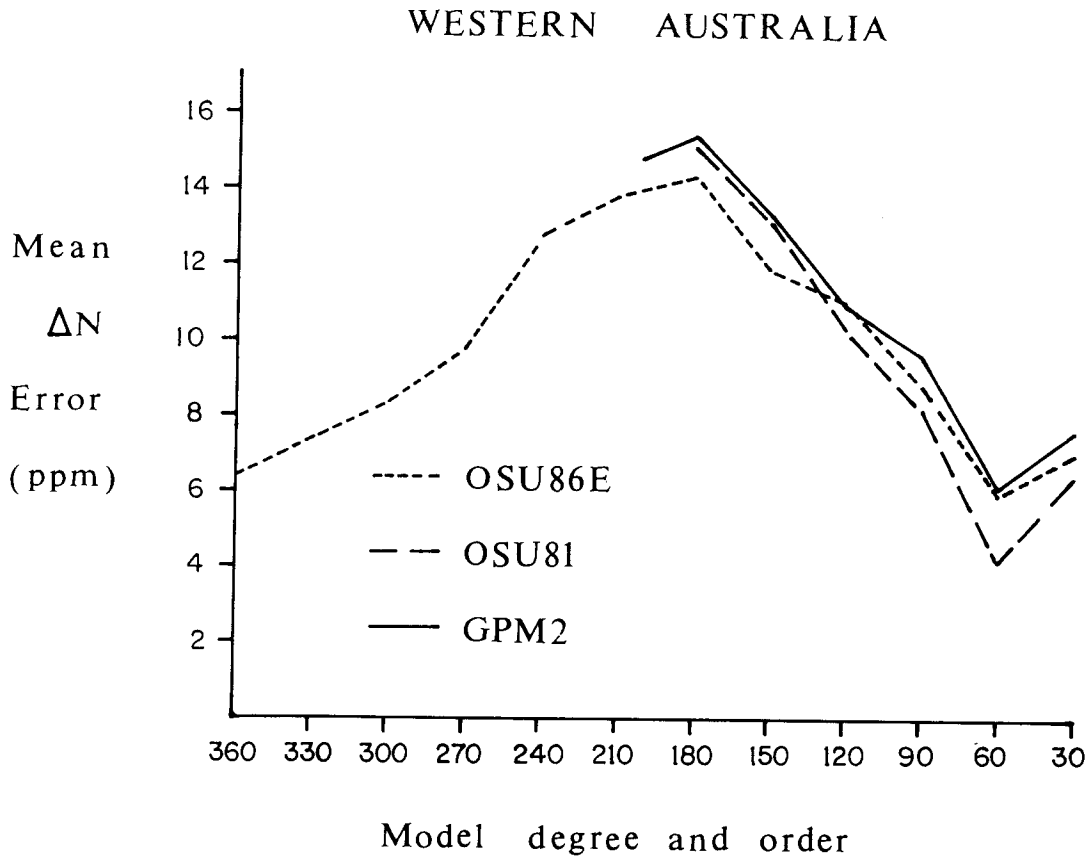

Figure 7.4 Comparison of OSU86E, OSU81 and GPM2.

This is also demonstrated in Figure 5.4 where the disagreement between gravity anomalies and the gravity anomalies generated by OSU81 at degree 180 is large in the region of the Western Australian network. We

can also see that from degree 180 down to degree 30 the three geopotential models behave in a very similar fashion but, unexpectedly, the error in ΔN actually improves with the geopotential models evaluated to lower orders. From degree 180 to 360, the error in ΔN using OSU86E steadily become less, reaching a minimum at degree 360 of 6 ppm.

At this stage one can only speculate as to the reasons for the large errors in ΔN and the behaviour of the geopotential models in the region of the Western Australian network. Perhaps the near vicinity of a plateau in the geoid, evident in Figure 5.2, is being reflected in the geopotential models or some erroneous data has gone into determination of the geopotential coefficients in this area.

7.1.4 Evaluating *N* Using RINT.

Heighting applications requiring the highest possible accuracy for ΔN may be computed using a combined solution, RINT, discussed in Section 6. The UNSW computer programs (see Section 6.1) compute the long wavelength component N_L using geopotential model OSU81 to n_{max}=180 which is combined with the short wavelength component N_S by evaluating the Stokes' integral in compartments bounded by rings, using point residual gravity anomalies.

ΔN_{grav} is the difference in N between the terminal points of a baseline. This can be compared to $\Delta N_{GPS-levelling}$ along the same baseline for each ring increment from ring 0 (using the geopotential model only) to ring 26 ($\psi_0 = 2.6°$ from the computation point).

The gravity data inside the rings should contain a sufficient number of gravity points with an even distribution that the mean gravity anomalies calculated for each compartment is truly representative of the gravity field in that compartment.

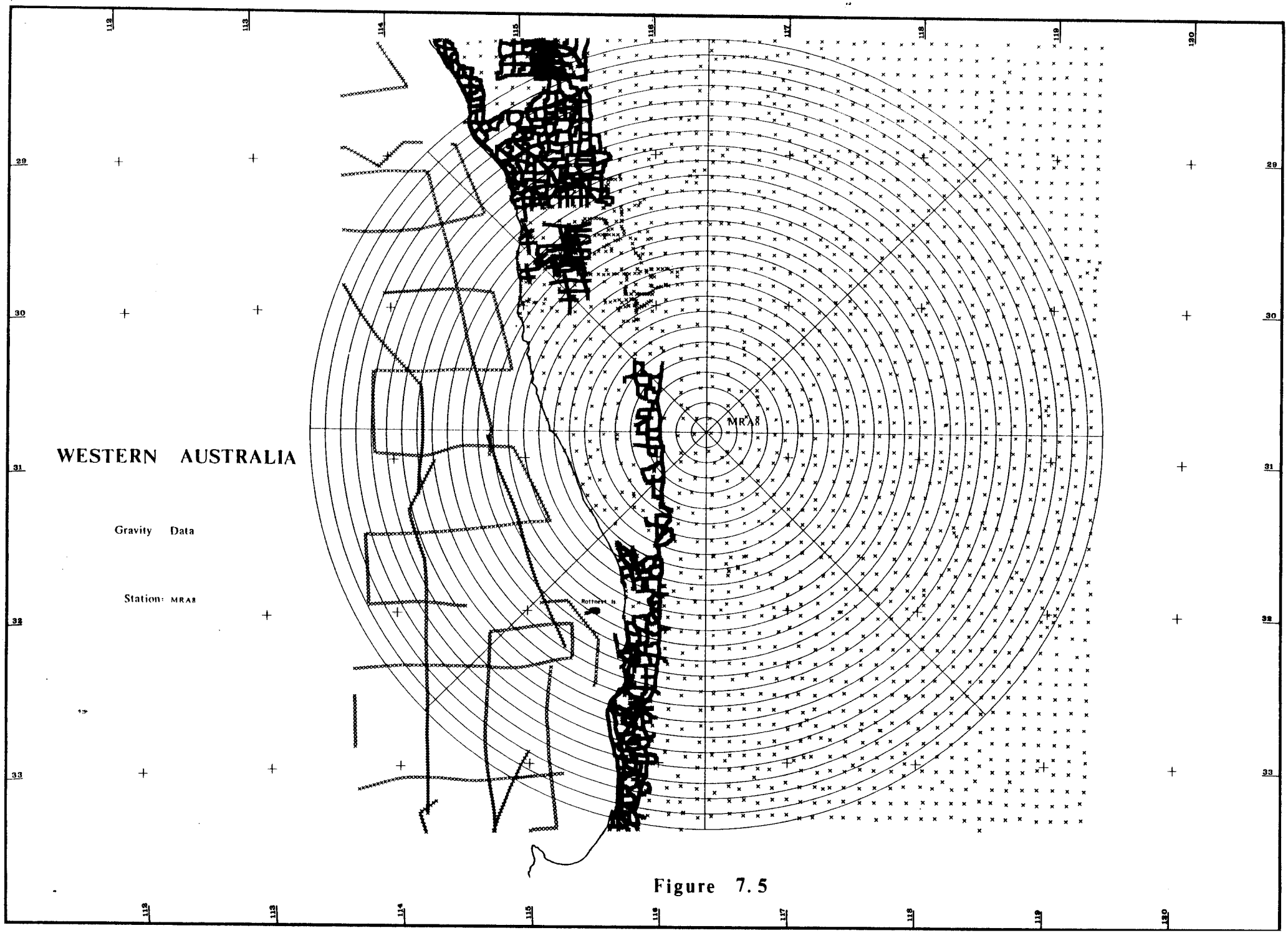
WESTERN AUSTRALIA
Gravity Data
Station: MRAS
MRAS
112
113
114
115
116
117
118
119
120
29
30
31
32
33

Figure 7.5

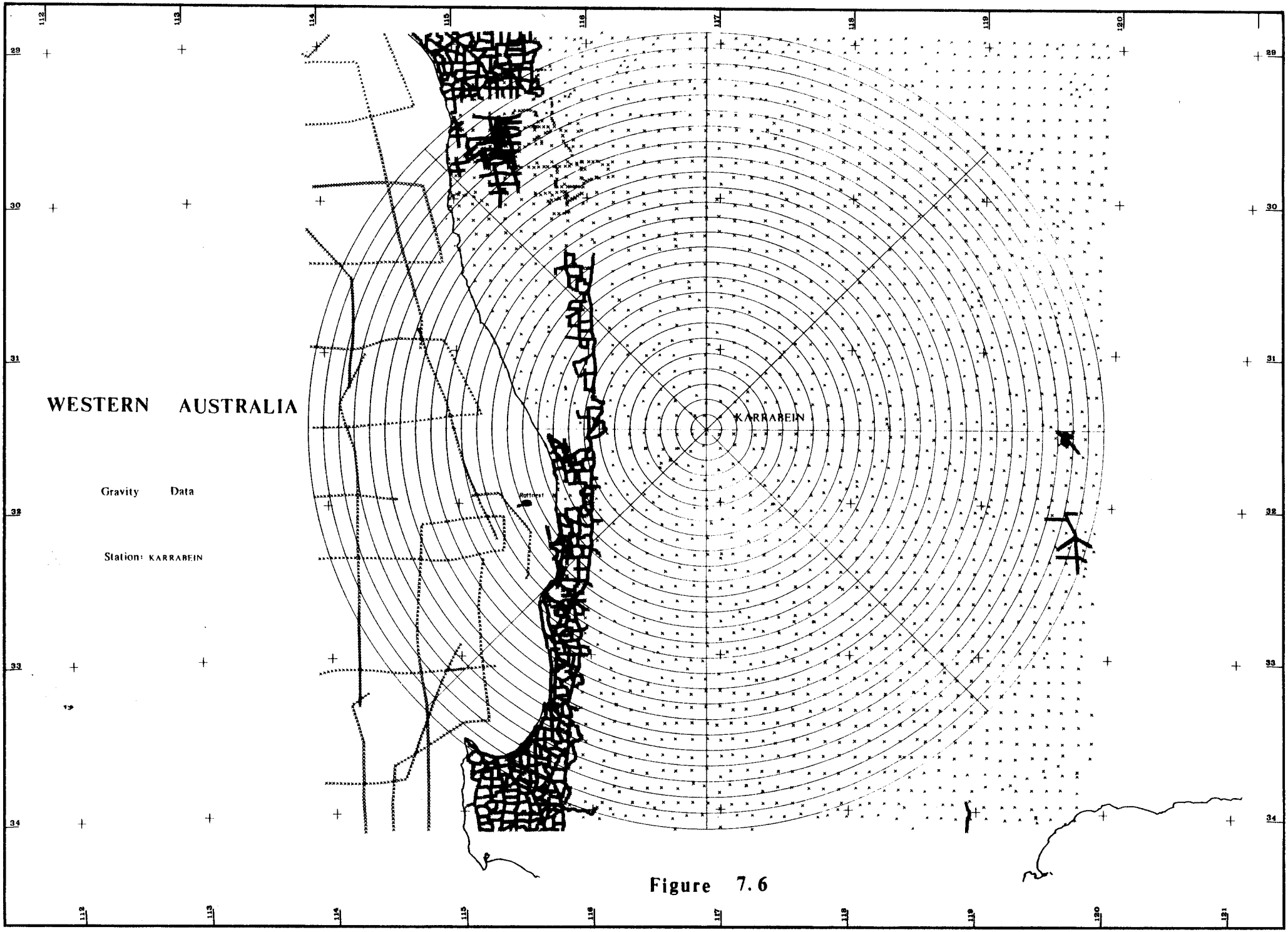
WESTERN AUSTRALIA
Gravity Data
Station: KARRABEIN
KARRABEIN
Rottnest

Figure 7.6

Figures 7.5 and 7.6 show the ring structure and the point gravity data, each marked with a cross, that was used to evaluate the Stokes' integral at station MRA8, in the north west of the network and station KARRABEIN, in the south east of the network. It can be seen that the gravity coverage in the region of the Western Australian network is complete and uniformly distributed. In the background, gravity has been observed on an evenly spaced grid which has been supplemented by gravity traverses along the coastline. The typical ships' tracks show the offshore gravity data.

The results of this analysis, computed using program GRAV08, is listed in Appendix C and also presented in Figure 7.7. The abscissa, or x-axis, shows the number of rings included in the integration while the ordinate, or y-axis, shows the mean error in $\Delta N_{grav} - \Delta N_{GPS-levelling}$ from Equation (6.6), for all lines in the network.

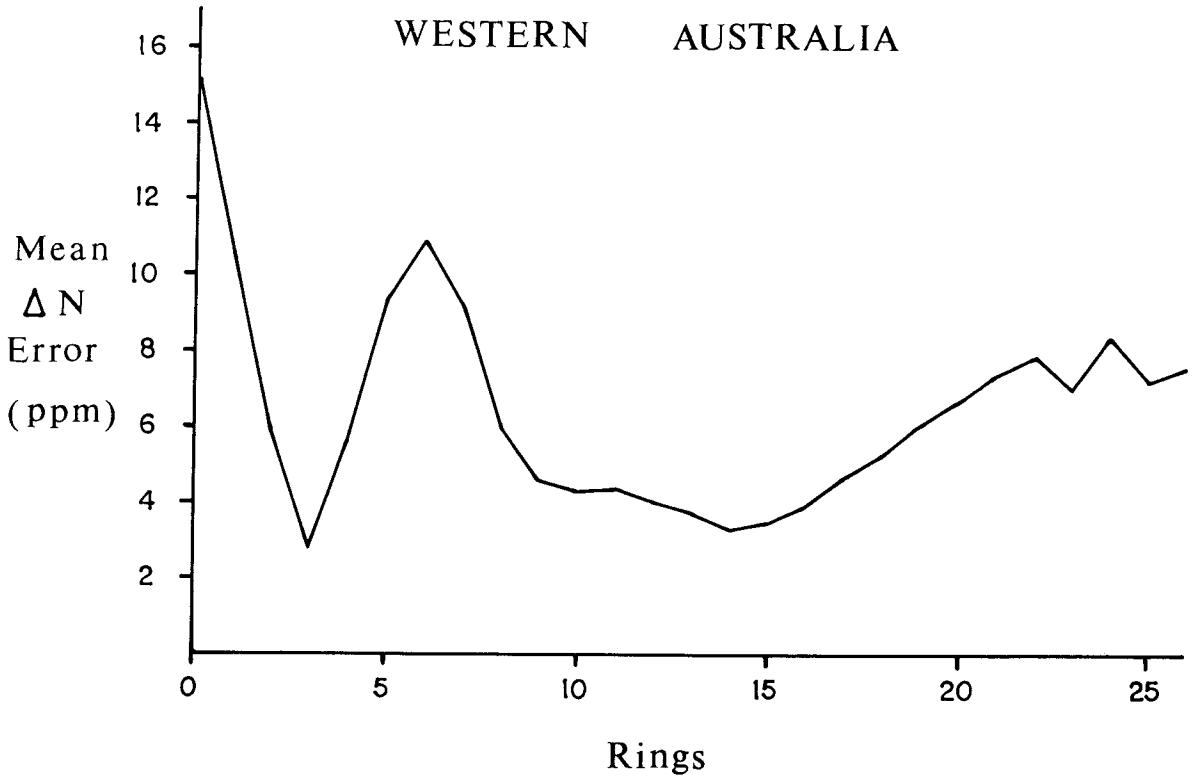

Figure 7.7 Results of tests using RINT in Western Australia.

It can be seen that at ring 0, using the geopotential model only, the error is quite large (>15 ppm), but the inclusion of even a small inner cap significantly improves the solution of ΔN. The curve is bimodal, exhibiting a

"W" shape that appears to be characteristic of RINT (Kearsley, 1988b). The two minima occur at ring 3 (3.5 ppm) and ring 14 (4.2 ppm), the first being quite definite whilst the second being a much flatter curve. Tests performed to investigate the cause of the "W" curve suggest that it is reflecting small errors in the higher order terms of the geopotential model (ibid).

7.2 South Australian Network.

The South Australian Phase 1 GPS network, shown in Figure 7.8, was observed in October-December 1985 using Macrometer V-1000 receivers. These receivers are independent of the codes because they square the L1 frequency signal to obtain the raw carrier wave phase. This makes it necessary for the receiver clocks to be synchronised by an external timing device. A Trimble 4000A GPS navigation receiver was used for the South Australian campaign. Also the satellite ephemerides had to be obtained externally from Litton Aero Service (Larden et al, 1986).

The strategy for processing the observations and performing the 3D network adjustment was outlined by Jones et al, (1987). The integer cycle ambiguities were not resolved because the majority of baselines were greater than 20 km making it impossible to model the atmospheric errors with certainty. This should not affect the accuracy of the ellipsoidal heights (see Section 4.3).

The processing of all GPS observations was done using BATCH_PHASER, a multi-station reduction program which also outputs a variance-covariance matrix that is used in the 3D adjustment of the network. The network adjustment was computed using program NEWGAN by Allman (Jones et al, 1987). The WGS72 ellipsoidal heights used in this study came from the adjusted coordinates output from NEWGAN.

A statistical analysis of the precision of the GPS data in the network was performed by Morgan et al, (1986) for the South Australian Department of Lands. This study included 172 independent baselines forming 72 geometrically independent loops. They found that the mean loop misclosure of the baseline vectors was 3.2 ppm (Morgan et al, 1986, p. 7).

SOUTH AUSTRALIA

GPS NETWORK – PHASE 1

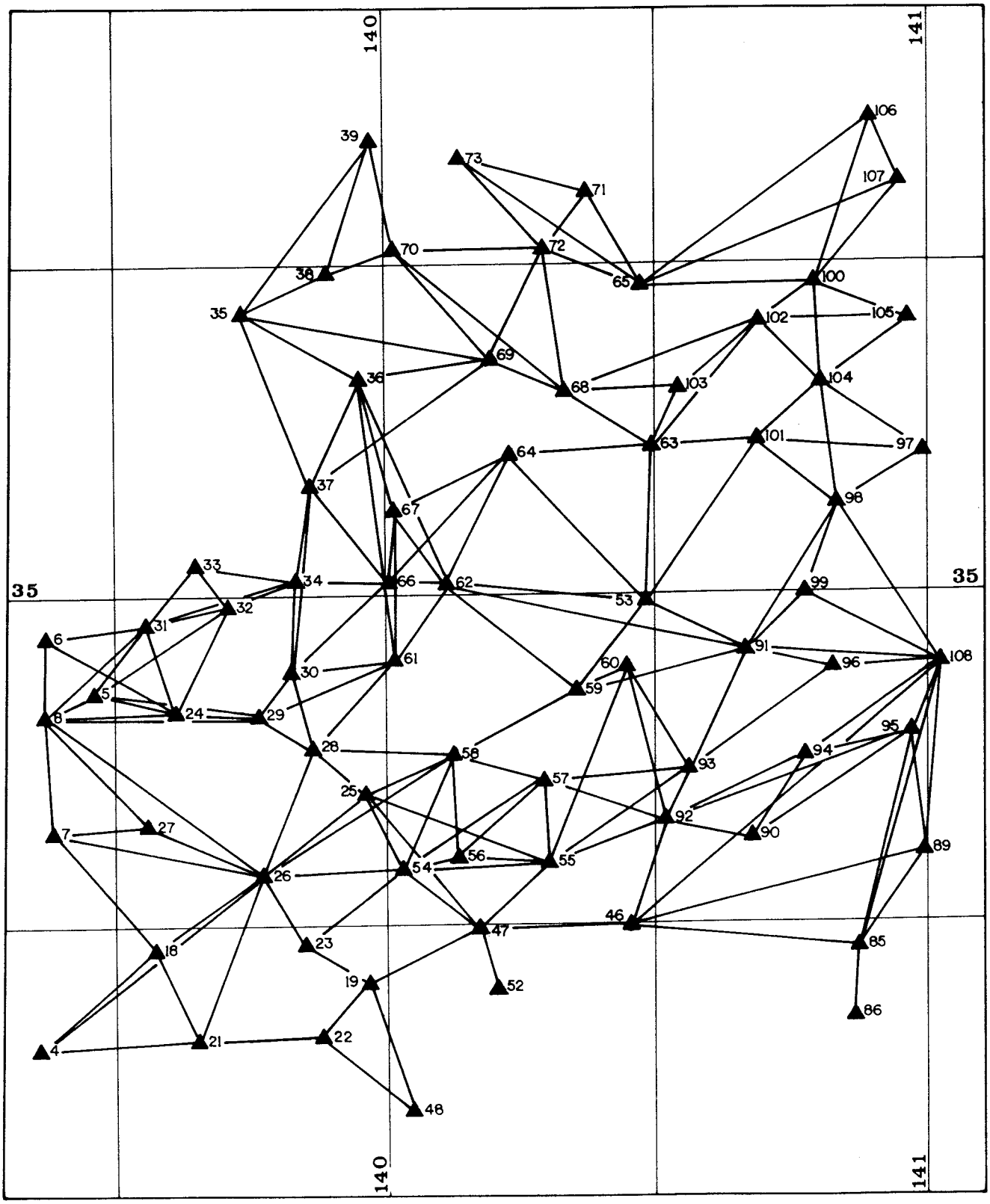

SOUTH AUSTRALIA

GEOID MAP

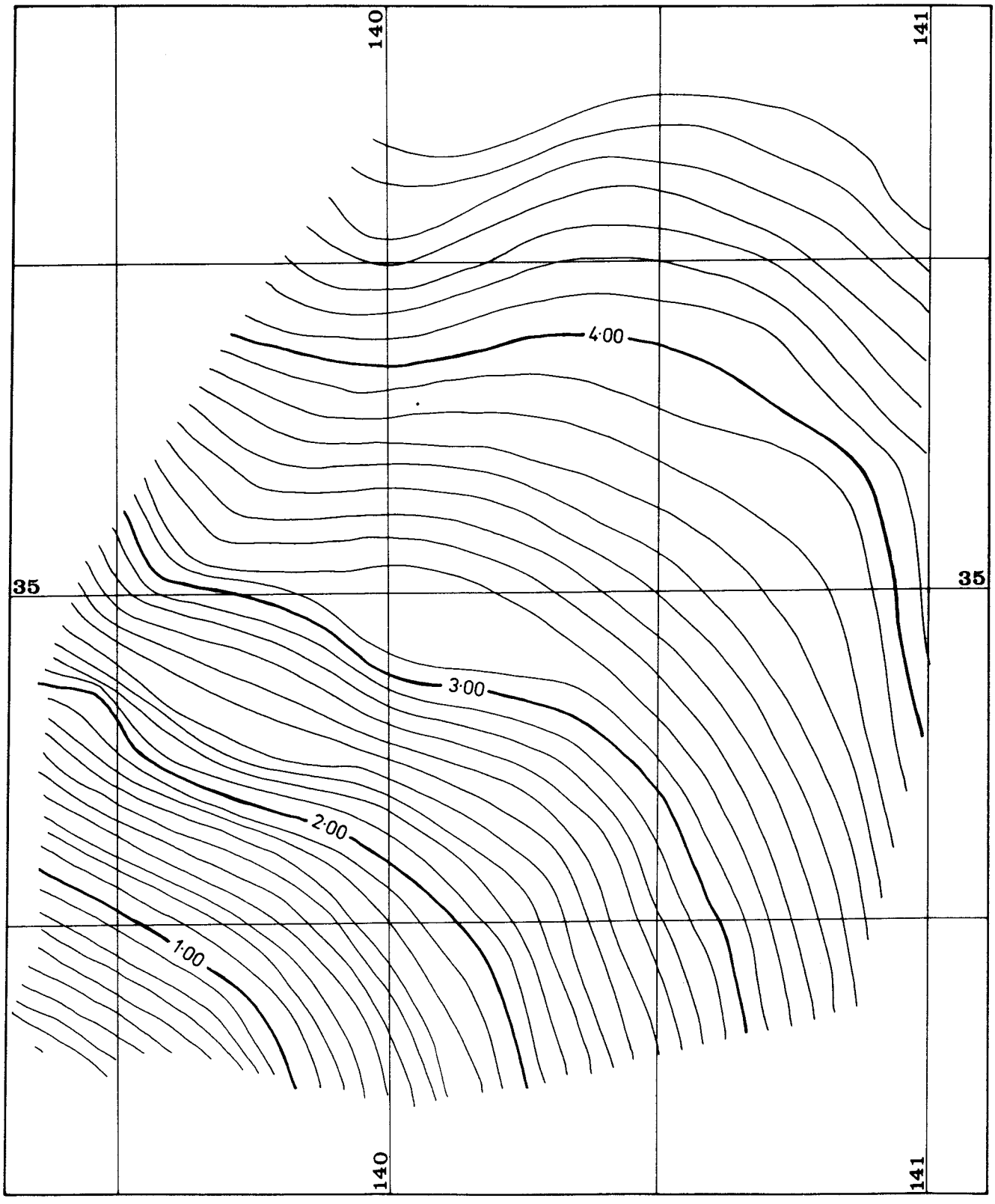

Contour Interval 10cm

Scale

0 10 20 30 40 50

(km)

Unfortunately separate height and horizontal loop misclosures were not computed and therefore we don't know the precision of the heights by themselves.

7.2.1 Interpolation of *N* from Contours.

There are 45 stations in the South Australian network that have both GPS and AHD heights. From the *N* values calculated at these stations a geoid plot was drawn with a contour interval of 10 cm. Figure 7.9 shows the geoid rising to the north east from 0 m to +4.7 m.

The slope of the geoid is irregular. This makes interpolating geoid heights for intermediate stations, especially at this scale and contour interval, uncertain over such a large area.

The Australian Survey Office in South Australia relevelled many of the existing control points in the network after the completion of the GPS survey to monitor any movements in points sited in sand dunes and to upgrade stations with fourth order or trigonometric heights. The relevelling revealed some differences with previously published heights, for example

Point	72 (6929/1397)	-0.323 m
	36 (6828/1264)	+0.117
	6 (6727/1099)	-0.225
	90 (7027/1051)	-0.343
	48 (6926/1548)	-2.024
	86 (7026/1353)	-1.426

which, if used, as fixed stations for interpolation would have propagated directly into the interpolating surface.

7.2.2 Interpolation of *N* from a Least Squares Fitted Plane.

Program LESQPL was used to calculate a least squares determined plane surface through the South Australian network using the same 45 stations as before which had both GPS and AHD heights (see Appendix F).

The coefficients A, B and C of the plane were computed to be,

A = +1.0727929E-05
B = +1.7652649E-05
C = -109.5566

with the standard deviation of the residuals being 0.352 m. The range in the residuals was 1.80 m, indicating that the "fit" of the plane to the control was not very good. The extent of the South Australian network, the irregular nature of the geoid and the poor quality of some AHD heights suggest that if geoid heights are interpolated they should be treated with caution and have a large error figure attached to them.

7.2.3 Gravimetric solution of N.

Tests were conducted to determine the agreement in ΔN using geopotential models OSU86E, OSU81 and GPM2 from degree 30 to their n_{max} in the South Australian region. Program GRAV08 was used to compute the differences (errors) with $\Delta N_{GPS-levelling}$ for all lines that had both a GPS and AHD height. This resulted in 527 line combinations generated for the whole network. If only those lines that had been observed with GPS had been used the sample size would have been too small because many lines involved stations that did not have an AHD height. Figure 7.10 shows the results.

We can see that the three geopotential models agree closely with each other from degree 180 down to degree 30, which is similar to the Western Australian experience. However, unlike the Western Australian region, the error in ΔN behaves more to expectations as it increases from 3.5 ppm at degree 180 to ≈15 ppm at degree 30. The error in ΔN decreases from degree 180 to degree 360 reaching a minimum of 2.4 ppm using model OSU86E. This is probably of sufficient accuracy, without including local gravity, for most users requirements, especially as this agreement is probably at the noise level of the GPS and AHD heights.

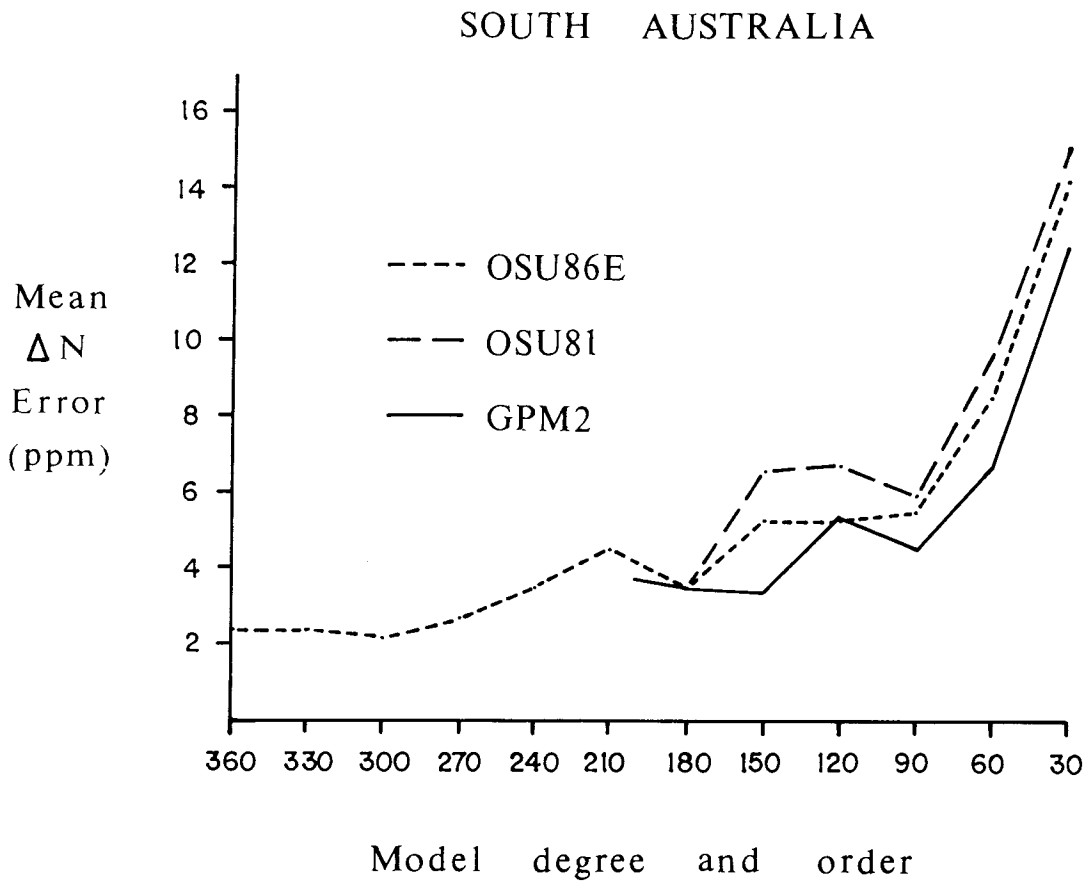

Figure 7.10 Comparison of OSU86E, OSU81 and GPM2.

The ability of OSU81 to recover gravity anomalies in the region of the South Australian network, shown in Figure 5.4, also reflects the agreement between the geopotential model and the gravity field.

7.2.4 Evaluating *N* Using RINT.

As for the tests in the Western Australian network (Section 7.1.4), the RINT method (Section 6) was used to compute ΔN for all lines in the South Australian network. The UNSW gravity programs were used to compute the long wavelength contribution N_L using OSU81 to degree 180 and the short wavelength contribution N_S by evaluating the Stokes' integral in compartments formed by concentric rings and radial lines.

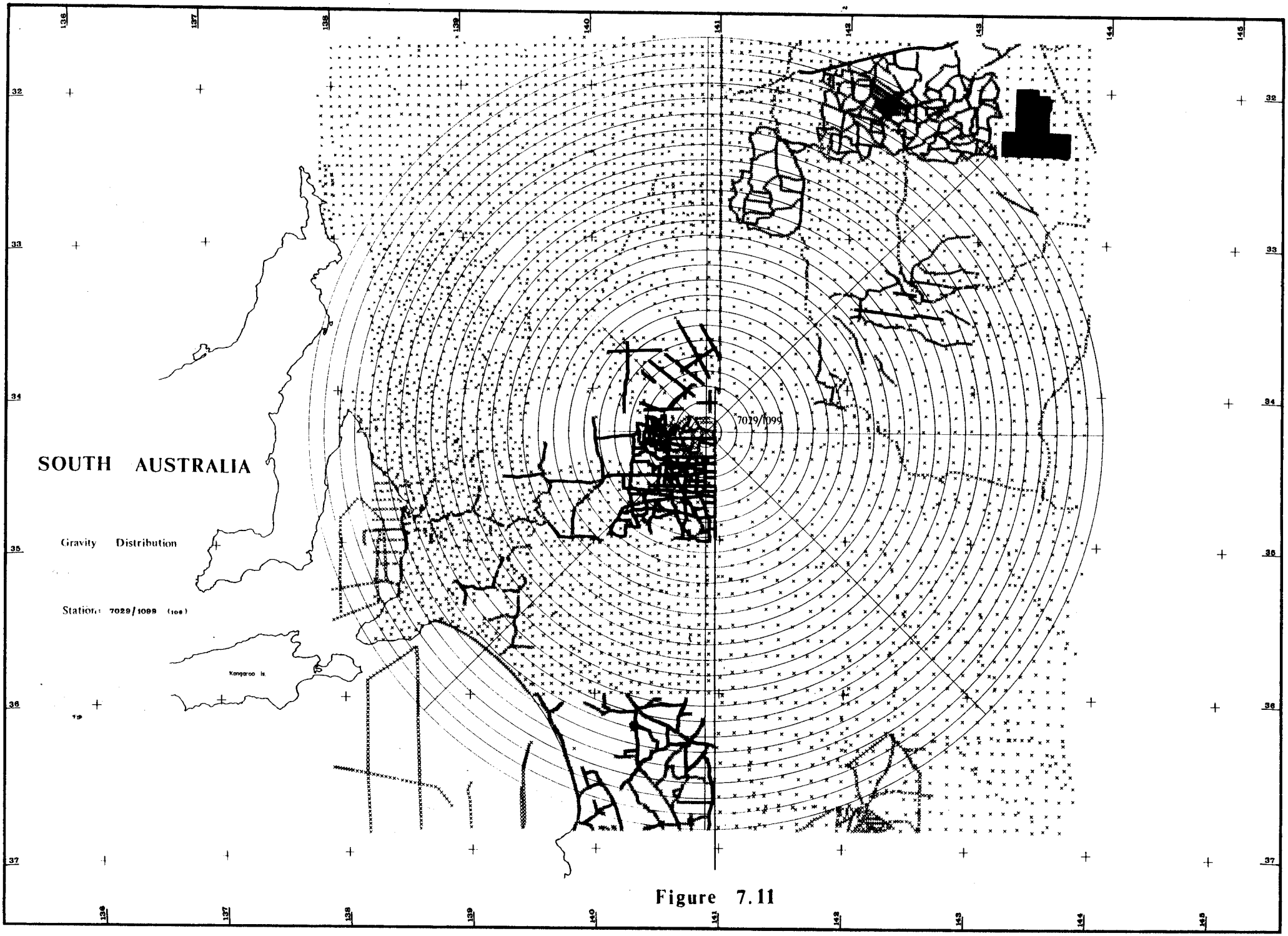
SOUTH AUSTRALIA
Gravity Distribution
Station: 7029/1099 (108)
7029/1099
Kangaroo Is.

Figure 7.11

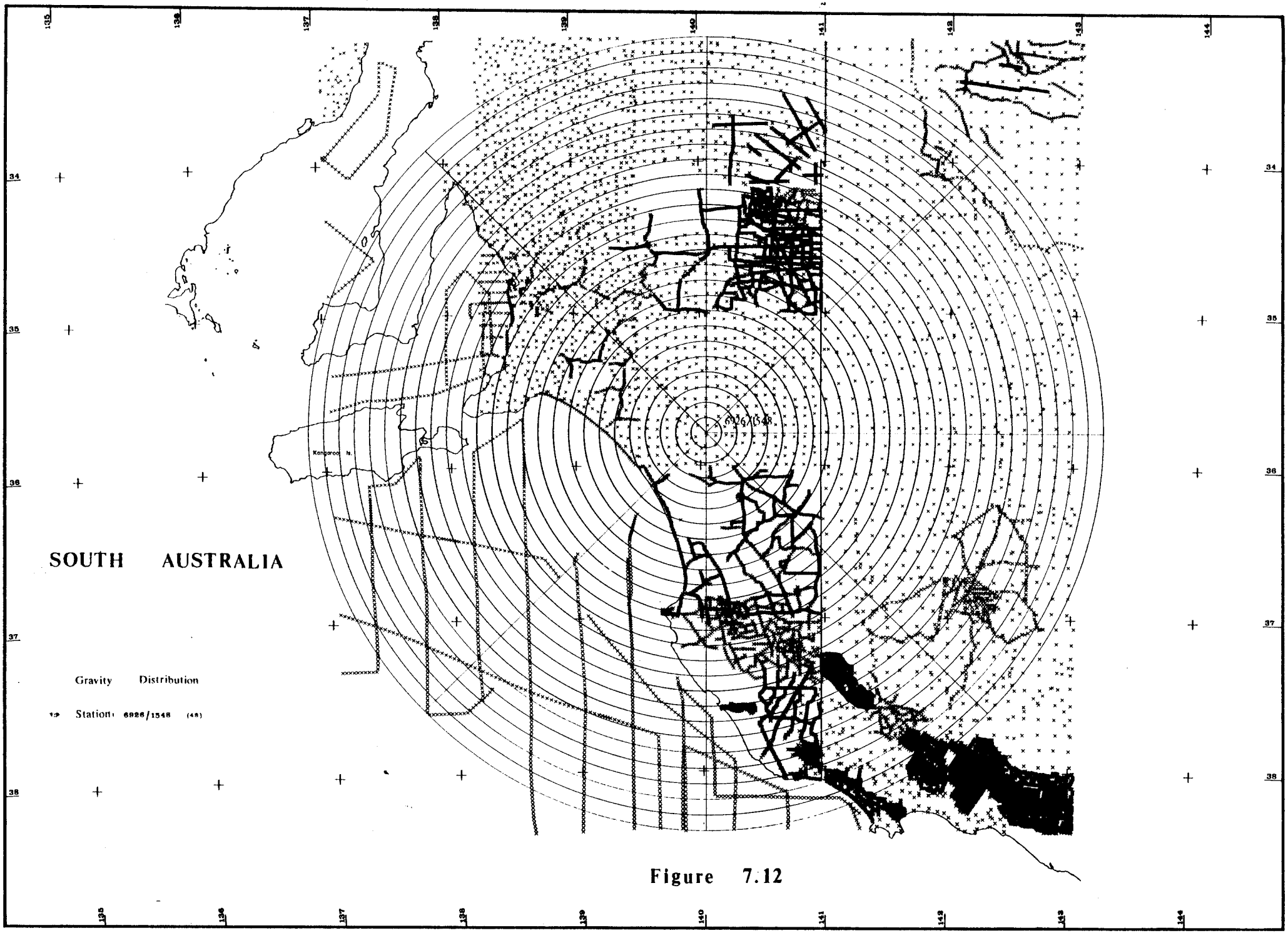
SOUTH AUSTRALIA
Gravity Distribution
Station 6926/1548 (48)
6926/1548
Kangaroo Is.

Figure 7.12

The gravity data available in the South Australian region, and used by program GRAV01 for station 7029/1099 (106) in the extreme north of the network and station 6926/1548 (48) in the south of the network is shown in Figures 7.11 and 7.12. They show the ring structure superimposed on a map with each gravity data point marked with a cross. It can be seen that the gravity coverage is complete within the rings. There is an even distribution of "background" gravity data observed on a systematic grid which has been supplemented by gravity traverses providing more intense gravity data in areas of geological interest. The offshore gravity coverage is also good, even up into Spencer's Gulf. However there appears to be no gravity data on Kangaroo Island but this is towards the extremity of the rings and shouldn't degrade the computation.

It can be seen that the computation of N_S for stations 7029/1099 and 6926/1548, even in this extreme case, involves gravity data within each ring system that is common to both stations. Therefore any systematic errors in the common gravity data within the overlapping areas will cancel when N is differenced between the two stations.

The computed ΔN_{grav} for all lines in the South Australian network were then compared for each ring contribution to $\Delta N_{GPS-levelling}$ for the same lines using program GRAV08. The lines were generated between all points that had both a GPS and AHD height in the network, making 527 combinations. The results are presented in Figure 7.13.

It can be seen that at ring 0, using the geopotential model only, the error in ΔN is 3.5 ppm, reflecting the good agreement between OSU81 and the gravity field in this area. The inclusion of even a small inner zone immediately improves the solution which reaches a minimum at ring 3 ($\psi_0 = 0.3°$). The slope of the curve is fairly flat and constant in the region from ring 3 to ring 20 making the choice of ψ_0 not critical. It is not until ring 15 that the error in ΔN is greater than 4 ppm.

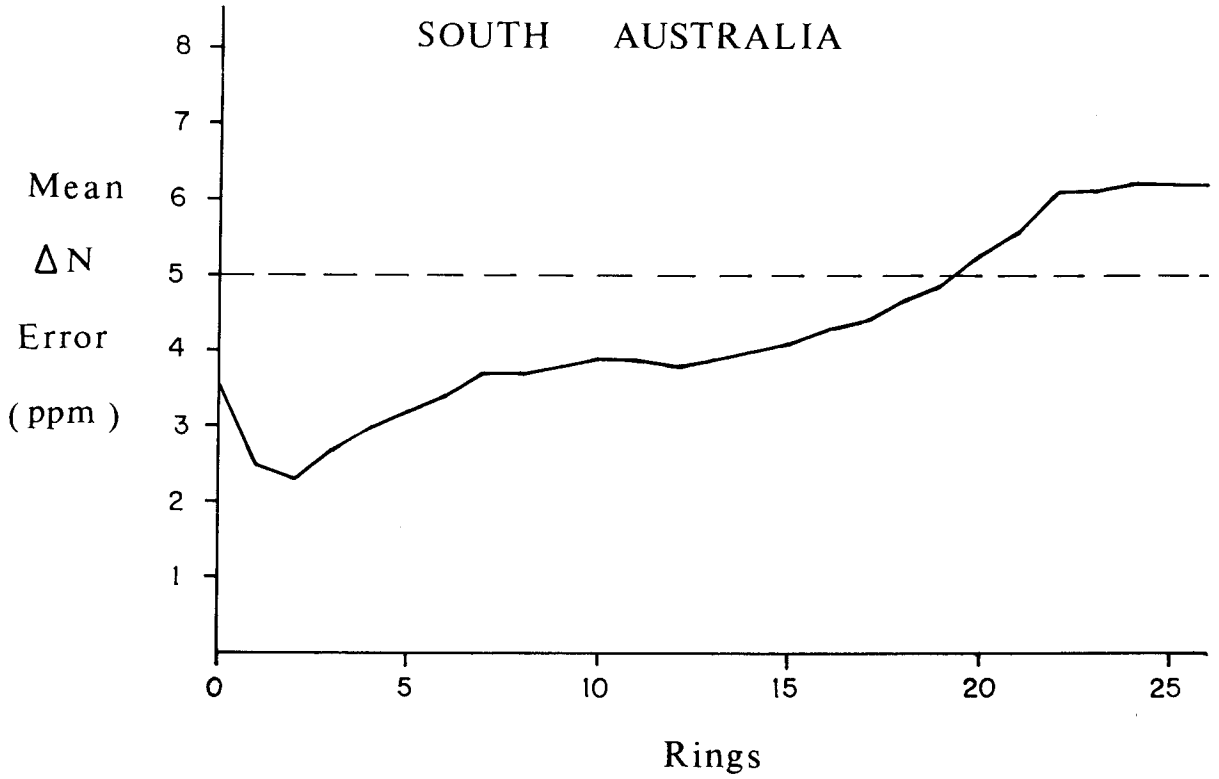

Figure 7.13 Results of tests using RINT in South Australia.

It is interesting that the "W" curve evident in the Western Australian network and in Canadian networks (Kearsley, 1988b) is not as obvious in the South Australian network. This may be due to small errors in the AHD heights of some stations.

Concurrent with the computation and analysis of ΔN for the South Australian network the Australian Survey Office were relevelling many existing stations in the region of the GPS network. A number of lines were isolated, containing common points, which were suspected of being outliers as the error in ΔN was much greater than the population. The ASO conducted field checks at these stations and did find errors in the heights (Section 7.2.1) which could have been caused by errors in the original levelling or settlement of the stations in sandy soils. The new heights were used in the analysis presented here.

7.3 The Future of Gravimetric Geoid Computations.

The computation of geoidal heights to a similar accuracy as that of GPS is now possible using techniques such as RINT provided there is sufficient gravity data that fulfils the conditions outlined by Kearsley (1984, p. 101). These conditions appear to be satisfied in the Australian region, except for the south east coast and the Gulf of Carpentaria (see Figure 5.3).

The precision of ΔN computed for networks in Western Australia and South Australia was between 2 ppm and 3 ppm. This is in agreement with the computed precision of networks in Manitoba and Ontario (Kearsley, 1988b, p. 6567) and appears to be about the noise level of the GPS and spirit levelled heights with which they are compared. Therefore there is little likelihood in the future for any improvement in the precision of computed geoid heights. However the use of higher order geopotential models, such as OSU86E, will enable a smaller cap to be used in which Stokes' integral is evaluated. The requirements of density and coverage for gravity data will be not so stringent because of the smaller cap used and because the geopotential model will give a much better estimate of the gravity field.

GPS, coupled with a method of accurately computing geoidal heights, will offer an independent method of detecting errors in existing levelling. Until now, the only statistics on the precision of levelling has been the agreement between a forward and backward levelling run and the height misclosure around a closed loop. Errors in heights could go undetected if two compensating errors were made or if the length of the perimeter of the closed loop was so great that an isolated error was insignificant when expressed as a fraction.

The South Australian experience shows that errors were able to be detected in existing levelling lines using GPS. Suspect lines were isolated by comparing ΔN_{grav} to $\Delta N_{GPS-levelling}$ which was subsequently confirmed by relevelling of those lines by the Australian Survey Office. This is much more efficient than relevelling all lines in an area to find an error.

I understand the South Australian Lands Department propose to occupy stations at the junction points used in the levelling adjustment for the AHD in the next stage of their GPS observed control point densification survey in 1988-1989. It is hoped that this will isolate any errors, if any, in the primary network. I will view those results with interest.

7.4 GPS and the Australian Height Datum.

The logical extension of these techniques is to incorporate GPS heights and computed geoidal heights into a readjustment of the Australian levelling network as independent observations. Tide gauge information for the 30 sites around the coastline, spanning a much longer period than before, should also be used with the best estimate of the sea surface topography at each gauge from models and satellite altimetry. This would be similar in practice to the readjustment of the Australian geodetic network (AGD66 - AGD84) incorporating Doppler stations to upgrade the whole network.

The observation equation between tide gauge sites would be of the form,

$$\text{GAUGE HEIGHT}_{1\text{-}2} + \text{SST}_{1\text{-}2} + \Delta H_{1-2} + (\Delta h_{1-2} - \Delta N_{1-2}) = 0$$

with each data type having an independently determined *a priori* variance used to weight the observations. The advantages of a combined adjustment using heterogeneous data from spirit levelling, GPS, computed geoid heights, tide gauge readings and an estimate of the sea surface topography at each tide gauge would be great. Such a combined adjustment

* would be able to detect any systematic errors in the original levelling,
* would be able to detect any gross errors in the original levelling,
* would mean the reference surface for all heights would be much closer to the geoid,
* would upgrade the accuracy of the whole height network.

This new height network (AHD89?) would have a much greater integrity than the existing AHD and would facilitate the inclusion of additional GPS heights into the height network. The reduction of observed data to the geoid, such as gravity, would also be closer to the truth.

8 CONCLUSIONS

This study shows that the Global Positioning System, with an appropriate computational strategy to determine the geoid-ellipsoid separation, can be used to obtain heights referred to the Australian Height Datum. We have looked at each of the three components in the equation, the Australian Height Datum, GPS ellipsoidal heights and the geoid-ellipsoid separation connecting the two.

The main points regarding the Australian Height Datum are summarised below.

* Heights in the AHD should be referred to as *normal orthometric heights*, and not as *orthometric heights*, because the orthometric correction applied to levelled height differences uses normal gravity and not observed gravity. The difference between the two, however, is quite small reaching a maximum of 1.9 cm across Australia.

* Heights in the AHD are referred to a warped surface not coincident with the geoid or any other equipotential surface. This is because the levelling network was adjusted between the mean sea level heights, held fixed, at 30 tide gauges around the Australian coastline based on three years of tide data.

* The difference between mean seal level and the geoid at each tide gauge station is equal to the sea surface topography at the tide gauge. This will be different at each tide gauge and is very much dependent on local conditions in the vicinity of the tide gauge site.

* The precision of the adjusted levelling is very close to second order specifications being $8.1\sqrt{k}$ mm. This gives the precision of relative height differences between the centre of Australia and the coastline of 0.34 m.

* There is a high probability that compensating gross errors in heights remain undetected in some levelling loops.

Accuracies of 2-4 ppm for GPS observed ellipsoidal heights using single frequency receivers are possible under the following conditions.

* The dominant error source is the delay of the signal through the troposphere. This error can be minimised, if WVR's are unavailable, by observing in stable weather conditions, keeping inter-station distances to a minimum and using a tropospheric model such as Hopfield or Saastamoinen.

* On short baselines the determination of the *a priori* coordinates of the fixed station is important. They can be found by transforming the AGD84 coordinates of a station in the geodetic network to WGS84 coordinates or by averaging pseudorange solutions over a long period.

* The residual error in the ionospheric delay can be minimised if the observations are made during night time and the broadcast ionospheric model is used.

* The user has very little control over the error in the satellite orbits. The error is approximately 20 metres currently which is satisfactory for ellipsoidal height determination at the 2-4 ppm level. Hopefully the orbits will not be degraded in the future when all the satellites have been launched.

* There is no improvement in the heights if the cycle ambiguities are resolved correctly weighed against the risk, especially over longer lines, that the heights will be degraded if they are resolved incorrectly. Therefore, there is no benefit in fixing the cycle ambiguities to integer values.

The accuracy requirements of users of geoid heights vary. A number of techniques of determining geoidal heights with differing accuracies were investigated.

* The simplest method, using only a pen and ruler, is to draw a contour map of geoid heights. Three or more stations with both GPS and AHD heights surrounding the network act as control from which the interpolating surface can be drawn. The accuracy of the interpolated heights is very much dependent on the scale of the drawing, the plotting accuracy, the accuracy of the heights at the control stations, the area of the network and the behaviour the the geoid within that area.

* The interpolating surface can be defined analytically, instead of graphically as above, using program LESQPL. An indication of how well the plane "fits" the control stations is given by the size of the residuals at each station.

* These two methods gave most satisfactory results in the Western Australian network because the AHD heights at the control stations were all first or second order and the area enclosed by the network is not very large. However, the results for the South Australian network were unsatisfactory because of the large extent of the network, the uncertainty of heights at some control stations and the irregular nature of the geoid in that area.

* The geoidal heights computed using high order geopotential models OSU81, GPM2 or OSU86E were much more accurate when differenced than the absolute values. A datum error occurs because the geopotential models refer to the GRS80 ellipsoid instead of the reference ellipsoid for GPS, WGS72, which has different defining parameters.

* The computed ΔN from the three models agree with each other very closely from degree 30 to 180. However, the agreement of the models with $\Delta N_{GPS-levelling}$ varies with the degree of the model and the region in Australia. The agreement of the models in the Western Australian network was poor, being 15 ppm, but in the South Australian network it was 4 ppm. There was significant improvement in ΔN for both networks when OSU86E was used at degree 360.

* The RINT technique was found to be most suitable for the precise computation of ΔN. Even if the agreement of ΔN using the geopotential model only was poor, as in the Western Australian network, the inclusion of even a small ($< 0.5°$) inner zone integration gave a significant improvement to the solution.

* The optimum size of the cap used for the inner zone integration is $0.5° < \psi_0 < 1.2°$ which is in agreement with expected theoretical value of $180°/n_{max}$ using OSU81 to n_{max}=180.

This study shows that it is possible to compute ΔN to an accuracy similar to that of GPS heights and that these heights can be used to supplement orthometric heights in the Australian Height Datum to an accuracy comparable to third order levelling. These techniques could also be used as an efficient means to isolate any errors in the existing levelling network or included with levelling, tide gauge heights and estimates of the sea surface topography at each tide gauge, in a new adjustment of the AHD.

9 BIBLIOGRAPHY

Anfiloff, W., Barlow, B.C., Murray, A., Denham, D., and Sandford, R. (1976) Compilation and Production of the 1976 1:5 000 000 Gravity Map of Australia. *BMR Journal of Australian Geology & Geophysics,* Vol 1, pp 273-276.

Angus-Leppan, P.V., (1982) The Frequency of Gravity Measurements for Levelling Reduction. *Australian Journal of Geodesy, Photogrammetry and Surveying. No. 36,* June, pp 65-82.

Blume, P.H., (1975) Standard Datum in New South Wales. *The Australian Surveyor, Vol. 27, No. 1,* March, pp 11-21.

Bomford, G. (1977) *Geodesy.* 3rd ed., Oxford University Press.

Bowie, R.R. and Avers, H.G. (1914) Fourth General Adjustment of the Precise Level Net in the US and the Resulting Standard Deviations. *US Coast and Geodetic Survey Special Publication No.28.*

Beutler, I., Bauersima, I., Gurtner, W., Rothacher, M., Schildknecht, T., Geiger, A., (1987) Atmospheric Refraction and Other Important Biases in GPS Carrier Phase Observations. presented at XIX General Assembly of the IAGG, Vancouver, Canada. 9-22 Aug.

Campbell, J. and Lohmar, F.J., (1985) On the Ionospheric Calibration of GPS Measurements. Proceedings of the Second European Working Group on Satellite Radio Positioning (SATRAPE). Saint-Mande, France. 4-6 Nov.

Carrera, G.H., (1984) Heights on a Deforming Earth. *Technical Report No. 107.* Department of Surveying Engineering, University of New Brunswick.

Castle, R.O. and Elliott, M.R., (1982) The Sea Slope Problem Revisited. *Journal of Geophysical Research, Vol. 87, No. B8,* August, pp 6989-7024.

Coco, D.S. Clynch, J.R., (1982) The Variability of the Tropospheric Range Correction due to Water Vapour Fluctuations. Proceedings of the Third Geodetic Symposium on Satellite Doppler Positioning, New Mexico State University, February.

Cohen, E.R. and Taylor, B.N., (1987) The Fundamental Physical Constants. *Physics Today,* August, BG 11-15.

Collins, J. and Leick, A., (1985) Analysis of Macrometer Networks with Emphasis on the Montgomery (PA) County Survey, proceedings of the First International Symposium on Precise Positioning with the Global Positioning System, Rockville, Maryland. 15-19 April, pp 677-693.

Collins, J., (1986) GPS Surveying Techniques. paper presented at the 28th Australian Survey Congress, Adelaide. April 5-12, pp 31-35.

Collins, J., (1987) GPS - What Does It All Mean? *(P.O.B. Point of Beginning) June-July, Vol. 12, No. 5,* pp 12-22.

Colombo, O.L., (1986) Ephemeris Errors of GPS Satellites. *Bulletin Geodesique No.60,* pp 64-84.

Cook, A.H., (1969) *Gravity and the Earth.* Wykeham Publications (London) Ltd.

Cumerford, N.J., (1987) An Investigation into the Precision and Error Propagation within part of the Australian Height Datum Primary Levelling Network. Undergraduate project, *Department of Surveying, Queensland Institute of Technology.*

Delikaraoglou, D., Beck, N., McArthur, D., Lochhead, L., (1985) On the Establishment of 3-D Geodetic Control by Interferometry with the TI-4100 GPS Receiver. First International Symposium on Precise Positioning with the Global Positioning System, Washington D.C. April 15-19, pp 645-655.

Denker, H., Torge, W., Wenzel, H.G., Lelgemann, D, Weber, G., (1986) Strategies and Requirements for a New European Geoid Determination. Proceedings of the International Symposium on the Definition of the Geoid, Florence, 26-30 May.

Denker, H., Wenzel, H.G., (1987) Local Geoid Determination and Comparison with GPS Results. Submitted to the IAG Section III Meeting Gsm3: The Challenge of the cm Geoid - Strategies and State of the Art. Vancouver, 9-22 August.

Dennis, A.R., (1986) STARFIX A New High-Precision Satellite Positioning System. presented at International Symposium On Marine Positioning, Reston, Virginia, 14-17 October.

Dodson, A.H., (1986) Refraction and Propagation Delays in Space Geodesy. *International Journal of Remote Sensing, Vol. 7, No. 4,* pp 515-524.

Donnelley, B., (1988) personal communication.

Dooley, J.C., and Barlow, B.C., (1976) Gravimetry in Australia, 1819-1976. *BMR Journal of Australian Geology & Geophysics,* Vol 1, pp 261-271.

Eckels, R., (1987) Surveying With GPS In Australia. *Unisurv S-28,* School of Surveying, University of New South Wales.

Engelis, T., Rapp, R.H., and Tscherning, C.C., (1984) The Precise Computation of Geoid Undulation Differences with Comparison to Results Obtained from Global Positioning System. *Geophysical Research Letters, Vol. 1, No. 9,* September, pp 821-824.

Engelis, T., Rapp, R.H., and Bock, Y., (1985) Measuring Orthometric Height Differences With GPS and Gravity Data. *Manuscripta Geodaetica, No. 10* pp 187-194.

Geiger, A., (1987) Simplified Error Estimation of Satellite Positioning. presented at the GPS Technology Workshop, Jet Propulsion Laboratory, Pasadena, 23 March.

Georgiadou, Y. and Kleusberg, A., (1986) Ionospheric Delay in GPS Observations. presented at American Geophysical Union Fall Meeting, Dec. 7-12, San Francisco, Ca.

Georgiadou, Y. and Kleusberg, A., (1988) On the Effect of Ionospheric Delay on Geodetic Relative GPS Positioning. *Manuscripta Geodeatica, Vol. 13, No. 1,* pp 1-8.

GEO/HYDRO, Inc., (1986) Project Report: GPS Survey of South West Seismic Zone for W.A. Department of Lands.

Gilliland, J.R., (1981) The Outer, Middle and Near Zone Effect on the Free-Air Geoid of South Australia. *Australian Journal of Geodesy, Photogrammetry and Surveying. No. 34,* June, pp 15-27.

Gilliland, J.R., (1982) A Free Air Geoid of South Australia. *Australian Journal of Geodesy, Photogrammetry and Surveying., No. 36,* June, pp 47-58.

Gilliland, J.R., (1983) Geoid Comparisions in South Australia. *Australian Journal of Geodesy, Photogrammetry and Surveying., No. 38,* June, pp 53-70.

Gilliland, J.R., (1987) An Australian Gravity Anomaly Data Bank for Geoid Determinations. *The Australian Surveyor, Vol. 33, No 7,* September, pp 578-581.

Granger, H.W., (1972) The Australian Height Datum. *The Australian Surveyor, Vol. 24, No. 4,* December, pp 228-237.

Grant, D.B., (1987) Tropospheric Errors in GPS. Paper presented at the Centenary GPS Conference, Royal Melbourne Institute of Technology, 24-26 August.

Grant, D.B., (1988) The Combination of Terrestrial and GPS Data for Earth Deformation Studies in New Zealand. *Unisurv S-32,* School of Surveying, University of New South Wales.

Hatch, W, and Goad, C., (1973) Mathematical Description of the ORAN Error Analysis Program. *Report No. 009-73*, National Aeronautics and Space Administration, Goddard Space Flight Centre, Greenbelt, Maryland, Aug.

Hein, G.W., (1985) Orthometric Height Determination Using GPS Observations and the Integrated Geodesy Adjustment Model. *NOAA Technical Report NOS 110 NGS 32,* National Oceanic and Atmospheric Administration. Rockville, Maryland.

Hein, G.W., (1986) The Role of GPS Data in Gravity Field Approximation or The Role of the Gravity Field in GPS Surveys. IAG Symposium on the Definition of the Geoid. Florence, 26-30 May.

Heiskanen, W. and Moritz, H., (1967) *Physical Geodesy.* W.H. Freeman and Co., San Francisco.

Henson, D.J. and Collier, E.A., (1986) Effects of the Ionosphere on GPS Relative Geodesy. Proc. of the IEEE Position Location and Navigation Symposium. Las Vegas, Texas. November.

Higgins, M., (1987) Transformation from WGS84 to AGD84 - An Interim Solution. Internal Report, Department of Mapping and Surveying, Queensland.

Hoar, G.J., (1982) *Satellite Surveying.* Magnavox Advanced Products and Systems Company.

Holloway, R.D. and Williamson, I.P., (1987) Life, The Universe and Everything Or Technology and the Surveyor - 1997. *The Australian Surveyor, Vol. 33 No. 6,* June, pp 511-518.

Hothem, L.D. and Williams, G.E., (1985) Proposed Revisions to Geodetic Survey Standards and Preliminary Specifications for Geodetic Surveys Using Relative Positioning GPS Techniques (DRAFT). National Geodetic Survey Unpublished Position Paper, May.

Jeremy, C.W., (1973) Errors in Precise Levelling. Thesis for Master of Surveying Science degree, School of Surveying, University of New South Wales.

Jones, A.C., Larden, D.R., and Allman, J.S., (1987) First Order geodetic Control using Multi-Station Global Positioning System Techniques. Proceedings of the 29th Australian Survey Congress, Perth, April, pp 218-244.

Kearsley, A.H.W., (1984) Precision Limitations and Data Requirements for the Determination of Relative Geoid Heights from Gravimetry. *Report No. 26,* University of Uppsala, Institute of Geophysics.

Kearsley, A.H.W., (1985) Towards the Optimum Evaluation of the Inner Zone Contribution to Geoidal Heights. *Australian Journal Geodesy, Photogrammetry Surveying, No. 42,* June, pp 75-98.

Kearsley, A.H.W., (1986) Data Requirements for Determining Precise Relative Geoid heights From Gravimetry, *Journal of Geophysical Research, Vol. 91, No. B9,* pp 9193-9201.

Kearsley, A.H.W. and Holloway, R.D., (1987) Tests on the Recovery of Precise Geoid Height Differences from Gravimetry. Paper presented at the Centenary GPS Conference, Royal Melbourne Institute of Technology, 24-26 August.

Kearsley, A.H.W., (1988a) The Determination Of The Geoid-Ellipsoid Separation For GPS Levelling, *The Australian Surveyor, Vol. 34, No. 1,* March, pp 11-18.

Kearsley, A.H.W., (1988b) Tests on the Recovery of Precise Geoid Height Differences from Gravimetry, *Journal of Geophysical Research, Vol. 93, No. B6,* June 10, pp 6559-6570.

King, R.W., Masters, E.G., Rizos, C., Stolz, A. and Collins, J., (1985) Surveying With GPS, *Monograph No. 9*, School of Surveying, University of New South Wales.

King, R.W., (1987) personal communication.

Klass, P.J., (1987) British Scientists Reveal Signal Format of Soviet Navsat. *Aviation Week & Space Technology*, April 13, pp 109-114.

Kleusberg, A., (1986a) Ionospheric Propagation Effects In Geodetic Relative Positioning, *Manuscripta Geodaetica, Vol. 11 No. 4* , pp 256-261.

Kleusberg, A., (1986b) GPS Antenna Phase Centre Variations. American Geophysical Union Fall Meeting, Dec. 7-12, San Francisco, Ca.

Klobuchar, J.A., (1986) Design and Characteristics of the GPS Ionospheric Time Delay Algorithm for Single Frequency Users. Presented at the Position Location and Navigation Symposium, Las Vegas, NV. Nov. 4-7.

Ladd, J.W., (1986) Establishment of a 3-Dimensional Geodetic Network using the Macrometer II™ Dual-Band Surveyor. Proceedings of the Fourth International Geodetic Symposium on Satellite Positioning, Austin, Texas, April 28 - May 2.

Landau, H. and Eissfeller, B., (1985) Optimization of GPS Satellite Selection For High Precision Differential Positioning. *Heft 19,* GPS Research 1985 at the Institute of Astronomical and Physical Geodesy, Universitarer Studiengang Vermessungswesen, Universitat der Bundeswehr, Munchen. FRG, March.

Larden, D.R., Jones, A.C., Warhurst, D.F., (1986) Implementation of GPS Technology in South Australia. paper presented at the 28th Australian Survey Congress, Adelaide, April 5-12, pp 31-35.

Llewellyn, S.K. and Bent, R.B., (1973) Documentation and Description of the Bent Ionospheric Model. *Report AD-772 733,* National Technical Information Service, Springfield, Va.

Mainville, A., (1987) Intercomparison of Various Geoid Computation Methods at GPS Stations. paper presented to the IAG Section III Meeting Gsm3: The Challenge of the cm Geoid - Strategies and State of the Art, Vancouver, 9-22 Aug.

Mather, R.S., (1973) A Solution to the Geodetic Boundary Value Problem to Order e^3, Publication X-592-73-11, Goddard Space Flight Centre, Greenbelt, Md., USA.

Mitchell, H.L., (1973) Relations Between Mean Sea Level And Geodetic Levelling In Australia. *Unisurv S-9,* School of Surveying, University of New South Wales.

Morgan, P., Chen, X., and Rogers, C., (1986) An Asssessment of the Internal Precision and Quality of GPS Data from the S.A. Geodetic Network Project. Research Project Report, School of Applied Science, Canberra College of Advanced Education.

Nakiboglu, S.M., Krakiwsky, E.J., Schwarz, K.P., Buffet, B., Wanless, B., (1985) A Multi-Station, Multi Pass Approach to Global Positioning System Improvement and Precise Positioning. *Contract Report No OST83-00340,* submitted to Geodetic Survey of Canada, Department of Energy, Mines and Resources.

National Mapping Council of Australia, (1979) The Australian Height Datum (AHD). *Special Publication 8*, Division of National Mapping, Department of National Development.

National Mapping Council of Australia, (1970) Standard Specifications and Recommended practices for Horizontal and Vertical Control Surveys. Division of National Mapping, Department of National Development.

Partis, I.J., (1988) The Use of Dual Frequency TRANSIT Measurements to Determine Ionospheric Corrections for Single Frequency GPS. *thesis for Graduate Diploma,* School of Surveying, University of New South Wales.

Prijanto, A., (1987) Problems in the Levelling Used to Establish the Vertical Control Network in Java, *thesis for Master of Surveying Science,* University of New South Wales.

Rapp, R.H., (1961) The Orthometric Height, *thesis submitted for Master of Science,* Ohio State University.

Rapp, R.H. (1981) The Earth's Gravity Field to Degree and Order 180 using SEASAT Altimeter Data, Terrestrial Gravity Data and Other Data. *Report No. 322,* Department of Geodetic Science and Surveying, Ohio State University, Columbus, Ohio, USA.

Rapp, R.H., (1982) A Fortran Program for the Computation of Gravimetric Quantities from High Degree Spherical Harmonic Expansions. *Report No. 334,* Department of Geodetic Science and Surveying, Ohio State University, Columbus, Ohio, USA.

Rapp, R.H., and Cruz, J.Y., (1986) Spherical Harmonic Expansions of the Earth's Gravitational Potential to Degree 360 using 30' Mean Anomalies. *Report No. 376*, Department of Geodetic Science and Surveying, Ohio State University, Columbus, Ohio, USA.

Rawer, K., Bilitza, D., and Ramakrishnan, S., (1978) Goals and Status of the International Reference Ionosphere. *Rev. Geophys. Space Phys. No 16,* pp 177-181.

Rizos, C.R., (1979) An Efficient Computer Technique for the Evaluation of Geopotential from Spherical Harmonic Models. *Australian Journal of Geodesy, Photogrammetry and Surveying, No. 31,* pp 161-169.

Roelse, A., Granger, H.W. and Graham, J.W., (1975) The Adjustment Of The Australian Levelling Survey 1970-1971. *Technical Report 12,* 2nd ed. Division of National Mapping.

Rothacher, M., Beutler, G., Gurtner, W., Geiger, A., Kahle, H.G., Schneider, D., (1986) The 1985 Swiss GPS-Campaign. presented at the Proceedings of the Fourth Geodetic Symposium on Satellite Positioning. Austin, Texas. April 28 - May 2.

Rush, G., (1986) The Adequacy of the Australian Height Datum. unpublished position paper, Department of Mapping and Surveying, Queensland.

Schodlbauer, A., (1986) Geodetic Height Systems In The Wake Of Advancing Technology. proceedings of the Fourth International Geodetic Symposium on Satellite Positioning. Austin, Texas. April 28 - May 2.

Scherrer, R., (1985) *The WM GPS Primer.* The Wild Magnavox Satellite Survey Company.

Schwarz, K.P. and Sideris, M.G., (1985) Precise Geoid Heights and Their Use In GPS Interferometry. *Report 85-004,* University of Calgary, September.

Schwarz, K.P., Sideris, M.G., and Forsberg, R., (1987) Orthometric Heights Without Levelling. *Journal of Surveying Engineering,* American Society of Civil Engineers, Vol. 113, No. 1, February, pp 28-40.

Sideris, M.G. and Schwarz, K.P., (1986) The Use of GPS and Doppler Heights in NAVD. Proceedings of the Fourth International Geodetic Symposium on Satellite Positioning, Austin, Texas, April 28 - May 2.

Smith Jr., E.K. and Weintraub, S., (1953) The Constants in the Equation for Atmospheric Refractive Index at Radio Frequencies. *Proc. IRE, 41,* pp 1035-1057.

Stolz, A., (1987) Lecture Notes, University of New South Wales.

Tscherning, C.C., and Forsberg, R., (1986) Geoid Determination in the Nordic Countries from Gravity and Height Data. Proceedings of the International Symposium on the Definition of the Geoid, Florence, 26-30 May.

Torge, W., (1980) *Geodesy.* Walter de Gruyter & Co., Berlin.

Trimble Navigation Ltd., (1986) *TRIMVEC™* GPS Survey Software Preliminary User's Manual. Part Number 11926 Rev. D, Trimble Navigation Limited, 585 North Mary Avenue, Sunnyvale, California. 94086.

Vanicek, P. and Krakiwsky, E., (1986) *Geodesy, The Concepts.* 2nd ed., Elsevier Science Publishers.

Vanicek, P., Carrera, G.H., Craymer, M.R., (1985) Corrections for Systematic Errors in the Canadian Levelling Network. *Contract Report 85-001,* Department of Energy, Mines and Resources Canada.

WM Satellite Survey Company, (1987) *PoPS™* Manual. Wild Heerbrugg Survey Corporation and Magnavox Survey Systems Inc, November edition.

Wells, D., as leader, (1986) *Guide To GPS Positioning.* Canadian GPS Associates, University of New Brunswick.

Wooden, W.H., (1985) NAVSTAR Global Positioning System: 1985, proceedings of the First International Symposium on Precise Positioning with the Global Positioning System, Rockville, Maryland. 15-19 April, pp 23-32.

Zilkoski, D.B., and Hothem, L.D., (1988) GPS Satellite Surveys and Vertical Control, presented at the GPS-88 Engineering Applications of GPS Satellite Surveying Technology at Nashville, Tennessee. 11-14 May.

10 APPENDIX A

Western Australia GPS Network - South West Seismic Zone

No.	Name	Latitude (WGS-72)	Longitude (WGS-72)	Height (WGS-72)	Height (AHD)
1	MRA8	-30.836005	116.639220	393.015	416.931
2	NMF705	-30.852247	116.795533	359.979	383.632
3	HD09	-31.003169	116.983791	377.135	400.589
4	PTH135	-31.027971	116.624541	313.975	338.041
5	HD10	-31.120361	116.929872	341.630	365.463
6	PTH136	-31.147490	116.631130	273.014	297.256
7	BERRING	-31.275797	116.918182	289.188	313.307
8	KARRABEIN	-31.524803	116.895302	273.112	297.482
9	NTHTOODYAY	-31.448026	116.557939	342.147	367.045
10	HD08	-30.994752	116.782171	314.202	338.010

11 APPENDIX B

South Australian GPS Network - Phase 1

No.	Name	Latitude (WGS-72)	Longitude (WGS-72)	Height (WGS-72)	Height (AHD
4	6726/1099	-35.6857338	139.3526459	36.225	36.125
5	6727/1063	-35.1455841	139.4593506	100.723	98.721
6	6727/1099	-35.0630798	139.3719940	84.712	82.424
7	6727/1819	-35.3580170	139.3833923	25.978	24.756
8	6727/1820	-35.1798820	139.3665161	66.206	64.412
18	6826/1001	-35.5381050	139.5683441	110.078	
19	6826/1120	-35.5906181	139.9694824	92.879	
21	6826/1122	-35.6762772	139.6489410	169.207	168.578
22	6826/2001	-35.6797028	139.8739471	35.711	
23	6826/2002	-35.5280685	139.8483734	55.002	
24	6827/1003	-35.1786156	139.6112061	116.439	114.048
25	6827/1065	-35.3042297	139.9644470	136.893	134.646
26	6827/1066	-35.4261856	139.7705383	29.054	
27	6827/1067	-35.3499260	139.5572662	41.590	
28	6827/1701	-35.2385559	139.8657990	135.767	
29	6827/1702	-35.1916618	139.7593079	135.856	
30	6827/1703	-35.1159477	139.8228455	119.885	117.184
31	6827/1704	-35.0458069	139.5584869	131.155	
32	6827/1705	-35.0178642	139.7082977	99.420	
33	6828/1003	-34.9389915	139.6469116	143.474	140.270
34	6828/1157	-34.9788933	139.8356628	137.832	134.661
35	6828/1256	-34.5741768	139.7383881	74.583	70.463
36	6828/1264	-34.6751976	139.9528046	76.203	72.358
37	6828/1701	-34.8336487	139.8615417	100.421	

South Australian GPS Network - Phase 1

No.	Name	Latitude (WGS-72)	Longitude (WGS-72)	Height (WGS-72)	Height (AHD
38	6828/1702	-34.5209160	139.8903198	83.623	
39	6829/1301	-34.3140182	139.9770966	68.277	63.587
46	6926/1501	-35.5057907	140.4513550	139.696	137.016
47	6926/1540	-35.5093842	140.1715851	114.425	112.376
48	6926/1548	-35.7859192	140.0483398	96.178	94.676
52	6926/1570	-35.6032295	140.1924744	115.928	
53	6927/1055	-35.0130157	140.4828644	114.316	110.845
54	6927/1056	-35.4198799	140.0293427	90.419	
55	6927/1301	-35.4105873	140.2976227	106.398	
56	6927/1302	-35.3976860	140.1377411	130.577	128.338
57	6927/1303	-35.2880974	140.2886353	123.449	
58	6927/1304	-35.2627907	140.1167450	119.770	
59	6927/1305	-35.1517487	140.2927551	123.687	120.601
60	6927/1306	-35.1195297	140.4469910	143.768	
61	6927/1307	-35.1007690	140.0234375	93.741	90.623
62	6928/1067	-34.9851913	140.1129913	101.431	98.271
63	6928/1070	-34.7756805	140.4885254	72.464	68.628
64	6928/1092	-34.7961159	140.2258301	78.558	74.872
65	6928/1116	-34.5347748	140.4714050	70.974	66.833
66	6928/1118	-34.9804649	140.0113525	90.484	87.376
67	6928/1301	-34.8896408	140.0265503	101.101	
68	6928/1302	-34.7107735	140.3435669	82.575	
69	6928/1303	-34.6530228	140.1966858	82.355	
70	6929/1232	-34.4782257	140.0172272	79.345	74.854

South Australian GPS Network - Phase 1

No.	Name	Latitude (WGS-72)	Longitude (WGS-72)	Height (WGS-72)	Height (AHD
71	6929/1394	-34.3911324	140.3711853	58.998	54.586
72	6929/1397	-34.4808083	140.2935944	70.967	66.734
73	6929/1399	-34.3440399	140.1356812	92.206	87.473
85	7026/ 24	-35.5684128	140.8929596	163.105	
86	7026/1353	-35.6427422	140.8639984	145.414	141.926
89	7027/1049	-35.3904076	140.9904175	149.161	
90	7027/1051	-35.3703270	140.6757355	132.071	128.800
91	7027/1124	-35.0901031	140.6653900	83.648	80.070
92	7027/1758	-35.3517075	140.5202942	107.110	
93	7027/1759	-35.2700615	140.5704956	114.281	111.106
94	7027/1760	-35.2917137	140.7700348	125.851	
95	7027/1761	-35.2350960	140.9714813	116.981	
96	7027/1763	-35.1150856	140.8320465	123.017	
97	7028/1004	-34.7892761	140.9897766	105.444	101.234
98	7028/1089	-34.8641129	140.8347931	57.890	54.012
99	7028/1098	-34.9992752	140.7720642	73.975	70.206
100	7028/1104	-34.5295906	140.7901154	71.056	67.114
101	7028/1113	-34.7683372	140.6854706	90.869	86.973
102	7028/1144	-34.5941467	140.6858521	74.167	70.060
103	7028/1304	-34.6849403	140.5495453	81.397	77.447
104	7028/1305	-34.6775169	140.8045349	68.713	
105	7028/1306	-34.5894394	140.9633789	64.570	60.100
106	7029/1099	-34.2829933	140.8927917	54.098	49.329
107	7029/7282	-34.3563766	140.9431458	64.304	59.528
108	7127/1100	-35.1057587	141.0222473	115.737	111.590

12 APPENDIX C

WESTERN AUSTRALIA GPS NETWORK
SOUTH WEST SEISMIC ZONE

RESULTS FROM PROGRAM GRAV08
COMPARISION OF ΔN FROM GRAVIMETRIC SOLUTION AND ΔN FROM THE DIFFERENCE BETWEEN GPS AND AHD HEIGHTS FROM RING 0 TO RING 26.

SCHOOL OF SURVEYING, U.N.S.W. DELTA N ANALYSIS
GRAV08 Ver 1.5 WA.DAT 19-MAY-88

WESTERN AUSTRALIA HEIGHT NETWORK
UNIVERSITY OF NEW SOUTH WALES

Control File: WAPTS.DAT Lines File: WALINES.DAT
Inner Zone File: WAIN.SUM Remote Zone File: OSU81_18.OUT

Number of Rings in Inner Zone: 0

LINE NO.	FROM	TO	DIST (km)	GRAVITY REMOTE	GRAVITY INNER	GRAVITY SUM	G.P.S.-LEVEL	DIFF (cm)	PPM
1	1	2	15.06	62.0	.0	62.0	26.3	-35.7	23.7
2	1	3	37.79	94.0	.0	94.0	46.2	-47.8	12.6
3	1	4	21.33	-42.0	.0	-42.0	-15.0	27.0	12.7
4	2	3	24.57	32.0	.0	32.0	19.9	-12.1	4.9
5	2	4	25.43	-104.0	.0	-104.0	-41.3	62.7	24.7
6	3	10	19.28	-62.0	.0	-62.0	-35.4	26.6	13.8
7	3	5	13.98	-33.0	.0	-33.0	-37.9	-4.9	3.5
8	4	10	15.50	74.0	.0	74.0	25.8	-48.2	31.1
9	4	6	13.27	-16.0	.0	-16.0	-17.6	-1.6	1.2
10	5	6	28.65	-119.0	.0	-119.0	-40.9	78.1	27.3
11	5	7	17.27	-27.0	.0	-27.0	-28.6	-1.6	.9
12	5	10	19.82	-29.0	.0	-29.0	2.5	31.5	15.9
13	6	10	22.24	90.0	.0	90.0	43.4	-46.6	21.0
14	6	7	30.83	92.0	.0	92.0	12.3	-79.7	25.8
15	6	8	48.81	57.0	.0	57.0	-12.8	-69.8	14.3
16	6	9	34.04	-75.0	.0	-75.0	-65.6	9.4	2.8
17	7	8	27.69	-35.0	.0	-35.0	-25.1	9.9	3.6
18	7	9	39.24	-167.0	.0	-167.0	-77.9	89.1	22.7
19	8	9	33.17	-132.0	.0	-132.0	-52.8	79.2	23.9

MEAN: 3.4 S.D. 50.7 R.M.S. 49.4 MEAN PPM: 15.1 RMS PPM: 17.9

SCHOOL OF SURVEYING, U.N.S.W. DELTA N ANALYSIS
GRAV08 Ver 1.5 WA.DAT 19-MAY-88
WESTERN AUSTRALIA HEIGHT NETWORK
UNIVERSITY OF NEW SOUTH WALES

Control File: WAPTS.DAT Lines File: WALINES.DAT
Inner Zone File: WAIN.SUM Remote Zone File: OSU81_18.OUT

Number of Rings in Inner Zone: 2

LINE NO.	FROM	TO	DIST (km)	GRAVITY REMOTE	GRAVITY INNER	GRAVITY SUM	G.P.S.-LEVEL	DIFF (cm)	PPM
1	1	2	15.06	62.0	-24.9	37.1	26.3	-10.8	7.2
2	1	3	37.79	94.0	-28.9	65.1	46.2	-18.9	5.0
3	1	4	21.33	-42.0	14.8	-27.2	-15.0	12.2	5.7
4	2	3	24.57	32.0	-4.0	28.0	19.9	-8.1	3.3
5	2	4	25.43	-104.0	39.7	-64.3	-41.3	23.0	9.0
6	3	10	19.28	-62.0	13.4	-48.6	-35.4	13.2	6.9
7	3	5	13.98	-33.0	1.8	-31.2	-37.9	-6.7	4.8
8	4	10	15.50	74.0	-30.3	43.7	25.8	-17.9	11.5
9	4	6	13.27	-16.0	6.0	-10.0	-17.6	-7.6	5.7
10	5	6	28.65	-119.0	47.9	-71.1	-40.9	30.2	10.5
11	5	7	17.27	-27.0	-3.8	-30.8	-28.6	2.2	1.3
12	5	10	19.82	-29.0	11.6	-17.4	2.5	19.9	10.1
13	6	10	22.24	90.0	-36.3	53.7	43.4	-10.3	4.6
14	6	7	30.83	92.0	-51.7	40.3	12.3	-28.0	9.1
15	6	8	48.81	57.0	-58.5	-1.5	-12.8	-11.3	2.3
16	6	9	34.04	-75.0	12.3	-62.7	-65.6	-2.9	.8
17	7	8	27.69	-35.0	-6.7	-41.7	-25.1	16.6	6.0
18	7	9	39.24	-167.0	64.0	-103.0	-77.9	25.1	6.4
19	8	9	33.17	-132.0	70.8	-61.2	-52.8	8.4	2.5

MEAN: 1.5 S.D. 16.9 R.M.S. 16.4 MEAN PPM: 5.9 RMS PPM: 6.7

SCHOOL OF SURVEYING, U.N.S.W. DELTA N ANALYSIS
GRAV08 Ver 1.5 WA.DAT 19-MAY-88

WESTERN AUSTRALIA HEIGHT NETWORK
UNIVERSITY OF NEW SOUTH WALES

Control File: WAPTS.DAT Lines File: WALINES.DAT
Inner Zone File: WAIN.SUM Remote Zone File: OSU81_18.OUT

Number of Rings in Inner Zone: 4

LINE NO.	FROM	TO	DIST (km)	GRAVITY REMOTE	GRAVITY INNER	GRAVITY SUM	G.P.S.-LEVEL	DIFF (cm)	PPM
1	1	2	15.06	62.0	-46.0	16.0	26.3	10.3	6.8
2	1	3	37.79	94.0	-70.6	23.4	46.2	22.8	6.0
3	1	4	21.33	-42.0	23.6	-18.4	-15.0	3.4	1.6
4	2	3	24.57	32.0	-24.6	7.4	19.9	12.5	5.1
5	2	4	25.43	-104.0	69.6	-34.4	-41.3	-6.9	2.7
6	3	10	19.28	-62.0	34.9	-27.1	-35.4	-8.3	4.3
7	3	5	13.98	-33.0	6.5	-26.5	-37.9	-11.4	8.2
8	4	10	15.50	74.0	-59.3	14.7	25.8	11.1	7.2
9	4	6	13.27	-16.0	5.7	-10.3	-17.6	-7.3	5.5
10	5	6	28.65	-119.0	93.5	-25.5	-40.9	-15.4	5.4
11	5	7	17.27	-27.0	-2.1	-29.1	-28.6	.5	.3
12	5	10	19.82	-29.0	28.4	-.6	2.5	3.1	1.6
13	6	10	22.24	90.0	-65.0	25.0	43.4	18.4	8.3
14	6	7	30.83	92.0	-95.5	-3.5	12.3	15.8	5.1
15	6	8	48.81	57.0	-104.0	-47.0	-12.8	34.2	7.0
16	6	9	34.04	-75.0	22.3	-52.7	-65.6	-12.9	3.8
17	7	8	27.69	-35.0	-8.5	-43.5	-25.1	18.4	6.6
18	7	9	39.24	-167.0	117.8	-49.2	-77.9	-28.7	7.3
19	8	9	33.17	-132.0	126.3	-5.7	-52.8	-47.1	14.2

MEAN: .7 S.D. 19.4 R.M.S. 18.9 MEAN PPM: 5.6 RMS PPM: 6.4

SCHOOL OF SURVEYING, U.N.S.W. DELTA N ANALYSIS
GRAV08 Ver 1.5 WA.DAT 19-MAY-88
WESTERN AUSTRALIA HEIGHT NETWORK
UNIVERSITY OF NEW SOUTH WALES

Control File: WAPTS.DAT Lines File: WALINES.DAT
Inner Zone File: WAIN.SUM Remote Zone File: OSU81_18.OUT

Number of Rings in Inner Zone: 6

LINE NO.	FROM	TO	DIST (km)	GRAVITY REMOTE	GRAVITY INNER	GRAVITY SUM	G.P.S.-LEVEL	DIFF (cm)	PPM
1	1	2	15.06	62.0	-59.9	2.1	26.3	24.2	16.1
2	1	3	37.79	94.0	-111.1	-17.1	46.2	63.3	16.8
3	1	4	21.33	-42.0	22.6	-19.4	-15.0	4.4	2.1
4	2	3	24.57	32.0	-51.2	-19.2	19.9	39.1	15.9
5	2	4	25.43	-104.0	82.5	-21.5	-41.3	-19.8	7.8
6	3	10	19.28	-62.0	61.6	-.4	-35.4	-35.0	18.2
7	3	5	13.98	-33.0	9.9	-23.1	-37.9	-14.8	10.6
8	4	10	15.50	74.0	-72.1	1.9	25.8	23.9	15.4
9	4	6	13.27	-16.0	-2.2	-18.2	-17.6	.6	.5
10	5	6	28.65	-119.0	121.6	2.6	-40.9	-43.5	15.2
11	5	7	17.27	-27.0	-2.5	-29.5	-28.6	.9	.5
12	5	10	19.82	-29.0	51.8	22.8	2.5	-20.3	10.2
13	6	10	22.24	90.0	-69.8	20.2	43.4	23.2	10.4
14	6	7	30.83	92.0	-124.1	-32.1	12.3	44.4	14.4
15	6	8	48.81	57.0	-127.7	-70.7	-12.8	57.9	11.9
16	6	9	34.04	-75.0	18.2	-56.8	-65.6	-8.8	2.6
17	7	8	27.69	-35.0	-3.6	-38.6	-25.1	13.5	4.9
18	7	9	39.24	-167.0	142.2	-24.8	-77.9	-53.1	13.5
19	8	9	33.17	-132.0	145.8	13.8	-52.8	-66.6	20.1

MEAN: 1.8 S.D. 36.7 R.M.S. 35.7 MEAN PPM: 10.9 RMS PPM: 12.5

SCHOOL OF SURVEYING, U.N.S.W. DELTA N ANALYSIS
GRAV08 Ver 1.5 WA.DAT 19-MAY-88

WESTERN AUSTRALIA HEIGHT NETWORK
UNIVERSITY OF NEW SOUTH WALES

Control File: WAPTS.DAT Lines File: WALINES.DAT
Inner Zone File: WAIN.SUM Remote Zone File: OSU81_18.OUT

Number of Rings in Inner Zone: 8

LINE NO.	FROM	TO	DIST (km)	GRAVITY REMOTE	GRAVITY INNER	GRAVITY SUM	G.P.S.-LEVEL	DIFF (cm)	PPM
1	1	2	15.06	62.0	-36.5	25.5	26.3	.8	.6
2	1	3	37.79	94.0	-92.2	1.8	46.2	44.4	11.8
3	1	4	21.33	-42.0	13.8	-28.2	-15.0	13.2	6.2
4	2	3	24.57	32.0	-55.7	-23.7	19.9	43.6	17.7
5	2	4	25.43	-104.0	50.3	-53.7	-41.3	12.4	4.9
6	3	10	19.28	-62.0	57.4	-4.6	-35.4	-30.8	16.0
7	3	5	13.98	-33.0	11.1	-21.9	-37.9	-16.0	11.4
8	4	10	15.50	74.0	-48.6	25.4	25.8	.4	.3
9	4	6	13.27	-16.0	-3.6	-19.6	-17.6	2.0	1.5
10	5	6	28.65	-119.0	91.4	-27.6	-40.9	-13.3	4.6
11	5	7	17.27	-27.0	-3.0	-30.0	-28.6	1.4	.8
12	5	10	19.82	-29.0	46.3	17.3	2.5	-14.8	7.5
13	6	10	22.24	90.0	-45.0	45.0	43.4	-1.6	.7
14	6	7	30.83	92.0	-94.4	-2.4	12.3	14.7	4.8
15	6	8	48.81	57.0	-99.3	-42.3	-12.8	29.5	6.0
16	6	9	34.04	-75.0	10.9	-64.1	-65.6	-1.5	.4
17	7	8	27.69	-35.0	-4.9	-39.9	-25.1	14.8	5.3
18	7	9	39.24	-167.0	105.2	-61.8	-77.9	-16.1	4.1
19	8	9	33.17	-132.0	110.1	-21.9	-52.8	-30.9	9.3

MEAN: 2.8 S.D. 21.5 R.M.S. 20.9 MEAN PPM: 6.0 RMS PPM: 7.9

SCHOOL OF SURVEYING, U.N.S.W. DELTA N ANALYSIS
GRAV08 Ver 1.5 WA.DAT 19-MAY-88

WESTERN AUSTRALIA HEIGHT NETWORK
UNIVERSITY OF NEW SOUTH WALES

Control File: WAPTS.DAT Lines File: WALINES.DAT
Inner Zone File: WAIN.SUM Remote Zone File: OSU81_18.OUT

Number of Rings in Inner Zone: 10

LINE NO.	FROM	TO	DIST (km)	GRAVITY REMOTE	GRAVITY INNER	GRAVITY SUM	G.P.S.-LEVEL	DIFF (cm)	PPM
1	1	2	15.06	62.0	-27.0	35.0	26.3	-8.7	5.8
2	1	3	37.79	94.0	-51.5	42.5	46.2	3.7	1.0
3	1	4	21.33	-42.0	16.4	-25.6	-15.0	10.6	5.0
4	2	3	24.57	32.0	-24.5	7.5	19.9	12.4	5.0
5	2	4	25.43	-104.0	43.4	-60.6	-41.3	19.3	7.6
6	3	10	19.28	-62.0	26.5	-35.5	-35.4	.1	.0
7	3	5	13.98	-33.0	6.3	-26.7	-37.9	-11.2	8.0
8	4	10	15.50	74.0	-41.4	32.6	25.8	-6.8	4.4
9	4	6	13.27	-16.0	-2.5	-18.5	-17.6	.9	.7
10	5	6	28.65	-119.0	59.1	-59.9	-40.9	19.0	6.6
11	5	7	17.27	-27.0	-10.0	-37.0	-28.6	8.4	4.9
12	5	10	19.82	-29.0	20.2	-8.8	2.5	11.3	5.7
13	6	10	22.24	90.0	-38.9	51.1	43.4	-7.7	3.5
14	6	7	30.83	92.0	-69.1	22.9	12.3	-10.6	3.4
15	6	8	48.81	57.0	-85.1	-28.1	-12.8	15.3	3.1
16	6	9	34.04	-75.0	10.6	-64.4	-65.6	-1.2	.3
17	7	8	27.69	-35.0	-16.0	-51.0	-25.1	25.9	9.4
18	7	9	39.24	-167.0	79.7	-87.3	-77.9	9.4	2.4
19	8	9	33.17	-132.0	95.7	-36.3	-52.8	-16.5	5.0

MEAN: 3.9 S.D. 12.7 R.M.S. 12.4 MEAN PPM: 4.3 RMS PPM: 5.0

SCHOOL OF SURVEYING, U.N.S.W. DELTA N ANALYSIS
GRAV08 Ver 1.5 WA.DAT 19-MAY-88

WESTERN AUSTRALIA HEIGHT NETWORK
UNIVERSITY OF NEW SOUTH WALES

Control File: WAPTS.DAT Lines File: WALINES.DAT
Inner Zone File: WAIN.SUM Remote Zone File: OSU81_18.OUT

Number of Rings in Inner Zone: 12

LINE NO.	FROM	TO	DIST (km)	GRAVITY REMOTE	GRAVITY INNER	GRAVITY SUM	G.P.S.-LEVEL	DIFF (cm)	PPM
1	1	2	15.06	62.0	-29.4	32.6	26.3	-6.3	4.2
2	1	3	37.79	94.0	-42.4	51.6	46.2	-5.4	1.4
3	1	4	21.33	-42.0	17.3	-24.7	-15.0	9.7	4.5
4	2	3	24.57	32.0	-13.0	19.0	19.9	.9	.4
5	2	4	25.43	-104.0	46.7	-57.3	-41.3	16.0	6.3
6	3	10	19.28	-62.0	16.7	-45.3	-35.4	9.9	5.1
7	3	5	13.98	-33.0	.5	-32.5	-37.9	-5.4	3.8
8	4	10	15.50	74.0	-43.0	31.0	25.8	-5.2	3.4
9	4	6	13.27	-16.0	-2.3	-18.3	-17.6	.7	.6
10	5	6	28.65	-119.0	56.9	-62.1	-40.9	21.2	7.4
11	5	7	17.27	-27.0	-9.0	-36.0	-28.6	7.4	4.3
12	5	10	19.82	-29.0	16.3	-12.7	2.5	15.2	7.7
13	6	10	22.24	90.0	-40.6	49.4	43.4	-6.0	2.7
14	6	7	30.83	92.0	-65.8	26.2	12.3	-13.9	4.5
15	6	8	48.81	57.0	-82.5	-25.5	-12.8	12.7	2.6
16	6	9	34.04	-75.0	8.0	-67.0	-65.6	1.4	.4
17	7	8	27.69	-35.0	-16.7	-51.7	-25.1	26.6	9.6
18	7	9	39.24	-167.0	73.9	-93.1	-77.9	15.2	3.9
19	8	9	33.17	-132.0	90.6	-41.4	-52.8	-11.4	3.4

MEAN: 4.4 S.D. 12.4 R.M.S. 12.1 MEAN PPM: 4.0 RMS PPM: 4.7

SCHOOL OF SURVEYING, U.N.S.W. DELTA N ANALYSIS
GRAV08 Ver 1.5 WA.DAT 19-MAY-88

WESTERN AUSTRALIA HEIGHT NETWORK
UNIVERSITY OF NEW SOUTH WALES

Control File: WAPTS.DAT Lines File: WALINES.DAT
Inner Zone File: WAIN.SUM Remote Zone File: OSU81_18.OUT

Number of Rings in Inner Zone: 14

LINE NO.	FROM	TO	DIST (km)	GRAVITY REMOTE	GRAVITY INNER	GRAVITY SUM	G.P.S.-LEVEL	DIFF (cm)	PPM
1	1	2	15.06	62.0	-35.8	26.2	26.3	.1	.0
2	1	3	37.79	94.0	-52.1	41.9	46.2	4.3	1.1
3	1	4	21.33	-42.0	18.9	-23.1	-15.0	8.1	3.8
4	2	3	24.57	32.0	-16.3	15.7	19.9	4.2	1.7
5	2	4	25.43	-104.0	54.7	-49.3	-41.3	8.0	3.1
6	3	10	19.28	-62.0	20.3	-41.7	-35.4	6.3	3.3
7	3	5	13.98	-33.0	2.7	-30.3	-37.9	-7.6	5.5
8	4	10	15.50	74.0	-50.7	23.3	25.8	2.5	1.6
9	4	6	13.27	-16.0	-3.1	-19.1	-17.6	1.5	1.1
10	5	6	28.65	-119.0	65.2	-53.8	-40.9	12.9	4.5
11	5	7	17.27	-27.0	-9.5	-36.5	-28.6	7.9	4.6
12	5	10	19.82	-29.0	17.6	-11.4	2.5	13.9	7.0
13	6	10	22.24	90.0	-47.6	42.4	43.4	1.0	.5
14	6	7	30.83	92.0	-74.7	17.3	12.3	-5.0	1.6
15	6	8	48.81	57.0	-92.1	-35.1	-12.8	22.3	4.6
16	6	9	34.04	-75.0	10.0	-65.0	-65.6	-.6	.2
17	7	8	27.69	-35.0	-17.3	-52.3	-25.1	27.2	9.8
18	7	9	39.24	-167.0	84.8	-82.2	-77.9	4.3	1.1
19	8	9	33.17	-132.0	102.1	-29.9	-52.8	-22.9	6.9

MEAN: 4.6 S.D. 11.8 R.M.S. 11.5 MEAN PPM: 3.3 RMS PPM: 4.2

SCHOOL OF SURVEYING, U.N.S.W. DELTA N ANALYSIS
GRAV08 Ver 1.5 WA.DAT 19-MAY-88
WESTERN AUSTRALIA HEIGHT NETWORK
UNIVERSITY OF NEW SOUTH WALES

Control File: WAPTS.DAT Lines File: WALINES.DAT
Inner Zone File: WAIN.SUM Remote Zone File: OSU81_18.OUT

Number of Rings in Inner Zone: 16

LINE NO.	FROM	TO	DIST (km)	GRAVITY REMOTE	GRAVITY INNER	GRAVITY SUM	G.P.S.-LEVEL	DIFF (cm)	PPM
1	1	2	15.06	62.0	-44.3	17.7	26.3	8.6	5.7
2	1	3	37.79	94.0	-69.0	25.0	46.2	21.2	5.6
3	1	4	21.33	-42.0	19.5	-22.5	-15.0	7.5	3.5
4	2	3	24.57	32.0	-24.7	7.3	19.9	12.6	5.1
5	2	4	25.43	-104.0	63.8	-40.2	-41.3	-1.1	.4
6	3	10	19.28	-62.0	28.7	-33.3	-35.4	-2.1	1.1
7	3	5	13.98	-33.0	1.2	-31.8	-37.9	-6.1	4.4
8	4	10	15.50	74.0	-59.9	14.1	25.8	11.7	7.5
9	4	6	13.27	-16.0	-3.9	-19.9	-17.6	2.3	1.7
10	5	6	28.65	-119.0	83.4	-35.6	-40.9	-5.3	1.9
11	5	7	17.27	-27.0	-5.7	-32.7	-28.6	4.1	2.4
12	5	10	19.82	-29.0	27.5	-1.5	2.5	4.0	2.0
13	6	10	22.24	90.0	-56.0	34.0	43.4	9.4	4.2
14	6	7	30.83	92.0	-89.1	2.9	12.3	9.4	3.0
15	6	8	48.81	57.0	-103.4	-46.4	-12.8	33.6	6.9
16	6	9	34.04	-75.0	1.2	-73.8	-65.6	8.2	2.4
17	7	8	27.69	-35.0	-14.3	-49.3	-25.1	24.2	8.8
18	7	9	39.24	-167.0	90.3	-76.7	-77.9	-1.2	.3
19	8	9	33.17	-132.0	104.6	-27.4	-52.8	-25.4	7.7

MEAN: 6.1 S.D. 14.1 R.M.S. 13.8 MEAN PPM: 3.9 RMS PPM: 4.7

SCHOOL OF SURVEYING, U.N.S.W. DELTA N ANALYSIS
GRAV08 Ver 1.5 WA.DAT 19-MAY-88

WESTERN AUSTRALIA HEIGHT NETWORK
UNIVERSITY OF NEW SOUTH WALES

Control File: WAPTS.DAT Lines File: WALINES.DAT
Inner Zone File: WAIN.SUM Remote Zone File: OSU81_18.OUT

Number of Rings in Inner Zone: 18

LINE NO.	FROM	TO	DIST (km)	GRAVITY REMOTE	GRAVITY INNER	GRAVITY SUM	G.P.S.-LEVEL	DIFF (cm)	PPM
1	1	2	15.06	62.0	-43.2	18.8	26.3	7.5	5.0
2	1	3	37.79	94.0	-82.9	11.1	46.2	35.1	9.3
3	1	4	21.33	-42.0	11.8	-30.2	-15.0	15.2	7.1
4	2	3	24.57	32.0	-39.7	-7.7	19.9	27.6	11.2
5	2	4	25.43	-104.0	55.0	-49.0	-41.3	7.7	3.0
6	3	10	19.28	-62.0	42.5	-19.5	-35.4	-15.9	8.3
7	3	5	13.98	-33.0	5.1	-27.9	-37.9	-10.0	7.2
8	4	10	15.50	74.0	-52.1	21.9	25.8	3.9	2.5
9	4	6	13.27	-16.0	-5.5	-21.5	-17.6	3.9	3.0
10	5	6	28.65	-119.0	84.0	-35.0	-40.9	-5.9	2.1
11	5	7	17.27	-27.0	-7.1	-34.1	-28.6	5.5	3.2
12	5	10	19.82	-29.0	37.4	8.4	2.5	-5.9	3.0
13	6	10	22.24	90.0	-46.6	43.4	43.4	.0	.0
14	6	7	30.83	92.0	-91.1	.9	12.3	11.4	3.7
15	6	8	48.81	57.0	-110.5	-53.5	-12.8	40.7	8.3
16	6	9	34.04	-75.0	-7.5	-82.5	-65.6	16.9	5.0
17	7	8	27.69	-35.0	-19.4	-54.4	-25.1	29.3	10.6
18	7	9	39.24	-167.0	83.6	-83.4	-77.9	5.5	1.4
19	8	9	33.17	-132.0	103.0	-29.0	-52.8	-23.8	7.2

MEAN: 7.8 S.D. 18.8 R.M.S. 18.3 MEAN PPM: 5.3 RMS PPM: 6.2

SCHOOL OF SURVEYING, U.N.S.W. DELTA N ANALYSIS
GRAV08 Ver 1.5 WA.DAT 19-MAY-88

WESTERN AUSTRALIA HEIGHT NETWORK
UNIVERSITY OF NEW SOUTH WALES

Control File: WAPTS.DAT Lines File: WALINES.DAT
Inner Zone File: WAIN.SUM Remote Zone File: OSU81_18.OUT

Number of Rings in Inner Zone: 20

LINE NO.	FROM	TO	DIST (km)	GRAVITY REMOTE	GRAVITY INNER	GRAVITY SUM	G.P.S.-LEVEL	DIFF (cm)	PPM
1	1	2	15.06	62.0	-37.5	24.5	26.3	1.8	1.2
2	1	3	37.79	94.0	-84.2	9.8	46.2	36.4	9.6
3	1	4	21.33	-42.0	4.2	-37.8	-15.0	22.8	10.7
4	2	3	24.57	32.0	-46.7	-14.7	19.9	34.6	14.1
5	2	4	25.43	-104.0	41.7	-62.3	-41.3	21.0	8.3
6	3	10	19.28	-62.0	43.9	-18.1	-35.4	-17.3	9.0
7	3	5	13.98	-33.0	7.8	-25.2	-37.9	-12.7	9.1
8	4	10	15.50	74.0	-44.6	29.4	25.8	-3.6	2.4
9	4	6	13.27	-16.0	-9.4	-25.4	-17.6	7.8	5.8
10	5	6	28.65	-119.0	71.2	-47.8	-40.9	6.9	2.4
11	5	7	17.27	-27.0	-12.8	-39.8	-28.6	11.2	6.5
12	5	10	19.82	-29.0	36.0	7.0	2.5	-4.5	2.3
13	6	10	22.24	90.0	-35.2	54.8	43.4	-11.4	5.1
14	6	7	30.83	92.0	-84.0	8.0	12.3	4.3	1.4
15	6	8	48.81	57.0	-112.3	-55.3	-12.8	42.5	8.7
16	6	9	34.04	-75.0	-10.9	-85.9	-65.6	20.3	6.0
17	7	8	27.69	-35.0	-28.3	-63.3	-25.1	38.2	13.8
18	7	9	39.24	-167.0	73.1	-93.9	-77.9	16.0	4.1
19	8	9	33.17	-132.0	101.4	-30.6	-52.8	-22.2	6.7

MEAN: 10.1 S.D. 22.1 R.M.S. 21.5 MEAN PPM: 6.7 RMS PPM: 7.7

SCHOOL OF SURVEYING, U.N.S.W. DELTA N ANALYSIS
GRAV08 Ver 1.5 WA.DAT 19-MAY-88

WESTERN AUSTRALIA HEIGHT NETWORK
UNIVERSITY OF NEW SOUTH WALES

Control File: WAPTS.DAT Lines File: WALINES.DAT
Inner Zone File: WAIN.SUM Remote Zone File: OSU81_18.OUT

Number of Rings in Inner Zone: 22

LINE NO.	FROM	TO	DIST (km)	GRAVITY REMOTE	GRAVITY INNER	GRAVITY SUM	G.P.S.-LEVEL	DIFF (cm)	PPM
1	1	2	15.06	62.0	-27.7	34.3	26.3	-8.0	5.3
2	1	3	37.79	94.0	-76.1	17.9	46.2	28.3	7.5
3	1	4	21.33	-42.0	1.6	-40.4	-15.0	25.4	11.9
4	2	3	24.57	32.0	-48.4	-16.4	19.9	36.3	14.8
5	2	4	25.43	-104.0	29.3	-74.7	-41.3	33.4	13.1
6	3	10	19.28	-62.0	34.8	-27.2	-35.4	-8.2	4.3
7	3	5	13.98	-33.0	11.5	-21.5	-37.9	-16.4	11.7
8	4	10	15.50	74.0	-42.9	31.1	25.8	-5.3	3.4
9	4	6	13.27	-16.0	-3.3	-19.3	-17.6	1.7	1.2
10	5	6	28.65	-119.0	63.0	-56.0	-40.9	15.1	5.3
11	5	7	17.27	-27.0	-10.5	-37.5	-28.6	8.9	5.1
12	5	10	19.82	-29.0	23.4	-5.6	2.5	8.1	4.1
13	6	10	22.24	90.0	-39.7	50.3	43.4	-6.9	3.1
14	6	7	30.83	92.0	-73.5	18.5	12.3	-6.2	2.0
15	6	8	48.81	57.0	-125.4	-68.4	-12.8	55.6	11.4
16	6	9	34.04	-75.0	-9.5	-84.5	-65.6	18.9	5.5
17	7	8	27.69	-35.0	-52.0	-87.0	-25.1	61.9	22.3
18	7	9	39.24	-167.0	64.0	-103.0	-77.9	25.1	6.4
19	8	9	33.17	-132.0	116.0	-16.0	-52.8	-36.8	11.1

MEAN: 12.1 S.D. 27.9 R.M.S. 27.2 MEAN PPM: 7.9 RMS PPM: 9.4

SCHOOL OF SURVEYING, U.N.S.W. DELTA N ANALYSIS
GRAV08 Ver 1.5 WA.DAT 19-MAY-88

WESTERN AUSTRALIA HEIGHT NETWORK
UNIVERSITY OF NEW SOUTH WALES

Control File: WAPTS.DAT Lines File: WALINES.DAT
Inner Zone File: WAIN.SUM Remote Zone File: OSU81_18.OUT

Number of Rings in Inner Zone: 24

LINE NO.	FROM	TO	DIST (km)	GRAVITY REMOTE	GRAVITY INNER	GRAVITY SUM	G.P.S.-LEVEL	DIFF (cm)	PPM
1	1	2	15.06	62.0	-29.6	32.4	26.3	-6.1	4.0
2	1	3	37.79	94.0	-78.0	16.0	46.2	30.2	8.0
3	1	4	21.33	-42.0	10.5	-31.5	-15.0	16.5	7.7
4	2	3	24.57	32.0	-48.4	-16.4	19.9	36.3	14.8
5	2	4	25.43	-104.0	40.1	-63.9	-41.3	22.6	8.9
6	3	10	19.28	-62.0	35.0	-27.0	-35.4	-8.4	4.3
7	3	5	13.98	-33.0	10.4	-22.6	-37.9	-15.3	10.9
8	4	10	15.50	74.0	-53.5	20.5	25.8	5.3	3.4
9	4	6	13.27	-16.0	-6.1	-22.1	-17.6	4.5	3.4
10	5	6	28.65	-119.0	72.0	-47.0	-40.9	6.1	2.1
11	5	7	17.27	-27.0	-5.0	-32.0	-28.6	3.4	2.0
12	5	10	19.82	-29.0	24.6	-4.4	2.5	6.9	3.5
13	6	10	22.24	90.0	-47.4	42.6	43.4	.8	.4
14	6	7	30.83	92.0	-77.0	15.0	12.3	-2.7	.9
15	6	8	48.81	57.0	-142.1	-85.1	-12.8	72.3	14.8
16	6	9	34.04	-75.0	-65.6	-140.6	-65.6	75.0	22.0
17	7	8	27.69	-35.0	-65.1	-100.1	-25.1	75.0	27.1
18	7	9	39.24	-167.0	11.5	-155.5	-77.9	77.6	19.8
19	8	9	33.17	-132.0	76.6	-55.4	-52.8	2.6	.8

MEAN: 21.2 S.D. 38.0 R.M.S. 37.0 MEAN PPM: 8.4 RMS PPM: 11.4

SCHOOL OF SURVEYING, U.N.S.W. DELTA N ANALYSIS
GRAV08 Ver 1.5 WA.DAT 19-MAY-88
WESTERN AUSTRALIA HEIGHT NETWORK
UNIVERSITY OF NEW SOUTH WALES

Control File: WAPTS.DAT Lines File: WALINES.DAT
Inner Zone File: WAIN.SUM Remote Zone File: OSU81_18.OUT

Number of Rings in Inner Zone: 26

LINE NO.	FROM	TO	DIST (km)	GRAVITY REMOTE	GRAVITY INNER	GRAVITY SUM	G.P.S.-LEVEL	DIFF (cm)	PPM
1	1	2	15.06	62.0	-39.9	22.1	26.3	4.2	2.8
2	1	3	37.79	94.0	-82.0	12.0	46.2	34.2	9.1
3	1	4	21.33	-42.0	11.9	-30.1	-15.0	15.1	7.1
4	2	3	24.57	32.0	-42.1	-10.1	19.9	30.0	12.2
5	2	4	25.43	-104.0	51.8	-52.2	-41.3	10.9	4.3
6	3	10	19.28	-62.0	41.0	-21.0	-35.4	-14.4	7.5
7	3	5	13.98	-33.0	13.0	-20.0	-37.9	-17.9	12.8
8	4	10	15.50	74.0	-52.9	21.1	25.8	4.7	3.1
9	4	6	13.27	-16.0	.5	-15.5	-17.6	-2.1	1.6
10	5	6	28.65	-119.0	81.4	-37.6	-40.9	-3.3	1.2
11	5	7	17.27	-27.0	8.4	-18.6	-28.6	-10.0	5.8
12	5	10	19.82	-29.0	28.0	-1.0	2.5	3.5	1.8
13	6	10	22.24	90.0	-53.5	36.5	43.4	6.9	3.1
14	6	7	30.83	92.0	-73.1	18.9	12.3	-6.6	2.2
15	6	8	48.81	57.0	-137.5	-80.5	-12.8	67.7	13.9
16	6	9	34.04	-75.0	-16.2	-91.2	-65.6	25.6	7.5
17	7	8	27.69	-35.0	-64.5	-99.5	-25.1	74.4	26.9
18	7	9	39.24	-167.0	56.9	-110.1	-77.9	32.2	8.2
19	8	9	33.17	-132.0	121.3	-10.7	-52.8	-42.1	12.7

MEAN: 11.2 S.D. 30.5 R.M.S. 29.7 MEAN PPM: 7.6 RMS PPM: 9.7

13 APPENDIX D

```
      PROGRAM LESQPL
      PARAMETER (MAXOBS=50)
C
C PROGRAM TO FIT AN OVERDETERMINED LEAST SQUARES
C PLANE TO A GPS HEIGHT NETWORK.
C ROBERT HOLLOWAY, UNSW.          13-MAR-1987
C
      IMPLICIT REAL*8 (A-H,O-Z)
      IMPLICIT INTEGER*2 (I-N)
      INTEGER*2 IN, IOUT, ISCRN, IKBD, ICHK
      INTEGER*2 NOBS, NUMB
      CHARACTER*10 MATID(MAXOBS), STNID, SNAME
      CHARACTER*20 FILEIN, FILEOUT
      CHARACTER*3 END
      REAL*8 MATA(MAXOBS,3), MATL(MAXOBS)
      REAL*8 MATRAN(3,MAXOBS), MATINV(3,3), MATEMP(3,3)
      REAL*8 MATD(3), MATRESULT(3),MATV(MAXOBS),MATVCV(MAXOBS)
      REAL*8 EAST,NORTH,GPSHGT,AHDHGT
      REAL*8 VAR,APOST,AHD
      REAL*8 PI,GRAD,DIRN,DEFLNE,DEFLNN,SEC
      COMMON /DEVICE/ FILEIN, FILEOUT
      COMMON /INOUT/ IN,IOUT,ISCRN,IKBD
C INITIALIZE DEVICE UNITS
      IN=1
      IOUT=2
      ISCRN=0
      IKBD=0
C INITIALISE VARIABLES
      NOBS=0
      NUMB=0
      PI=DACOS(-1.0D0)
C
C PROMPT FOR INPUT FILE NAME, OUTPUT FILE NAME
C
      WRITE (ISCRN,30)
30    FORMAT (//,12X,'Program LESQPL (LEast SQuares PLane fit).')
      WRITE (ISCRN,50)
50    FORMAT (//,12X,' Input file name : ?  ',$)
      READ (IKBD,100) FILEIN
100   FORMAT (A20)
      OPEN (IN,FILE=FILEIN,STATUS='OLD',FORM='FORMATTED',
     #IOSTAT=ICHK)
      IF (ICHK.NE.0) GO TO 1500
      WRITE (ISCRN,150)
150   FORMAT (12X,' Output file name : ? ',$)
      READ (IKBD,100) FILEOUT
```

```
      WRITE (ISCRN,175)
175   FORMAT (//,12X,'I am working .....')
C
C COUNT THE NUMBER OF OBSERVATIONS
C
200   READ (IN,250,ERR=1375) STNID,AMGE,AMGN,GPSHGT,AHDHGT
250       FORMAT (A10,F10.3,F12.3,2F8.3)
          IF (STNID.EQ.'999') GO TO 300
          NOBS=NOBS+1
          GO TO 200
300   CONTINUE
      IF (NOBS.LT.3) GO TO 1400
305   CONTINUE
      READ (IN,310,END=320) SNAME,EAST,NORTH,ELLIPHT
310       FORMAT (A10,F10.3,F12.3,F8.3)
          NUMB=NUMB+1
          GO TO 305
320   CONTINUE
      REWIND IN
C
C CLEAR ALL ARRAYS OF EXTRANEOUS DATA
C
      DO 7100 J=1,NOBS
          MATL(J)=0.0
          MATV(J)=0.0
          MATVCV(J)=0.0
          DO 7050 K=1,3
              MATA(J,K)=0.0
              MATD(K)=0.0
7050      CONTINUE
7100  CONTINUE
      DO 7250 N=1,3
          MATRESULT(N)=0.0
          DO 7200 I=1,NOBS
              MATRAN(N,I)=0.0
              DO 7150 M=1,3
                  MATEMP(N,M)=0.0
                  MATINV(N,M)=0.0
7150          CONTINUE
7200      CONTINUE
7250  CONTINUE

C
C READ IN DATA FROM INPUT FILE
C
      DO 7350 K=1,NOBS
          READ (IN,7300) STNID,AMGE,AMGN,GPSHGT,AHDHGT
7300      FORMAT (A10,F10.3,F12.3,2F8.3)
          UNDUL = GPSHGT-AHDHGT
          MATL(K) = UNDUL
          MATID(K) = STNID
          MATA(K,1) = AMGE
          MATA(K,2) = AMGN
```

```
          MATA(K,3) = 1.0D0
 7350   CONTINUE
 C
 C LEAST SQUARES EQUATION IS X=(INV(A(T)*A)) (A(T)*L)
 C
        CALL TRANSPOSE (MATA,MAXOBS,3,MATRAN)
        CALL MATMUL (MATRAN,MATA,3,MAXOBS,3,MATEMP)
        CALL INVERT (MATEMP,MATD,3)
        CALL MATMUL (MATRAN,MATL,3,MAXOBS,1,MATINV)
        CALL MATMUL (MATEMP,MATINV,3,3,1,MATRESULT)
 C
 C CALCULATE RESIDUALS
 C
        CALL MATMUL (MATA,MATRESULT,MAXOBS,3,1,MATV)
        CALL MATSUB (MATV,MATL,MAXOBS,1,MATVCV)

 C
 C PRINT OUT RESULTS
 C
        OPEN (IOUT,FILE=FILEOUT,STATUS='NEW',FORM='FORMATTED')
        WRITE (IOUT,322) FILEIN, FILEOUT
 322    FORMAT (3X,'Input data file is ',A20,1X,'Output file is ',A20,/)
        WRITE (IOUT,325)
 325    FORMAT (3X,72('-'),//,7X,'FIT AN OVERDETERMINED',
       #' LEAST SQUARES PLANE TO A GPS HEIGHT NETWORK',/,12X,
       #'GENERAL EQUATION OF PLANE IS  N = Ae + Bn + C'//,3X,72('-'),//)
        WRITE (IOUT,350) MATRESULT(1)
 350    FORMAT (15X,' CO-EFFICIENT A = ',F18.12)
        WRITE (IOUT,400) MATRESULT(2)
 400    FORMAT (15X,' CO-EFFICIENT B = ',F18.12)
        WRITE (IOUT,450) MATRESULT(3)
 450    FORMAT (15X,' CO-EFFICIENT C = ',F10.4,//)
        WRITE (IOUT,475)
 475    FORMAT (5X,'STATION ID',4X,'EASTING',4X,'NORTHING',3X,
       # 'UNDULATION',2X,'RESIDUAL',/)
 C
 C PRINT OUT CO-ORDINATES, UNDULATIONS AND RESIDUALS
 C
        DO 550 J=1,NOBS
        WRITE (IOUT,500) MATID(J),MATA(J,1),MATA(J,2),MATL(J),MATVCV(J)
 500    FORMAT (5X,A10,2X,F10.3,F13.3,F9.3,2X,F7.3)
 550    CONTINUE
 C
 C CALCULATE STANDARD DEVIATION OF RESIDUALS
 C
        STDEV=0.0D0
        DO 560 K=1,NOBS
           STDEV = MATVCV(K) * MATVCV(K) + STDEV
 560    CONTINUE
        STDEV = DSQRT(STDEV/(NOBS-1))
        WRITE (IOUT,570) STDEV
 570    FORMAT (/,30X,'STD DEV OF RESIDUALS = ',F5.3)
 C
```

```
C CALCULATE APOST VARIANCE  VTV/n-r
C
      APOST=0.0
      VAR=0.0
      IF (NOBS.EQ.3) GO TO 625
      DO 600 N=1,NOBS
         APOST=MATVCV(N) * MATVCV(N) + APOST
600   CONTINUE
      VAR = APOST/(NOBS-3)
C
625   CONTINUE
      WRITE (IOUT,650) NOBS, VAR
650   FORMAT (//,5X,'NUMBER OF COMMON POINTS IS ',I2,4X,'APOST ',
     #'VARIANCE =',F10.7)
C
C CALCULATE MAXIMUN GRADIENT OF PLANE AND DIRECTION
C
      GRAD=DSQRT(MATRESULT(1)*MATRESULT(1)+MATRESULT(2)*
     #MATRESULT(2))
      GRAD=GRAD*1000000.0D0
      DIRN=DATAN(DABS(MATRESULT(1)/MATRESULT(2)))
      IF (MATRESULT(1).LT.0.0) GO TO 750
      IF (MATRESULT(2).LT.0.0) GO TO 700
      GO TO 850
700   DIRN=PI-DIRN
      GO TO 850
750   IF (MATRESULT(2).LT.0.0) GO TO 800
      DIRN=2*PI-DIRN
      GO TO 850
800   DIRN=PI+DIRN
850   CONTINUE
      CALL RAD2DEG (DIRN, IDEG, IMIN, ASEC)
      WRITE (IOUT,900) GRAD,IDEG,IMIN,ASEC
900   FORMAT (5X,'MAXIMUM SLOPE = ',F7.2,' mm/km',4X,'DIRECTION ',
     #'OF MAX SLOPE =',I4,I3,F5.1)
C
C CALCULATE DEFLECTION OF THE VERTICAL
C
      DEFLNE = MATRESULT(1)/PI*180.0D0*3600.0D0
      DEFLNN = MATRESULT(2)/PI*180.0D0*3600.0D0
      DEFLNE = -DEFLNE
      DEFLNN = -DEFLNN
      WRITE (IOUT,950) DEFLNE, DEFLNN
950   FORMAT (5X,'DEFLECTIONS OF THE VERTICAL     Eta(E) =',
     #F6.2,'",3X,'Xi(N) =',F6.2,'",//)
C
C CALCULATE AHD HEIGHT FOR INTERPOLATED POINTS
C
      IF (NUMB.EQ.0) GO TO 1600
      WRITE (IOUT,1000)
1000  FORMAT (5X,'TABLE OF INTERPOLATED POINTS TO AHD',/)
      WRITE (IOUT,1050)
1050  FORMAT (5X,'STATION ID',4X,'EASTING',4X,'NORTHING',3X,'AHD HEIGHT',/)
```

```
C
      READ (IN,1100) END
1100  FORMAT(A3)
1150  READ (IN,1200,END=1300) SNAME,EAST,NORTH,GPSHGT
1200     FORMAT (A10,F10.3,F12.3,F8.3)
         AHD =
GPSHGT-(EAST*MATRESULT(1)+NORTH*MATRESULT(2)+MATRESULT(3))
         WRITE (IOUT,1250) SNAME, EAST, NORTH, AHD
1250   FORMAT (5X,A10,2X,F10.3,F13.3,F9.3)
      GO TO 1150
1300  CONTINUE
      WRITE (IOUT,1350) NUMB
1350  FORMAT (/,5X,'NUMBER OF INTERPOLATED POINTS IS ',I2)

C
C CLOSE OUTPUT FILE
C
      ENDFILE IOUT
      CLOSE (IOUT,STATUS='KEEP')
      CLOSE (IN,STATUS='KEEP')
      GO TO 1600
1375  WRITE (ISCRN,1380)
1380  FORMAT (8X,' *** ERROR *** Input file wrong format.')
      STOP
1400  WRITE (ISCRN,1450)
1450  FORMAT (8X,' *** WARNING *** Less than 3 control points. '
      #'Unable to solve for plane.')
      STOP
1500  WRITE (ISCRN,1550)
1550  FORMAT (12X,' *** WARNING *** Input file does not exist.')
      STOP
1600  WRITE (ISCRN,1650) FILEOUT
1650  FORMAT (/////,12X,' Program finished successfully',
     # ' ....Output file is  ',A20,/////)
      END

      SUBROUTINE INVERT(A,D,M)
      IMPLICIT REAL*8 (A-H,O-Z)
      REAL*8 A(M,M),D(M)
C     INTEGER*2 M
C
C INVERTS A SQUARE MATRIX
C (MAT A)INV = MAT A   (M COLS, M ROWS)
C D IS A MATRIX DEFINED AT BEGINNING OF PROGRAM - TEMPORARY
C
C SCALE MATRIX TO AVOID OVERFLOW AND IMPROVE CONDITION
C NUMBER THE SAME WAY AS CALCULATING CORRELATION MATRIX
C STORE SCALE FACTORS (SQ ROOT OF DIAGONAL) IN D.
C
      DO 10 I=1,M
         D(I) = DSQRT(A(I,I))
         IF (DABS(D(I)).LT.1.0D-18) GO TO 100
10    CONTINUE
```

```
C
C THIS TESTS IF ONE OF THE DIAGONAL TERMS IS ZERO,
C IF IT IS, MATRIX CANNOT BE INVERTED AND PROGRAM STOPS
C
C REDUCE A
      DO 30 I=1,M
         DO 20 J=1,M
            A(I,J)=A(I,J)/D(I)/D(J)
20       CONTINUE
30    CONTINUE
C
      DO 70 I=1,M
         F=A(I,I)
         A(I,I)=1.0D0
         DO 40 J=1,M
            A(I,J)=A(I,J)/F
40       CONTINUE
         DO 60 J=1,M
            IF(I.EQ.J) GO TO 60
            F=A(J,I)
            A(J,I)=0.0D0
            DO 50 K=1,M
               A(J,K)=A(J,K)-A(I,K)*F
50          CONTINUE
60       CONTINUE
70    CONTINUE
C
C RESCALE TO GIVE TRUE INVERSE
C
      DO 90 I=1,M
         DO 80 J=1,M
            A(I,J)=A(I,J)/D(I)/D(J)
80       CONTINUE
90    CONTINUE
      RETURN
C
100   WRITE(*,110) I,F
110   FORMAT(' FATAL ERROR. DIAGONAL TERM ',I2,' EQUALS ',D10.3)
      STOP 'STOPPED IN INVERT'
      END

      SUBROUTINE TRANSPOSE (RMATB,IR,IC,RMATA)
C TO TRANSPOSE MATRIX IN SITU
C LOCAL VARIABLES
      INTEGER*2 I,J
      INTEGER*2 IR,IC
      REAL*8    RMATB(IR,IC)
      REAL*8    RMATA(IC,IR)
      DO 20 I = 1,IR
         DO 10 J = 1,IC
            RMATA(J,I) = RMATB(I,J)
```

```
10          CONTINUE
20      CONTINUE
        END

        SUBROUTINE  MATMUL (RMATB,RMATC,IRB,ICB,ICC,RMATA)
C MULTIPLICATION OF TWO MATRICES
C
C LOCAL VARIABLES
        INTEGER*2 I,J,K
        INTEGER*2 IRB,ICB,ICC
        REAL*8    RMATB(IRB,ICB), RMATC(ICB,ICC)
        REAL*8    RMATA(IRB,ICC)
C
        DO 30 I = 1,IRB
           DO 20 J = 1,ICB
              DO 10 K = 1,ICC
                 RMATA(I,K)=RMATA(I,K)+(RMATB(I,J)*RMATC(J,K))
10            CONTINUE
20         CONTINUE
30      CONTINUE
        END
C

        SUBROUTINE  MATSUB (RMATB,RMATC,IR,IC,RMATA)
C SUBTRACTING TWO MATRICES; MATB - MATC = MATA
C
C LOCAL VARIABLES
        INTEGER*2 I,J
        INTEGER*2 IR,IC
        REAL*8    RMATB(IR,IC),RMATC(IR,IC)
        REAL*8    RMATA(IR,IC)
C
        DO 20 I = 1,IR
           DO 10 J = 1,IC
              RMATA(I,J) = RMATB(I,J) - RMATC(I,J)
10         CONTINUE
20      CONTINUE
        END
```

```
      SUBROUTINE RAD2DEG (RAD,IDECDEG,IMIN,SEC)
C
C CONVERTS RADIANS TO DEG, MINS AND SECONDS
C
      IMPLICIT REAL*8 (A-H,O-Z)
      IMPLICIT INTEGER*2 (I-N)
      REAL*8 MIN
C
      PI=DACOS(-1.0D0)
      FACT=180.0D0/PI
C
      DDMS=RAD*FACT
      DECDEG=DINT(DDMS)
      MIN=DABS((DDMS-DECDEG)*60.0D0)
      SEC=DABS((MIN-DINT(MIN))*60.0D0)
      IDECDEG=INT(DECDEG)
      IMIN=INT(MIN)
C
C TEST IF DEGREES ARE GREATER THAN 360 AND
C MINS AND SECS ARE NOT GREATER 60.
C
100   IF (IDECDEG.GT.360) THEN
        IDECDEG=IDECDEG-360
        GOTO 100
      ENDIF
      IF (SEC.GE.59.99995) THEN
        IMIN=IMIN+1
        SEC=SEC-60.0
      ENDIF
      IF (IMIN.GE.60) THEN
        IF (IDECDEG.LT.0) THEN
          IDECDEG=IDECDEG-1
          IMIN=IMIN-60
        ELSE
          IDECDEG=IDECDEG+1
          IMIN=IMIN-60
        ENDIF
      ENDIF
      RETURN
      END
```

14 APPENDIX E

WESTERN AUSTRALIA

FIT AN OVERDETERMINED LEAST SQUARES PLANE TO A GPS HEIGHT NETWORK

GENERAL EQUATION OF PLANE IS N = Ae + Bn + C

CO-EFFICIENT A = .000020386494
CO-EFFICIENT B = .000012325885
CO-EFFICIENT C = -114.6127

STATION ID	EASTING	NORTHING	*N*	RESIDUAL
MRA 8	465374.677	6588373.432	-23.916	-.002
NMF 705	480325.935	6586611.166	-23.653	+.018
HD 9	498328.152	6569903.015	-23.454	-.020
KARRABEIN	489934.988	6512086.189	-24.370	+.013
NTH TOOD	457872.171	6520516.113	-24.898	-.009

STD DEV OF RESIDUALS = .016

NUMBER OF COMMON POINTS IS 5
MAXIMUM SLOPE = 23.82 mm/km
DEFLECTIONS OF THE VERTICAL

APOST VARIANCE = .0004831
DIRECTION OF MAX SLOPE = 58 50 32.7
Eta(E) = -4.21" Xi(N) = -2.54"

TABLE OF INTERPOLATED POINTS TO AHD

STATION ID	EASTING	NORTHING	AHD HEIGHT
PTH 135	464042.484	6567094.202	338.182
PTH 136	464715.309	6553850.296	297.371
HD 8	479079.076	6570815.757	338.057
HD 10	493188.937	6556913.253	365.369
BERRING	492086.875	6539685.494	313.161

NUMBER OF INTERPOLATED POINTS IS 5

15 APPENDIX F

SOUTH AUSTRALIA

FIT AN OVERDETERMINED LEAST SQUARES PLANE TO A GPS HEIGHT NETWORK
GENERAL EQUATION OF PLANE IS N = Ae + Bn + C

CO-EFFICIENT A = .000010727929
CO-EFFICIENT B = .000017652649
CO-EFFICIENT C = -109.5566

STATION ID	EASTING	NORTHING	*N*	RESIDUAL
4	350933.713	6049643.037	0.100	+.900
5	359601.401	6109592.523	2.002	+.150
6	351548.191	6118735.766	2.288	-.061
7	353119.811	6086039.374	1.222	+.444
8	351261.393	6105772.674	1.794	+.201
21	377732.183	6051101.604	0.629	+.685
24	373541.377	6106252.061	2.382	-.140
25	405853.801	6092712.461	2.247	+.103
30	392905.713	6113296.301	2.701	-.127
33	376432.914	6132872.951	3.204	-.461
34	393722.553	6129664.534	3.171	-.299
35	384278.589	6173440.791	4.120	-.577
36	404063.751	6162462.998	3.845	-.283
39	405885.101	6202537.989	4.690	-.401
46	450245.358	6070711.595	2.680	-.242
47	424876.333	6070136.354	2.049	+.106
48	413996.565	6039363.762	1.502	-.007
53	452818.535	6125376.911	3.471	-.041
56	421331.388	6082164.211	2.239	+.091
59	435708.168	6110216.514	3.086	-.107
61	410537.644	6115156.053	3.118	-.322
62	419042.576	6128225.918	3.160	-.042
63	453551.044	6151336.215	3.836	+.060

STATION ID	EASTING	NORTHING	*N*	RESIDUAL
64	429202.612	6149317.908	3.686	-.086
65	451493.035	6178406.164	4.141	+.211
66	409761.311	6128663.160	3.108	-.082
70	409753.488	6184365.247	4.491	-.481
71	442196.836	6194281.931	4.412	+.121
72	435132.623	6184290.721	4.233	+.048
73	420503.756	6199344.298	4.733	-.344
86	487686.521	6055652.682	3.488	-.914
90	470543.871	6085825.012	3.271	-.349
91	469524.171	6116924.565	3.578	-.118
93	460041.880	6097347.171	3.175	-.162
97	499064.566	6150310.824	4.210	+.157
98	484695.946	6142059.611	3.878	+.189
99	479389.802	6126742.796	3.769	-.030
100	480737.852	6179087.742	3.942	+.736
101	471218.187	6152588.033	3.896	+.212
102	471191.792	6171904.223	4.107	+.342
103	458049.951	6161344.510	3.950	+.171
105	496651.694	6172877.578	4.470	+.269
106	490132.330	6206446.964	4.769	+.493
107	494836.525	6196093.975	4.776	+.353
108	502028.340	6115214.025	4.147	-.368

STD DEV OF RESIDUALS = .352

NUMBER OF COMMON POINTS IS 45
MAXIMUM SLOPE = 20.66 mm/km
DEFLECTIONS OF THE VERTICAL

APOST VARIANCE = .1299424
DIRECTION OF MAX SLOPE = 31 17 16.9
Eta(E) = -2.21" Xi(N) = -3.64"

Publications from

THE SCHOOL OF SURVEYING, THE UNIVERSITY OF NEW SOUTH WALES.

All prices include postage by surface mail. Air mail rates on application. (Effective July 1988)

To order, write to Publications Officer, School of Surveying, The University of New South Wales, P.O. Box 1, Kensington N.S.W., 2033 AUSTRALIA

NOTE: ALL ORDERS MUST BE PREPAID

UNISURV REPORTS - G SERIES

Price (including postage): $3.50

G14. A. Stolz, "The computation of three dimensional Cartesian coordinates of terrestrial networks by the use of local astronomic vector systems", Unisurv Rep. 18, 47 pp.

G16. R.S. Mather et al, "Communications from Australia to Section V, International Association of Geodesy, XV General Assembly, International Union of Geodesy and Geophysics, Moscow 1971", Unisurv Rep. 22, 72 pp.

G17. Papers by R.S. Mather, H.L. Mitchell & A. Stolz on the following topics:- Four-dimensional geodesy, Network adjustment and Sea surface topography, Unisurv G17, 73 pp.

G18. Papers by L. Berlin, G.J.F. Holden, P.V. Angus-Leppan, H.L. Mitchell & A.H. Campbell on the following topics:- Photogrammetry co-ordinate systems for surveying integration, Geopotential networks and Linear measurement, Unisurv G18, 80 pp.

G19. R.S. Mather, P.V. Angus-Leppan, A. Stolz & I. Lloyd, "Aspects of four-dimensional geodesy", Unisurv G19, 100 pp.

G20. Papers by J.S. Allman, R.C. Lister, J.C. Trinder & R.S. Mather on the following topics:- Network adjustments, Photogrammetry, and 4-Dimensional geodesy, Unisurv G20, 133 pp.

G21. Papers by E. Grafarend, R.S. Mather & P.V. Angus-Leppan on the following topics:- Mathematical geodesy, Coastal geodesy and Refraction, Unisurv G21, 100 pp.

G22. Papers by R.S. Mather, J.R. Gilliland, F.K. Brunner, J.C. Trinder, K. Bretreger & G. Halsey on the following topics:- Gravity, Levelling, Refraction, ERTS imagery, Tidal effects on satellite orbits and Photogrammetry, Unisurv G22, 96 pp.

G23. Papers by R.S. Mather, E.G. Anderson, C. Rizos, K. Bretreger, K. Leppert, B.V. Hamon & P.V. Angus-Leppan on the following topics:- Earth tides, Sea surface topography, Atmospheric effects in physical geodesy, Mean sea level and Systematic errors in levelling, Unisurv G23, 96 pp.

G24. Papers by R.C. Patterson, R.S. Mather, R. Coleman, O.L. Colombo, J.C. Trinder, S.U. Nasca, T.L. Duyet & K. Bretreger on the following topics:- Adjustment theory, Sea surface topography determinations, Applications of LANDSAT imagery, Ocean loading of Earth tides, Physical geodesy, Photogrammetry and Oceanographic applications of satellites, Unisurv G24, 151 pp.

G25. Papers by S.M. Nakiboglu, B. Ducarme, P. Melchior, R.S. Mather, B.C. Barlow, C. Rizos, B. Hirsch, K. Bretreger, F.K. Brunner & P.V. Angus-Leppan on the following topics:- Hydrostatic equilibrium figures of the Earth, Earth tides, Gravity anomaly data banks for Australia, Recovery of tidal signals from satellite altimetry, Meteorological parameters for modelling terrestrial refraction and Crustal motion studies in Australia, Unisurv G25, 124 pp.

G26. Papers by R.S. Mather, E.G. Masters, R. Coleman, C. Rizos, B. Hirsch, C.S. Fraser, F.K. Brunner, P.V. Angus-Leppan, A.J. McCarthy & C. Wardrop on the following topics:- Four-dimensional geodesy, GEOS-3 altimetry data analysis, analysis of meteorological measurements for microwave EDM and Meteorological data logging system for geodetic refraction research, Unisurv G26, 113 pp.

G27. Papers by F.K. Brunner, C.S. Fraser, S.U. Nasca, J.C. Trinder, L. Berlin, R.S. Mather, O.L. Colombo & P.V. Angus-Leppan on the following topics:- Micrometeorology in geodetic refraction, LANDSAT imagery in topographic mapping, adjustment of large systems, GEOS-3 data analysis, Kernel functions and EDM reductions over sea, Unisurv G27, 101 pp.

G29. Papers by F.L. Clarke, R.S. Mather, D.R. Larden & J.R. Gilliland on the following topics:- Three dimensional network adjustment incorporating ξ, η and N, Geoid determinations with satellite altimetry, Geodynamic information from secular gravity changes and Height and free-air anomaly correlation, Unisurv G29, 87 pp.

From June 1979 Unisurv G's name was changed to Australian Journal of Geodesy, Photogrammetry and Surveying. These can be ordered from The Managing Editor, Australian Journal of Goedesy, Photogrammetry and Surveying, Institution of Surveyors - Australia , Box 4793 G.P.O., Sydney, N.S.W., 2001, AUSTRALIA.

UNISURV REPORTS - S SERIES

S8 - S19	Price (including postage):		$7.50
S20 onwards	Price (including postage):	Individuals	$18.00
		Institutions	$25.00

S8 A. Stolz, "Three-D Cartesian co-ordinates of part of the Australian geodetic network by the use of local astronomic vector systems", Unisurv Rep. S 8, 182 pp, 1972.

S9 H.L. Mitchell, "Relations between MSL & geodetic levelling in Australia", Unisurv Rep. S 9, 264 pp, 1973.

S10 A.J. Robinson, "Study of zero error & ground swing of the model MRA101 tellurometer", Unisurv Rep. S 10, 200 pp, 1973.

S12. G.J.F. Holden, "An evaluation of orthophotography in an integrated mapping system", Unisurv Rep. S 12, 232 pp, 1974.

S14. Edward G. Anderson, "The Effect of Topography on Solutions of Stokes` Problem", Unisurv Rep. S 14, 252 pp, 1976.

S15. A.H.W. Kearsley, "The Computation of Deflections of the Vertical from Gravity Anomalies", Unisurv Rep. S 15, 181 pp, 1976.

S16. K. Bretreger, "Earth Tide Effects on Geodetic Observations", Unisurv S 16, 173 pp, 1978.

S17. C. Rizos, "The role of the gravity field in sea surface topography studies", Unisurv S 17, 299 pp, 1980.

S18. B.C. Forster, "Some measures of urban residual quality from LANDSAT multi-spectral data", Unisurv S 18, 223 pp, 1981.

S19. Richard Coleman, "A Geodetic Basis for recovering Ocean Dynamic Information from Satellite Altimetry", Unisurv S 19,332 pp, 1981.

S20. Douglas R. Larden, "Monitoring the Earth's Rotation by Lunar Laser Ranging", Unisurv Report S 20, 280 pp, 1982.

S21. R.C. Patterson, "Approximation and Statistical Methods in Physical Geodesy", Unisurv Report S 21, 179 pp, 1982.

S25. Ewan G. Masters, "Applications of Satellite Geodesy to Geodynamics", Unisurv Report S25, 208 pp, 1984.

S26. Andrew Charles Jones, "An Investigation of the Accuracy and repeatability of Satellite Doppler relative positioning techniques", Unisurv Report S26, 222 pp, 1984.

S27. Bruce R. Harvey, "The Combination of VLBI and Ground Data for Geodesy and Geophysics", Unisurv Report S27, 239 pp, 1985.

S28. Rod Eckels, "Surveying with GPS in Australia", Unisurv S28, 220 pp, 1987.

S29. Gary S. Chisholm, "Integration of GPS into hydrographic survey operations", Unisurv S29, 190 pp, 1987.

S30. Gary Alan Jeffress, "An investigation of Doppler satellite positioning multi-station software", Unisurv S30, 118 pp, 1987.

S31. Jahja Soetandi, "A model for a cadastral land information system for Indonesia", Unisurv S31, 168 pp, 1988.

S33. R. D. Holloway, "The integration of GPS heights into the Australian Height Datum", Unisurv S33, 151 pp.,1988.

S34. Robin C. Mullin, "Data update in a Land Information Network", Unisurv S34, 168 pp. 1988.

PROCEEDINGS

Prices include postage by surface mail

P1. P.V. Angus-Leppan (Editor), "Proceedings of conference on refraction effects in geodesy & electronic distance measurement", 264 pp. Price: $6.50

P2. R.S. Mather & P.V. Angus-Leppan (Eds), "Australian Academy of Science/International Association of Geodesy Symposium on Earth`s Gravitational Field & Secular Variations in Position", 740 pp. Price $12.50

MONOGRAPHS

Prices include postage by surface mail

M1. R.S. Mather, "The theory and geodetic use of some common projections", (2nd edition), 125 pp. Price $9.00

M2. R.S. Mather, "The analysis of the earth's gravity field", 172 pp. Price $5.50

M3. G.G. Bennett, "Tables for prediction of daylight stars", 24 pp. Price $2.00

M4. G.G. Bennett, J.G. Freislich & M. Maughan, "Star prediction tables for the fixing of position", 200 pp. Price $5.00

M5. M. Maughan, "Survey computations", 98 pp. Price $8.00

M6. M. Maughan, "Adjustment of Observations by Least Squares", 61 pp. Price $7.00

M7. J.M. Rueger, "Introduction to Electronic Distance Measurement", (2nd Edition), 140 pp. Price $14.00

M8. A.H.W. Kearsley, "Geodetic Surveying". 77pp. Price $8.00

M9. ** R.W. King, E.G. Masters, C. Rizos, A. Stolz and J. Collins, "Surveying with GPS", 128 pp

M10. W. Faig, "Aerial Triangulation and Digital Mapping", 102. pp. Price $13.00

M11. W.F. Caspary, "Concepts of Network and Deformation Analysis", 183 pp. Price $22.00

M12. F.K. Brunner, "Atmospheric Effects on Geodetic Space Measurements", 110 pp. Price $13.00

** No longer for external sale from the School of Surveying. Now published by Ferd. Dümmlers Verlag, Kaiserstrasse 31 - 37, D - 5300 Bonn 1, Federal Republic of Germany